

---

Civil Engineering Theses

Civil Engineering

---

Spring 5-1-2019

## Experimental Investigation of Adobe Structures with Digital Image Correlation

Ashmita Wasti

Follow this and additional works at: [https://scholarworks.uttyler.edu/ce\\_grad](https://scholarworks.uttyler.edu/ce_grad)



Part of the Civil Engineering Commons

---

### Recommended Citation

Wasti, Ashmita, "Experimental Investigation of Adobe Structures with Digital Image Correlation" (2019).  
*Civil Engineering Theses*. Paper 14.  
<http://hdl.handle.net/10950/1327>

This Thesis is brought to you for free and open access by the Civil Engineering at Scholar Works at UT Tyler. It has been accepted for inclusion in Civil Engineering Theses by an authorized administrator of Scholar Works at UT Tyler. For more information, please contact [tgullings@uttyler.edu](mailto:tgullings@uttyler.edu).

EXPERIMENTAL INVESTIGATION OF ADOBE STRUCTURES WITH  
DIGITAL IMAGE CORRELATION

by

ASHMITA WASTI

A thesis submitted in partial fulfillment  
of the requirements for the degree of  
Master of Science in Civil Engineering  
Department of Civil Engineering

Michael McGinnis, Ph.D., Committee Chair

College of Engineering

The University of Texas at Tyler  
May 2019

The University of Texas at Tyler  
Tyler, Texas



The University of Texas at Tyler  
Tyler, Texas

This is to certify that the Master's Thesis of

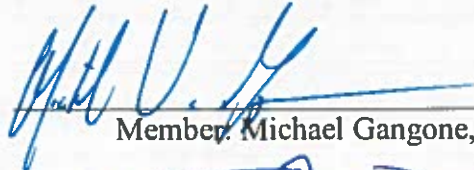
ASHMITA WASTI

has been approved for the thesis requirement on  
April 2, 2019  
for the Master of Science of Civil Engineering degree

Approvals:




Thesis Chair: Michael McGinnis, Ph.D., P.E.



Member: Michael Gangone, Ph.D.



Member: Gokhan Saygili, Ph.D., P.E.



Chair, Department of Civil Engineering

 FOR JK

Dean, College of Engineering

© Copyright 2019 by Ashmita Wasti

All rights reserved.

## Acknowledgements

At first, I would like to thank my thesis advisor Dr. Michael McGinnis. This thesis would not have been possible without him. I would like to thank him for providing constant supervision and guidance throughout this project.

I am thankful to Dr. Michael Gangone for his endless support throughout the research.

I express my gratitude towards my committee Dr. Gokhan Saygili and Dr. Brad Weldon for providing suggestions whenever necessary.

I would like to thank Grad School of University of Texas at Tyler for helping in my research and New Mexico State University for providing funding for the completion of this project.

I would like to thank Department of Civil Engineering for their continuous support.

This thesis would not have been possible without the hard work and dedication of the graduate students involved with this project at NMSU: Eduardo Davila, Judit Garcia, and Diego Garcia Vera. Their contributions are gratefully acknowledged.

This material is based upon work supported in part by the National Science Foundation (NSF) under NSF Cooperative Agreement Number EEC-1449501. Any opinions, findings and conclusions, or recommendations expressed in this material are those of the author(s), and do not necessarily reflect those of the NSF.

In addition, I am grateful for the love and support from my family and friends who have helped me throughout the process.

## Table of Contents

List of Tables .....	v
List of Figures .....	vi
Abstract .....	ix
Chapter One Introduction .....	1
1.1 Problem Statement .....	1
1.2 Research Relationship .....	2
1.3 Research Objectives .....	3
1.4 Research Significance and Scope .....	3
1.5 Construction of adobe specimens .....	4
1.6 3D-DIC .....	5
1.7 Organization of Thesis .....	5
Chapter Two Background .....	8
2.1 Classification of adobe .....	8
2.3 Experiments Performed on Adobe .....	9
2.3.1 Study of Mechanical Properties of Adobe Bricks in Ancient Construction .....	9
2.3.2 Seismic Strength of Adobe Masonry .....	10
2.3.3 Influence of Natural Stabilizers and Natural Fibers on the Mechanical Properties of adobe Bricks .....	11
2.2.4 Determination of Bending Strength Using Three-Point Test .....	13
2.3.5 Micromechanical assessment of adobe masonry assemblages based on experimental data sets .....	13

2.3.6 Adobe Bricks Under Compression: Experimental Investigation and Derivation of Stress–Strain Equation.....	14
2.4 In-plane behavior and retrofitting method of mud-brick walls.....	15
2.5 Study of shear strength of adobe clay bricks using DIC.....	16
2.6 Determination of Modulus of Elasticity .....	16
2.7 Repair of Adobe Building by Clay-Based Grout Injection.....	20
2.8 Digital Image Correlation (DIC) Technology in Civil Engineering.....	21
2.8.1 Measurement of Crack Opening .....	21
2.8.2 DIC in Biomechanics.....	23
2.8.3 DIC Applications at The University of Texas at Tyler.....	23
2.8.4 Study of Geomaterials.....	23
Chapter Three Digital Image Correlation Systems.....	25
3.1 Introduction.....	25
3.2 History of Digital Image Correlation.....	25
3.3 Working Mechanism.....	26
3.4 Advantages of using DIC.....	29
3.5 Disadvantages of DIC .....	30
Chapter Four Specimen Design .....	31
4.1 Adobe Used.....	31
4.2 MOR Specimens .....	31
4.3 Wall Test Specimens.....	33
4.4 Prism Specimens.....	35

4.5 Summary of the Specimens .....	36
Chapter Five Modulus of Rupture Test .....	40
5.1 2017 Testing Procedure .....	40
5.1.1 Results.....	46
5.2 2018 Testing.....	46
5.2.1 Results.....	53
5.3 2019 Testing.....	54
5.3.2 Results.....	58
5.3 Conclusions.....	58
Chapter Six Experimental Testing of Adobe Walls.....	59
6.1 July 2017 Testing.....	59
6.1.2 Discussion .....	66
6.2 January 2018 Testing .....	66
7.2.2 Discussion .....	71
7.3 Summary and Conclusions .....	72
Chapter Seven Compression Testing for Modulus of Elasticity.....	74
7.1 2017 testing.....	74
7.1.1 Results.....	79
7.2 2019 testing.....	80
7.2.1 Result .....	84
8.3 Analysis and Discussion .....	90

Chapter Nine Summary and Conclusions .....	95
9.1 Summary from Wall Tests .....	95
9.2 Summary from Modulus of Rupture Tests .....	96
9.3 Summary from Prism Tests .....	97
9.4 Overall Conclusions.....	97
Future Work.....	99

## List of Tables

Table 2.1 Modulus of elasticity for bricks .....	17
Table 2.2 Modulus of elasticity for houses and walls (Silveria 2012).....	20
Table 4.1. Summary of the specimen along with their specifications .....	37
Table 6.1. Matrix of Wall Test Specimens .....	59
Table 6.2. Summary of Wall tests with maximum load and shear strain at maximum load .....	73
Table 7.1. Summary Results of compression test 2017 .....	79
Table 7.2. Summary of Results of compression test 2019.....	90
Table 7.3. Calculation of Modulus of Elasticity .....	92
Table 7.4. Comparison of Modulus of Elasticity values with Literature Values.....	92
Table 9.1. Summary of MOR test.....	96



## List of Figures

Figure 2.1: Adobe Specimen Tested in Compression.....	13
Figure 2.2. Stress- strain results for brick specimen under uniaxial compression.....	17
(a) Results from global measurements (b) Results from local measurements.....	17
Figure2.3. Wall specimen during testing. ....	18
Figure 2.4. Application of load in the wall .....	18
Figure 2.5. Stress strain curve for House 2 and Wall 2. ....	19
Figure 2.3. schematic representation of DIC .....	27
Figure 2.4. Patterns on the specimen. ....	28
Fig 2.5. DIC calibration procedure .....	29
Figure 4.1. (a) Preparation of adobe mix and (b) Sun dried adobe bricks.....	31
Figure 4.2. MOR specimen (a) before (b) during and (c) after loading.....	32
Figure 4.3. Wall specimen (a) before loading and (b) after loading.....	33
Figure 4.4. Reinforcement Pattern 1.....	35
Figure 4.5. Reinforcement Pattern 2.....	35
Figure 4.6. Prism specimen (a) before (b) during and (c) after loading .....	36
Figure 5.1. Longitudinal strains for specimen 1 and 2 at different loads. ....	42
Figure 5.2. Longitudinal surface strains for MOR specimens 3 and 4 .....	43
Figure 5.3. Longitudinal surface strains for MOR specimens 5B and 5.....	44
Figure 5.4. Longitudinal surface strains for MOR specimens 6 and 7. ....	45
Figure 5.5. Longitudinal strain for specimen 65 and 66.....	47
Figure 5.6. Longitudinal strain for MOR specimen 67 and 68.....	48

Figure 5.7. Longitudinal strains for specimen 69 and 70 .....	49
Figure 5.8. Longitudinal strains for specimen 74 and 75 .....	50
Figure 5.9. longitudinal strain for specimen 71 and 77 .....	51
Figure 5.10. Longitudinal strain for specimen 78 and 80 .....	52
Figure 5.11. Longitudinal strains for sample 81 .....	53
Figure 5.12. Major strain for specimen 202 and 203 .....	55
Figure 5.13. Major strain for specimen 205 and 206, .....	56
Figure 5.14. Longitudinal strain for specimen 207 and 208. ....	57
Figure 5.15. Longitudinal strain for specimen 209 and 210. ....	58
Figure 6.1. Major strain for Wall 1 and 2 .....	61
Figure 6.2. Major strain for Wall 3 and 4 .....	63
Figure 6.3. Major strain for Wall 6 .....	65
Figure 6.3 Major strains for Wall 7 and 8.....	68
Figure 6.5. Load vs. Horizontal displacement for four points shown in Figure for Wall 7. .....	69
Figure 6.7 Load vs. horizontal displacement for four points shown in figure for Wall 8.	70
Figure 6.8. Illustration of dimensions used in equation (1).....	71
Figure 6.9 Load vs shear strain for all walls.....	72
Figure 6.10. Load Vs Shear Strain.....	72
Figure 7.1. Cube specimens showing top and bottom five points .....	74
Figure 7.2. Stress vs. stress plots for specimen 1.....	75
Figure 7.3. Stress vs. stress plots for specimen 2.....	76
Figure 7.4. Stress vs. stress plots for specimen 3.....	76

Figure 7.5. Stress vs. stress plots for specimen 4.....	77
Figure 7.6. Stress vs. stress plots for specimen 5.....	77
Figure 7.7. Major strains for specimen at particular loads. ....	79
Figure 7.8.Stress vs. stress plots for specimen 6.....	80
Figure 7.9. Stress vs. stress plots for specimen 7.....	80
Figure 7.10. Stress vs. stress plots for specimen 8.....	81
Figure 7.11.: Stress vs. stress plots for specimen 9 .....	81
Figure 7.13. Stress vs. stress plots for specimen 11.....	82
Figure 7.14. Stress vs. stress plots for specimen 12.....	83
Figure 7.15. Stress vs. stress plots for specimen 13.....	83
Figure 7.16. Stress vs. stress plots for specimen 14.....	84
Figure 7.17: Stress vs. stress plots for specimen .....	84
Figure 7.18. Major strains for specimen at particular given loading condition.....	88
Figure 7.19. Major strains for different loads for specimen 6. ....	89
Figure 7.20. Graph showing $E_2$ , $E_3$ , $E_4$ , $E_5$ .....	91

## Abstract

### EXPERIMENTAL TESTING OF ADOBE STRUCTURES WITH DIGITAL IMAGE CORRELATION

Ashmita Wasti

Thesis Chair: Michael McGinnis, Ph.D.

The University of Texas at Tyler  
May 2018

Adobe brick (or Mudbrick) is commonly used as a construction material for residential structures in the Southwest portion of the United States. Adobe bricks are formed from mud that is composed of sand, silt, clay and water that is further mixed with straw then allowed to dry in the open environment. The straw aids in providing reinforcement for the brick and helping the brick dry more evenly which in turn reduces the amount of shrinkage cracks. The final product is a strong, durable, heavy brick used in the construction of homes. While this practice of adobe brick construction has been around for centuries there is still a lot of unknowns regarding the mechanical properties of the bricks particularly at different material compositions, reinforcement levels and moisture contents. This research investigates the material properties of adobe through traditional material and structural testing and through the use of digital image correlation to measure surface strains of the test specimens. Three types of testing were completed: material tests measuring the compressive strength of brick prisms, material tests measuring the bending strength of small modulus of rupture specimens, and structural tests

measuring the in-plane lateral load capacity of one quarter scale walls. In 3-D DIC, the measured object is photographed with a pair of digital cameras before, during and after a load event, and a stochastic pattern marked on the object is tracked from one set of images to the next such that a full field of displacements is derived. Major findings were:

- DIC was a valuable tool for measuring displacements and strains in adobe materials and structures.
- DIC was able to allow visualization of adobe material failure modes and failure progression.
- Fibers within adobe bricks allowed the material to reach large deformations prior to complete collapse.
- This was the first study to use DIC on multiple faces of compression specimens to measure deformations in order to determine Modulus of Elasticity (E).
- The value for Modulus of Elasticity for the adobe used in this project was between 39,000 and 51,000 psi, depending on the method of calculation.

## Chapter One

### Introduction

This study focuses on the investigation of the mechanical properties of adobe at varying moisture condition and reinforcement levels. This research investigates the material properties of adobe through traditional material and structural testing and through the use of digital image correlation to measure surface strains of the test specimens. Three types of testing were completed: material tests measuring the compressive strength of brick prisms, material tests measuring the bending strength of small modulus of rupture specimens, and structural tests measuring the in-plane lateral load capacity of one quarter scale walls. This chapter is further categorized into the following sections: (1) Problem Statement, (2) Research Relationship, (3) Research Objectives, (4) Research Significance and Scope, (5) Methodology, (6) Summary of the Thesis, and (7) Organization of the Thesis.

#### **1.1 Problem Statement**

Adobe construction is popular in the Southwest part of United States. The history of adobe construction can be traced back to the nineteenth century. Adobe is a common building material which is easily and cheaply available, doesn't require skilled manpower for construction, and is environmentally friendly (Silveira, 2012). Good thermal and sound insulation properties along with ease of repair and maintenance makes adobe popular. However, adobe has low compressive strength compared to traditional building materials like timber and concrete and has poor durability as it is affected by climatic conditions such as heavy rainfall, erosion, and groundwater. Frequent contact of adobe with water leads to the absorption of water

which results in swelling and on drying leads to shrinkage. Thus, it is necessary to understand the behavior of adobe with varying moisture contents and improve its properties so that it can better serve a useful purpose.

This thesis focuses on studying the mechanical behavior of adobe at different moisture contents and with different reinforcing materials. Digital Image Correlation (DIC) was used to capture the strains and displacements on the surface of adobe specimens to characterize their structural performance. Small-scale beams and prisms were used to determine the elastic modulus and modulus of rupture of the material. Quarter scale wall specimens were tested under lateral loading with realistic boundary conditions. Characterization of this building material was able to be completed as a result of the testing outlined in this thesis.

## **1.2 Research Relationship**

This research was completed in partnership between The University of Texas at Tyler (UT Tyler) and New Mexico State University (NMSU). NMSU is one of four university partners in the Engineering Research Center for Bio-mediated and Bio-inspired Geotechnics (CBBG) funded by the National Science Foundation (started in 2015). **Dr. Paola Bandini** is the campus principal investigator of the grant for NMSU and leads the *Infrastructure Construction Thrust* for the Center. The material presented herein is based upon work supported in part by the National Science Foundation (NSF) under NSF CA No. EEC-1449501. This material is based upon work supported in part by the National Science Foundation (NSF) under NSF CA No. EEC-1449501. Any opinions, findings and conclusions or

recommendations expressed in this material are those of the authors and do not necessarily reflect those of NSF.

### **1.3 Research Objectives**

Adobe is a cheaply available naturally occurring material, which is one of the reasons for its popularity. Construction using adobe is easy and of low-cost. In addition, it has good thermal and acoustic properties. Apart from its advantages, adobe shows poor resistance to moisture (absorption) making it vulnerable during heavy rainfall and ground water conditions. Adobe construction is not safe in places susceptible to erosion and high moisture. Therefore, it is necessary to find ways to improve the strength of adobe at different moisture contents.

Few have studied the use of DIC on adobe. The main objective of this research is

- To investigate whether DIC can be used to capture displacements and strains of adobe surfaces.
- To study the applicability of DIC to capture and provide insight on adobe material and structural behavior.
- To study and document material properties of adobe such as Modulus of Elasticity and material failure modes using DIC.

### **1.4 Research Significance and Scope**

It is believed that more than 30% of the world population still resides in earthen homes (Qualiarini, 2010). Adobe structures that are not properly designed for lateral loading are highly susceptible to seismic forces and may not be safe to live in. To improve its structural stability, it is important to find ways to increase the strength



of adobe structures. In addition to studying the applicability of DIC on adobe, study of the mechanical properties of adobe and the effects of reinforcing materials on the strength of adobe is also explored.

This research is one of few experiments on adobe using DIC. DIC will be described in detail in Chapter Three of this thesis. This thesis explores behavior of adobe consisting of different moisture content and reinforcement materials under various loading conditions while being monitored by DIC systems.

Some specific tasks achieved by this thesis are described below:

- Using DIC and load data, analyze the compressive behavior of adobe prisms (cubes) with different moisture and reinforcement levels to determine the Elastic Modulus and failure mode of the material
- Analyze the behavior of adobe at different moisture and reinforcement levels under 3-point bending using DIC to monitor initiation of cracking and crack growth.
- Monitor laboratory scale walls made from adobe under lateral loading to determine their failure mechanisms and load deformation response at different moisture and reinforcement levels using DIC

### **1.5 Construction of adobe specimens**

The center for Bio-meditated and Bio-inspired Geotechnics (CBBG) at New Mexico State University was responsible for construction of the three types of specimens used in this work. Compression prisms were three bricks tall with each brick approximately 2 inches high. Modulus of Rupture specimens were

approximately 16 in. \* 4 in. \* 4 in. The walls were quarter scale with final dimensions 5ft \* 2.5ft \*2.5 ft. Variables in the testing (described in individual chapters) included moisture content and fiber type, fiber length and percentage of fiber content. This thesis primarily focuses on the behavior of the adobe specimens as captured by DIC. For traditional measurements and methods not described herein, readers are directed to the center for Bio-Meditated and Bio-Inspired Geotechnics (CBBG). (Davila, 2019).

## **1.6 3D-DIC**

Three-Dimensional Digital Image Correlation (3D-DIC) is an image processing technique that uses a distinct pattern on the surface of an object where the cameras track the movement of that pattern. As the pattern moves software is able to calculate displacements in and out of plane then correlate those displacements to strains. Due to this method being non-contact, it is easier to setup and, in many cases, use compared to traditional instrumentation methods. In this project, three different types of camera system, 2M, Hi-spec and IL5 systems were used. As explained earlier this is one of the first experiments using DIC on adobe.

## **1.7 Organization of Thesis**

The remaining sections of this thesis are organized as follows:  
Chapter 2- Background: In this chapter a short description of adobe including its properties is provided. In addition, previous research with adobe from other researchers is discussed in brief. This chapter also gives a short description of DIC and some other areas research areas where DIC has been used.

Chapter 3- DIC: This chapter gives a detail information about the Digital Image Correlation Technology (DIC), which is used for analysis in the current studies. This section gives the history related to DIC, its working mechanism, limitations of the method and some of the previous applications of this method not only in engineering but also in biomedical studies and geotechnical studies.

Chapter 4 – Specimen Design: The specimens used in the experiment are made from adobe with varying levels of reinforcement and moisture content. This chapter provides a general description of the type of adobe used. It gives detailed description of the adobe specimens used for the wall tests, MOR tests and prism tests.

Chapter 5- Modulus of Rupture Test: This chapter explains the three point bending tests performed on adobe beam specimens and the findings of these experiments.

Chapter 6- Wall Tests: This chapter describes the testing procedure, analysis and the outcomes for the wall test. Five wall tests were performed in January 2017 and two additional in July 2018.

Chapter 7- Modulus of Elasticity Test: Multiple adobe prisms (cubes) were constructed and tested in March 2019 and 2017. This chapter describes the basic testing procedure used in the experiment, how the analysis was done, and the results for the individual tests performed.

Chapter 8 – DIC lessons learned: This chapter includes the lessons learned from DIC. Factors that need to be considered while using DIC on adobe are explained.

Chapter 9 – Summary and Conclusions: A summary of the research program and its major findings is presented in this section.

Chapter 10- Future Work: Tasks that need to be performed to further understand adobe behavior are recommended in this section.

## Chapter Two

### Background

The word “adobe” is derived from Arabic word “al-tob” which means “the brick”. Adobe construction has been popular for many years. The oldest structure on the earth is made of adobe which can be dated back to 8000 BC. It is locally available, low cost, recyclable and possess good thermal properties. (Smith, 1982) Adobe can be produced manually or mechanically. During the production of adobe, strengthening materials like straw or sisal fibers are generally added which helps the adobe to dry out evenly and prevents cracking. However, over time the use of adobe in construction has decreased. Analysis have been done with the work in this thesis using DIC to study the behavior of adobe structures.

#### **2.1 Classification of adobe**

Adobe bricks can be classified into six different types (Smith, 1982) as described below:

1. Traditional bricks: Traditionally adobe brick is composed of sand, silt and clay. Straw was added to provide additional strength to the brick. Straw provides reinforcement to the brick and reduces shrinkage during drying. During the construction, mud mortar was added between the two bricks creating a strong bond. To prevent erosion from water, plaster or cement stucco can be spread on the wall annually.
2. Semi-stabilized adobe bricks: Such bricks are constructed in similar manner as traditional brick, except in this brick stabilizers like Portland cement or

- bituminous emulsion or asphaltic emulsion are added during the construction process so that the bricks obtained are partially water resistant. Such bricks cannot resist heavy rainfall.
3. Stabilized brick: Such bricks contain enough admixtures to make the brick water resistant. No exterior protection like plaster or cement stucco is required for this kind of brick.
  4. Terron: Such bricks are generally made from turf or cut sod and its use is similar to traditional bricks.
  5. Pressed adobe: Bricks obtained from pressing the stabilized or traditional adobe materials with the use of hydraulic machine are known as pressed adobe bricks. Such bricks possess high tensile and compressive strengths. Stabilizer should be added in such bricks otherwise they disintegrate when in contact with water.
  6. Burnt adobe bricks: Such bricks usually take a little more time for manufacturing than traditional bricks. They are generally cured in low temperature firing.

## **2.3 Experiments Performed on Adobe**

In this section, experiments done on adobe structures to study their behavioral properties is explained. Also, studies done to understand the impact of adding fibers or chemicals are explained in brief.

### **2.3.1 Study of Mechanical Properties of Adobe Bricks in Ancient Construction**

(Silveira, 2012) presented a paper which investigated the mechanical properties of the adobe bricks. The adobe brick samples were taken from an existing structure in Aveiro, Portugal. The adobe bricks were collected from houses and land dividing walls. Compression tests and splitting tests were performed on cylindrical specimens. A uniform load was applied and increased continuously until the specimen failed. The result showed that the tensile strength for the land dividing walls were larger than the houses whereas the compressive strength and modulus of elasticity were higher for houses than the land dividing walls. The lateral forces that are generated during an earthquake generate bending stress on the wall. Since the tensile strength of the wall is known to be negligible it is not able to withstand seismic loads. It can be concluded that seismic safety was not given much concern during the construction of adobe buildings and no reinforcement on adobe was found due to which the structure failed to withstand the seismic actions.

### **2.3.2 Seismic Strength of Adobe Masonry**

(Vargas, 1986) conducted a study to understand the seismic strength of adobe structures and also the effect of additives in adobe structures. For this, soil samples from six different zones of Peru were selected. In order to maintain the uniformity in the test results, the sample specimens were prepared in a soil mixer and by the same technician. During the construction of the adobe bricks, the specimens were dried in the shade to prevent cracking due to drying. A Diagonal Compression Test was conducted to determine the seismic strength of the adobe masonry. The results suggested that the strength of adobe structures is highly dependent on the degree of micro cracking of soil mortar due to drying shrinkage. The adobe structures made

with soil of high clay content had less strength. Also, the bricks had higher strength which were dried in the shade than those which were dried in the sun.

Similarly, some additives like cement (amount larger than 10%) and sand, sodium carbonate, manure (in small content) helped to increase the compressive strength of the adobe bricks whereas addition of lime, manure (in larger content) decreased the strength. It was also noticed that construction done from the adobe bricks after one week of their manufacturing had higher strength. Moreover, using straw as additives increased the strength of the adobe masonry. However, simultaneous addition of sand and straw did not improve the strength of the adobe masonry. Before placing, it is suggested to wet the bricks to increase the strength of the construction.

### **2.3.3 Influence of Natural Stabilizers and Natural Fibers on the Mechanical Properties of adobe Bricks**

Adobe has low compressive strength and energy absorption capacity and adobe alone cannot withstand high loads and seismic forces. It is important to improve the properties of adobe by adding natural fibers or stabilizers which ultimately can withstand higher loads.

(Qualiarini, 2010) published a paper which explains how the mechanical properties of Roman ancient adobe bricks changes by varying the content of straw and coarse sand into the mixture to produce them. Compression tests were performed on 80 samples where straw was added as reinforcement and coarse sand as natural stabilizer. The result suggested excessive increase in the coarse sand make the compressive strength worse if the straw content is low whereas if the addition of



coarse sand is limited, straw does not have significant effect on compressive strength.

(Lutfullah turanli, 2010) studied the use of additives and plaster mesh in adobe wall panels. Diagonal Compressive Axial Load Tests were performed in order to determine the load capacity. The result concluded that plaster mesh provides increased strength and energy absorption capacity increasing the friction along the weak horizontal joint in adobe wall.

(Quintilio Piattoni, 2011) studied the mechanical properties of earthen bricks using theoretical and experimental approach. A total of 70 bricks were molded and compacted manually. For the reinforcement, short straw and coarse sand was added. External features like cracks on the surface of the material and lack of material was noted visually. Hydraulic press was used for the compression test. Compressive force and vertical displacement were recorded for each test. Displacement was measured with the aid of a transducer which was attached to the lower platen in order to compensate for the irregularity of the sample and to reduce the friction between the plates and the sample. Water content was also calculated for the sample at the end of each test. Out of all of the specimens, compression test was performed on 20 specimens. Two tests were conducted for each of the different compositions. The result showed that the lowest compressive strength is for the samples that had high coarse sand and low straw content which suggests that addition of straw fibers doesn't have much influence on the strength on the bricks if the sand content is limited. The high content of sand determines high value of Young's modulus. The test also concluded that as the aspect ratio increases, compressive strength decreases.

#### **2.2.4 Determination of Bending Strength Using Three-Point Test**

(C. Galan-Marin, 2010) studied the behavior of clay-based soil stabilized with alginate (a natural polymer from brown cells of algae) and reinforced with raw unprocessed sheep's wool. Specimen preparation was done under Spanish-European standards. Three-point bending test was performed to determine the bending strength of the specimen as shown in Figure 2.1.



*Figure 2.1: Adobe Specimen Tested in Compression*

Stress-strain curves for flexural tests and compressive tests were derived. The graph for stress-strain curve shows that for soil with no addition of fibers, the specimen fails immediately after the ultimate load. However, if the soil has fibers, then this process is little smooth. The results showed that the addition of stabilizer as alginate and wool as a reinforcing material was successful in increasing the compressive strength of the soil specimen.

#### **2.3.5 Micromechanical assessment of adobe masonry assemblages based on experimental data sets**

(Caporale, 2015) conducted an experiment which measured the strength and elastic moduli of adobe bricks. Compression and tensile strength tests were done to calculate the mechanical properties of adobe masonry. Experimental data analysis based on the mechanical properties for the adobe bricks were collected from a large experimental database which was developed by Augenti. A data analysis was performed using the database for most of the mechanical properties of adobe bricks. Correlations between tensile, compressive and Young's Modulus were derived using robust regression analysis. However, micromechanical analysis was given a key emphasis for the study. The scope of the study was to derive a critical curve so that critical stresses could be identified. It was also used to calculate principle stresses and to define the mechanical behavior of masonry walls based on the properties of bricks. The use of mortar during the construction of the masonry was also a focus of study because the failure of the interface between them was also a concern. The use of regression analysis on the large number of data present gave equation which predicted mechanical properties of adobe brick masonry with good  $R^2$  values.

### **2.3.6 Adobe Bricks Under Compression: Experimental Investigation and Derivation of Stress–Strain Equation**

(Illampas C. I., 2014) conducted a study where adobe bricks with various samples were used for testing. The samples used had straw fibers (2-30mm) in length and chinks and marls (4-35mm) in diameter. The specimen was cut dry from adobe bricks and were placed for uniaxial compression test. A stress rate of 0.1 megapascals per second was applied until failure. In all tests, deformations were measured from the relative displacement of the machines' loading platens. This

tends to overestimate true strains; however, the texture and size of the specimens did not allow the application of strain gauges or other strain measuring devices. DIC was used in the current study to solve this issue. Compression failure of the cubes were characterized by bulging of the specimen with vertical cracks. The specimen did not fail instantly but developed deformation before it failed. Straw fibers held the material together and delayed ultimate failure.

At early stages of testing consolidation starts to occur. The void spaces present in the specimen are filled by the soil particles until a steady state is reached. After reaching the steady state, in the second stage of testing the deformation tends to increase linearly until the maximum stress level is reached. After the maximum stress is reached the specimen go through compression softening up to the ultimate strain is obtained.

#### **2.4 In-plane behavior and retrofitting method of mud-brick walls**

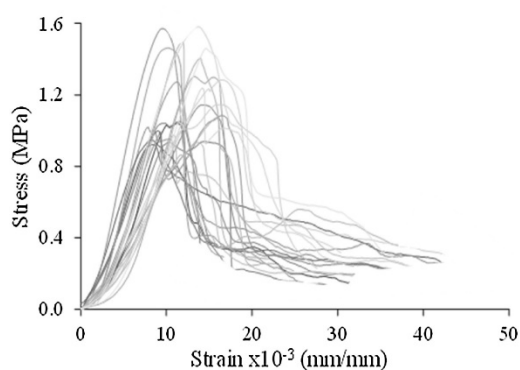
(F. Tootoonchy, 2015) studied the in-plane behavior of scaled adobe walls at different levels of vertical loads. After identifying the damage mechanism, proper retrofitting method was suggested. During test, walls were laterally loaded by hydraulic jack. LVTDs were installed on the wall to study the deformation on the wall. For each test, behavior of walls were measured in terms of lateral load displacement. The result shows brittle failure of the walls as a result of applying high vertical loads. Also, energy absorption and ductility of wall is increased by the application of tarpaulin belts and polypropylene lace together. (Fulvio Parisi, 2015)

## 2.5 Study of shear strength of adobe clay bricks using DIC

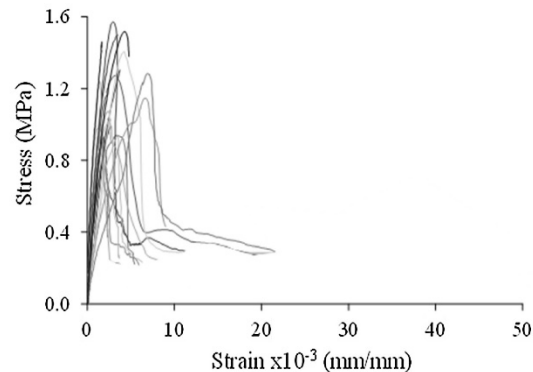
(Kabir, 2018) studied the shear strength of adobe clay brick of three different mixes at constant fiber volume, moisture content and soil type. Straw and Nylon were two types of fibers used. Comparison in the behavior of adobe with fibers and without fibers were performed using 2D- Digital Image Correlation (DIC). Tire fiber had positive effect on the strength of adobe and the plastic behaviors of the straw fiber reinforced specimen was higher than the other.

## 2.6 Determination of Modulus of Elasticity

(Aguilar, 2017) performed three point bending test, uniaxial compression test and splitting test in prismatic brick specimen to study the behavior of earthen structures in Peru. Localized deformation of the specimens was carried out with Digital Image Correlation (DIC). Prismatic specimens of different size for different tests were designed. Strains labeled global deformation were obtained from displacement measurements of the load cell. Strains labeled local deformation were obtained from DIC measurements of the middle third of compressive specimens. These strains are shown in Figure 2.2 (a) and (b).



(a)



(b)

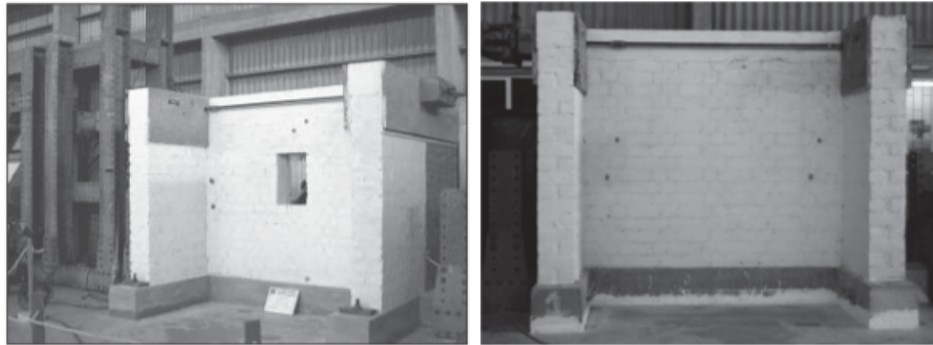
Figure 2.2. Stress- strain results for brick specimen under uniaxial compression  
 (a) Results from global measurements (b) Results from local measurements

*Table 2.1 Modulus of elasticity for bricks*

<i>Material</i>	$f_c$	$E_{local}$	$E_{global}$
	<i>(psi)</i>	<i>(psi)</i>	<i>(psi)</i>
Brick	Average	24366	116,172
		21,320	

From table 2.1,  $E_{global}$  corresponds to the secant elasticity modulus calculated considering 30% $f_c$ -60% $f_c$ .  $E_{local}$  corresponds to secant modulus of elasticity considering 0-33% of  $f_c$ . The average value for  $E_{local}$  obtained is approximately six times higher than from global deformation. This showed the importance of using DIC to measure deformations. The  $E_{global}$  values were heavily influenced by deformation of the testing apparatus as opposed to the DIC measurements ( $E_{local}$ ) which only include material deformation. Finally, the DIC measurements of this study were performed on only one face of the specimen. Any out of plane distortion of the specimens (as for example with the measured face in higher compression than the obscured, unmeasured face) could heavily influence the calculated  $E_{local}$  values and could not be captured.

(Blondet, 1978) , performed experiment on three I-shaped adobe walls which were similar in size. One wall had a window opening and other two did not as shown in figure2.3 (a) and (b) respectively. All of the three walls were not reinforced.



(a) with window opening  
(Blondet, 1978)

(b) without window opening  
(Blondet, 1978)

*Figure 2.3. Wall specimen during testing.*



*Figure 2.4. Application of load in the wall*  
(Blondet, 1978)

The wall was loaded horizontally from the top corner with the aid of hydraulic actuator as shown in Figure 2.4. Horizontal cracks appear at the bottom of the wall while diagonal cracks appear from both direction of the wall. The walls without windows were stiff initially than the walls with windows. From the cyclic test, the modulus of elasticity for full scale adobe walls was suggested to be 29,000 psi to 32,000 psi.

(Silveira, 2012) investigated the brick specimens obtained from land dividing walls and houses. Compression tests and splitting tests were performed in cylindrical

adobe specimens. The specimen was loaded until failure, with the measurements as shown in Figure 2.5.

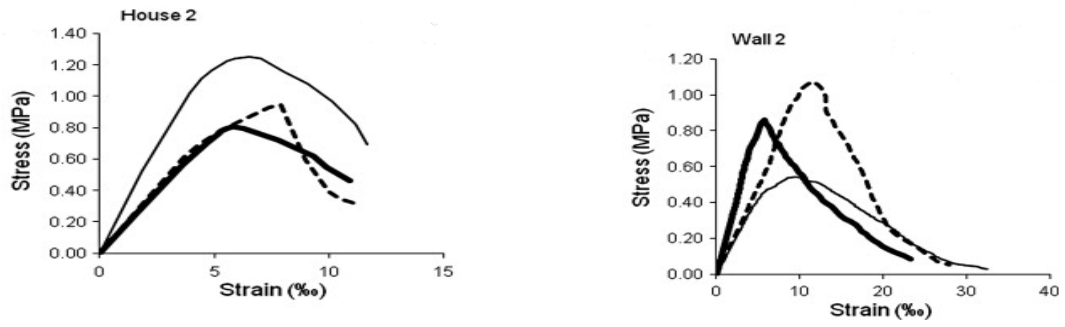


Figure 2.5. Stress strain curve for House 2 and Wall 2.  
(Silveria 2012)



*Table 2.2 Modulus of elasticity for houses and walls (Silveria 2012)*

<i>Specimen from</i>	<i>Modulus of elasticity (MPa)</i>	<i>Specimen from</i>	<i>Modulus of elasticity (MPa)</i>
H1	273	W1	138
H2	203	W2	117
H3	97	W4	200
H4	51	W5	340
H5	448	W6	209
H9	87	W7	94
H10	334	W9	114
H11	143	W10	127

The Modulus of elasticity obtained from stress-strain curves ranges between 51 MPa (approx. 7,400 psi) to 448 MPa (approx. 65,000 psi) for specimens taken from houses whereas for the specimen taken from land dividing walls, values ranges in between 94 MPa (approx. 13,600 psi) to 340 MPa (approx. 49,300 psi). The correlation between modulus of elasticity and compressive strength was also studied and result shows

$$E=181 f_c \text{ for houses}$$

$$E= 163 f_c \text{ for land dividing walls, where } f_c= \text{ compressive strength.}$$

## **2.7 Repair of Adobe Building by Clay-Based Grout Injection**

Grouts are generally added to the voids or cracks which when filled hardens and provides adhesion between the materials permitting the stress transfer. Grout

injection is an easy and cost-effective method of repair. (Illampas L. C., 2017) studied the effectiveness of injecting clay-based grout in cracks occurred in adobe wall due to series of lateral load cycles. At first, adobe wall was subjected to ten lateral loading and unloading cycles. After the loading, damage was observed in the form of diagonal shear crack from the corner, horizontal cracks, bending of wall. For the repair of the damage, clay -based grout (made from the same soil from which the adobe bricks were made) mixed with limestone powder was injected in the cracks. The result suggests that clay based grouting injection was successful in reestablishing the structural stability of adobe structures. This practice seems to be an easy and cost-effective means of strengthening adobe structures.

## **2.8 Digital Image Correlation (DIC) Technology in Civil Engineering**

Various technologies have been discovered for the measurement of strain and displacement. Of the many technologies available today, Digital Image Correlation (DIC) is gaining popularity specially in the field of mechanics. It is also popularly known as a contactless technique, which provides useful solutions to aggressive, hot, corrosive environments. Three Dimensional (3D) DIC uses a set of images to calculate the displacements. In DIC, the measured object is photographed with a pair of digital cameras before, during and after a load event, and a stochastic pattern marked on the object is tracked from one set of images to the next such that full field displacements are derived. Apart from engineering, DIC is also used in medical field. Some examples showing the uses of DIC are provided in this section.

### **2.8.1 Measurement of Crack Opening**

(Lees, 2017) used DIC to measure the crack opening displacement in reinforced concrete structures. The test consists of two series of reinforced concrete beams. The first series consists of seven beams having the same dimensions and subjected to the same loading condition. They differ with each other in reinforcement ratios, concrete strength, concrete covers and reinforcement surface profiles. Three-point bend test was performed on the beams. DIC setup included a single digital lens reflex camera (DSLR) of high resolution. Light was properly adjusted so that the obtained images are clear. The images thus obtained was analyzed using Geo PIV software. The images were taken for each test under different loading condition. The crack mouth opening displacement (CMOD) values for the tested specimens were determined from the displacement vectors of the DIC analysis results. The result show that concrete strength does not have much influence on the crack opening.

### **2.8.2 DIC in Biomechanics**

DIC has found its application not only in engineering but also in biomedical. It is very difficult to obtain precise data on tissues, bones, ligaments. In order to obtain precise data, the specimen to be tested should be left undamaged by the testing procedure. DIC provides a useful solution to these kind of problems as it is non-contact technique. (Tyson, 2010) conducted an experiment using DIC in ligament joints. (Pablo de Heras Ciechowski, 2012) conducted an experiment using DIC and concluded that this technology has potential in other medical applications also such as surgery or facial malformations, aesthetic facial procedures and more.

### **2.8.3 DIC Applications at The University of Texas at Tyler**

McGinnis (McGinnis M. J., 2005) has been prolific in applying DIC to study various structural materials and systems. His research group has applied DIC to glass windows (McGinnis M. J., 2009), Concrete beams (McGinnis M. J., 2015), Walls and slabs (McGinnis M. J., 2013), Ultra High-Performance Concrete beams and bridges (Manning, 2016), Rammed earth and adobe (McGinnis M. J., 2012). They have shown the applicability of DIC in characterizing and visualizing structural behavior across a broad range of materials, a wide variety of loading scenarios (static, dynamic, earthquake, fire, etc.) , and in lab, field and in-situ environments (McGinnis M. J., 2015).

### **2.8.4 Study of Geomaterials**

DIC has various applications in the area of geotechnical engineering as well. (Aydilek, 2002) used DIC to determine the pore structure parameters of the geotextile filters. The images of the geotextiles were captured using monochrome

cameras and the images were analyzed by using codes developed in LabView. Further, strain distribution in geosynthetics was also defined.

DIC was used to study the mechanical properties of soil. (Bergliv, 2016) conducted a laboratory experiment which shows that it is possible to measure degradation in standardized degradation test using two dimensional (2D) DIC. (Rodriguez, 2012) used image analysis to study the particle shape classification for coarse-grained soils.

## Chapter Three

### Digital Image Correlation Systems

#### **3.1 Introduction**

In mechanics, various devices and instruments are used for the measurement of displacement and strain. The strain gauge was popular for measuring strain but in the beginning of 1980s, a new technology came to light known as Digital Image Technology or commonly known as DIC. This is an image technology which uses cameras to track the movement of a pattern on the surface of an object as that object is being loaded. This is a non-contact and non-destructive technique used in various engineering applications, like measurement of displacements and strains, finite element verification, structural analysis and many more. It works on the combination of image correlation technique with triangulation principle.

This section presents a brief description of (1) History related to DIC, (2) Working mechanism (how it works), (3) The limitations of DIC, and (4) Previous applications of the technology.

#### **3.2 History of Digital Image Correlation**

Digital Image Correlation (DIC) is a non-contact technique which provides useful solutions to aggressive, hot, corrosive environments. DIC was proposed at the beginning of 1980s. It is an image-based technology which uses digital images for calculating displacements and strains. The basic principle behind this technology is called photogrammetry.

With the development in photographic methods, photogrammetry has developed into four major phases (Sutton et al., 2009): (1) plane photogrammetry

(1850-1900), (2) analog photogrammetry (1900-1950), (3) analytical photogrammetry (1950-1985) and (4) digital photogrammetry (1985-present). Among them digital photogrammetry is being directly used however the three other phases had great contributions in mathematical development.

The beginning of digital imaging can be traced back to 1950s where Hobrough correlated high-resolution reconnaissance photography with high precision survey photography to obtain more detailed information of ground condition. Digitized images became more popular after the 1960s. Analyzing the digital images and extracting the measurement data from those images became much easier as various methods and approaches were developed after 1970s. 2D DIC was the first progression from photogrammetry principles to correlation systems. It has proved to be successful in measuring the surface deformation of materials subjected to various loadings (mechanical, thermal or any other). Mechanical properties of the material such as Young's Modulus, thermal expansion coefficient, and Poisson's ratio can also be identified using 2D-DIC along with load data provided from an external source. Along with the method comes its limitations. Measurement of deformation of material with curved surface is not possible with 2D-DIC. This method is limited to in-plane measurement only. To overcome this limitation 2D-DIC was advanced to 3D-DIC which is more practical and effective as it can be used for 3D profile and measuring the deformation of both planar and curved surfaces.

### **3.3 Working Mechanism**

DIC is an image technology, which uses digital images from a camera system. This is a non-contact and non-destructive technique that has found its way

in various engineering applications. Most commonly it measures displacements that can then be converted into strains. DIC is also useful in verification of finite element models, and analysis of structures. It works on the combination of image correlation technique with triangulation principle. Figure 2 shows a schematic representation of DIC system.



*Figure 2.3. schematic representation of DIC*

In 3D-DIC, two cameras are mounted on the bar such that the distance between these two cameras is known. The cameras are fixed and the working distance between the cameras is constant throughout the process. The distance between the object and the cameras is based on triangulation principle. The camera captures the images of the specimen which contains number of patterns. Generally, spray paint or permanent marker is used to make the patterns. The patterns on the specimen should be such that each of them should be uniquely identified. Figure 2.4 shows a sample with patterns used during DIC technique. The imaging area is



divided into number of small facets, size of the facets is usually 5-10-pixel square. The center of each facet acts as a measurement point. These facets are tracked in each successive image with sub-pixel accuracy. (Schmidt, 2003) 3D coordinates of the specimen to be tested are computed using photogrammetry principle from which displacements and corresponding strains of the specimen can be calculated. As long as the object remain in the field of view of the cameras, deformations can be measured.

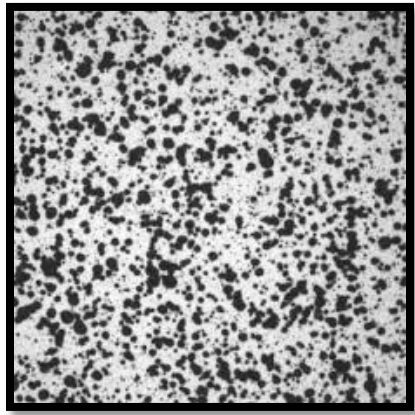


*Figure 2.4. Patterns on the specimen.*

The quality of measurement relies on the calibration process. For the calibration process, calibration panels are photographed from different distances and orientation from the test object as per the instructions shown in the computer system. Figure 2.5 shows calibration process which includes calibration panel, specimen and the cameras. Required number of adjustments are made to establish precise relation between the two digital cameras.

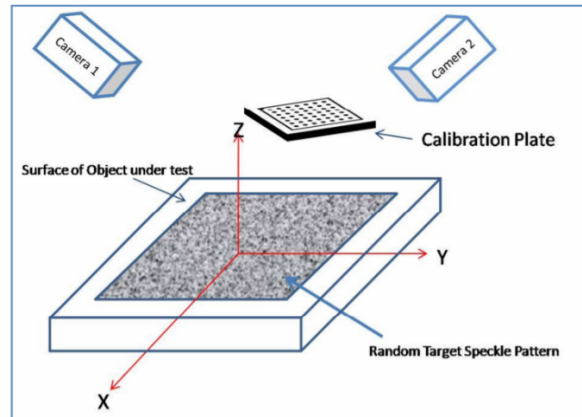


*Fig 2.5. DIC calibration procedure*

Now, the object to be measured is subjected under loading condition. During loading, the pattern deforms along with the object. The two digital cameras mounted on the bar captures the image before, during and after the loading condition and the stochastic pattern marked on the object is tracked from one set of images to the next. Facets of size 15-20 square pixels is defined across the entire imaging area. Tracking the measurement of these facet points, full field displacement can be obtained.

### **3.4 Advantages of using DIC**

As compared to conventional technique, DIC is a non-contact technique which provides accurate measurement of the structures even in the typical outdoor environments.

In most cases, the setup of the DIC is quite simple and easy. DIC has been proven to work in many different fields not just engineering. DIC is cost effective technique that can be cheaply deployed and is accurate. (Fayyad, 2014)

### **3.5 Disadvantages of DIC**

As DIC works on photogrammetry principle, proper lightning is necessary for the test. If the image is dark, then the system will not be able to identify the facets properly and it will be difficult to yield proper results. While using image technology, proper care should be taken that there is no obstruction between the object and the camera such that the obtained image is clear, and details can be studied properly. If the image is unclear, then desired results cannot be obtained. 2D-DIC uses only one camera system and is capable of measuring in-plane displacement only. Even a slight out-of-plane displacement can give measurement errors in collected data. In 3-D, any alteration in the position of camera after calibration results in error of the experiment. In such cases, the whole calibration process should be repeated.

## Chapter Four

### Specimen Design

#### 4.1 Adobe Used

Specimens for Wall tests, MOR tests and prism tests were constructed from naturally occurring soil found in parts of New Mexico which is composed of 74% clay and 26% sand. The mixture as shown in Figure 4.1 (a) was mixed with water and compacted manually in wooden box. The final obtained bricks were sun dried for no less than one week prior to the construction of adobe specimens as shown in Figure 4.2(b). Full scale bricks measure (length x width x thickness) 14 in. (36 cm) x 10 in. (25 cm) x 4 in. (10 cm) and quarter scale bricks measure 3.5 in. (6.4 cm) x 2.5 in. (5.1 cm) x 1 in. (2.5 cm).



(a)

(b)

*Figure 4.1. (a) Preparation of adobe mix and (b) Sun dried adobe bricks*

#### 4.2 MOR Specimens

A 3-point bend test on adobe beams were completed to determine the Modulus of Rupture (MOR) of the material. Each beam was 7.62 cm wide by 13 cm deep and 40.64 cm long (3 in. x 4 in. x 16 in.) and contained different water contents

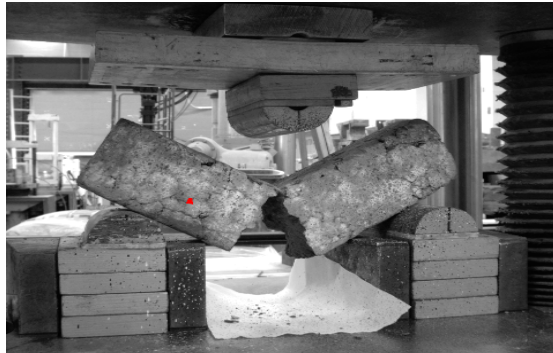
and natural fibers for reinforcement. The beams were constructed and then tested in the Structural Engineering and Materials Laboratory at New Mexico State University (NMSU) using a Tinius Olson axial loading machine. The testing took place in July 2017, January 2018 and March 2019. The beams were patterned with paint to track the surface deformations as a load was applied in the displacement control at the rate of 2.54 mm/min (0.1 in/min). A sample test specimen is shown in Figure 4.2.



(a)



(b)



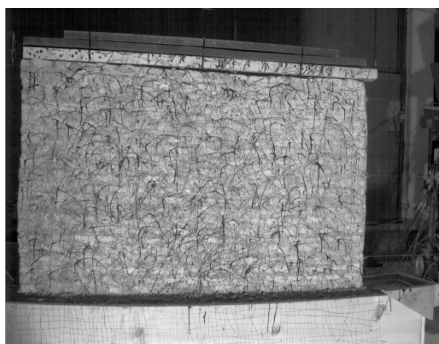
(c)

*Figure 4.2. MOR specimen (a) before (b) during and (c) after loading*

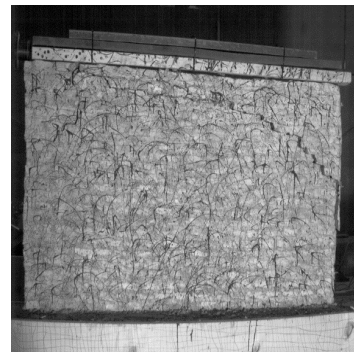
A pair of cameras were positioned on one side of the specimen. The cameras captured a pair of images at a rate of three images per second. The images were processed using 3D DIC to track the surface strains at different loading stages.

### 4.3 Wall Test Specimens

Multiple wall specimens were designed and constructed in the Structural Engineering and Materials Laboratory at New Mexico State University. Each wall was 1.52 m wide by 0.762m tall (5 ft. x 2.5 ft.) and tested under lateral loading from a single point load at the top of the wall. Seven of these wall tests were monitored with DIC. Six walls were to be tested in July 2017, with one wall failing prior to the testing. Two more walls were tested and monitored with DIC in January 2018. Table 4.1 shows the matrix of wall test configurations that were tested. According to Davila (2019), the bricks from these walls were made with straw fibers no greater than 1 inch in length and no more than 2% of the adobe by weight.



(a)



(b)

*Figure 4.3. Wall specimen (a) before loading and (b) after loading.*

Each wall was patterned on the front face for the camera systems to capture the in-plane and out-of-plane movement under an applied lateral load at the top of the wall.

Figure 4.3 shows a typical wall test specimen. Each wall was constructed on an earthen foundation, which was patterned to allow the DIC to capture any movement of the foundation under the lateral wall loading. Two reinforcement patterns were used for the wall test. Jute twine was used as a natural reinforcing material. In Reinforcement pattern 1 as shown in Figure 4.4, jute twines were tied to the foundation bricks of the wall and is placed throughout the height of the wall through the mortar joints. Reinforcement Pattern 2 as shown in Figure 4.5 has two root-like systems with three different jute twine reinforcement chords each. One of the jute twine chord travels vertically through the mortar joints, another chord travels vertically towards the center of the wall and the third one travels out of the wall towards mid-height of the wall. A 2x4 piece of dimension lumber was attached to the top of the wall to allow for better load transfer across the top. Each wall was loaded using a manual hydraulic jack with a load cell sandwiched between the jack and the wall specimen. A pair of images (one image from each of the two cameras) were captured prior to loading of the wall and used as a baseline. Loading was then applied, and images were captured at different loading increments. The images were processed using 3D DIC to obtain displacements and strains of the wall.

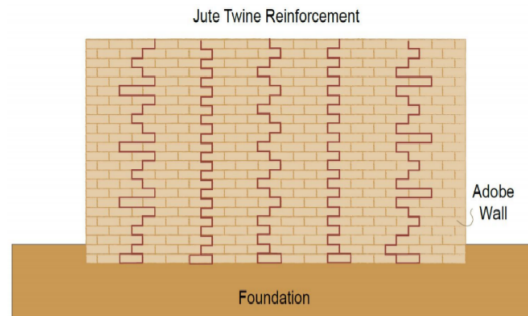


*Figure 4.4. Reinforcement Pattern 1. (Davila 2019)*

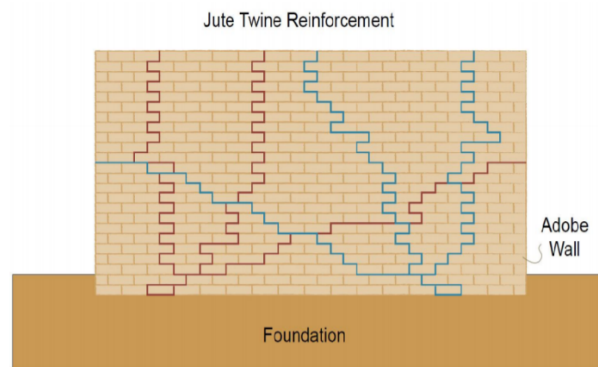


*Figure 4.5. Reinforcement Pattern 2. (Davila, 2019)*

#### **4.4 Prism Specimens**

Prism (cube) specimens were created to determine the elastic modulus of the adobe at different moisture and reinforcement levels. The cubes were 7 in. x 5 in. x 5 in. and loaded in compression until failure. A camera system was placed on two opposite faces of the cube to track the displacements as the specimen was loaded. See Figure 4.6 for a picture of a cube specimen being tested. As the specimen was loaded, the cameras took pictures approximately every 1 second. The displacements from DIC were combined with the load data from the Tinius Olson machine to produce a stress-strain curve.





(a)



(b)



(c)

*Figure 4.6. Prism specimen (a) before (b) during and (c) after loading*

#### **4.5 Summary of the Specimens**

The different types of specimen used for the Wall tests, MOR tests and Prism tests are summarized in Table 4.1 below including the type of moisture content, reinforcement materials and date of test. The index is an additional identifier for each test.

Table 4.1. Summary of the specimen along with their specifications

<i>Index</i>	<i>test</i>	<i>Reinforcement</i>	<i>Moisture content (%)</i>	<i>Fiber length</i>	<i>Fiber %</i>
1	wall	Straw (in bricks) Reinf. Pattern1	3.03%		
2	wall	Straw (in bricks) Reinf. Pattern2	2.80 %		
3	wall	Straw in bricks) Reinf. Pattern 2	3.86%		
4	wall	None	4.26%		
6	wall	Straw (in bricks) Reinf. Pattern 2	4.48%		
7	wall	None	1.77%		
8	wall	Straw (in bricks) Reinf pattern 2	8.55%		
1	MOR	palm	2.6	1.2	0.33
2	MOR	palm	3.1	1.2	0.33
3	MOR	palm	2.6	1.2	0.33
4	MOR	straw	2.6	1.2	0.33
5	MOR	Jute	4.93	1.2	0.33
5B	MOR	Jute	4.93	1.2	0.33
6	MOR	sisal	3.23	1.2	0.33
7	MOR	None	3.14	No	No
65	MOR	None	4.22	No	No

66	MOR	None	4.35	No	No
67	MOR	Straw	4.88	1.22	0.33
68	MOR	Straw	6.9	1.2	0.33
69	MOR	Straw	3.6	1.2	0.33
70	MOR	Sisal	5.21	1.2	0.33
71	MOR	Sisal	3.17	1.2	0.33
72	MOR	Sisal	4.76	1.2	0.33
74	MOR	None	6.33	No	No
75	MOR	None	6.06	No	No
77	MOR	Straw	6.45	1.2	0.33
78	MOR	Straw	6.02	1.2	0.33
80	MOR	sisal		1.2	0.33
81	MOR	sisal		1.2	0.33
202	MOR	None		1.2	0.66
203	MOR	Sisal		1.2	0.66
204	MOR	Sisal		1.2	0.66
205	MOR	Sisal		1.2	0.66
206	MOR	Sisal		2.4	0.33
207	MOR	Sisal		2.4	0.33
208	MOR	Sisal		2.4	0.33
209	MOR	Sisal		2.4	0.66
210	MOR	Sisal		2.4	0.66
211	MOR	Sisal		2.4	0.66

---

1	prism	sisal	4.16	1.2	0.33
2	prism	sisal	6.19	1.2	0.33
3	prism	jute	6.85	1.2	0.33
4	prism	straw	2.96	1.2	0.33
5	prism	palm	3.11	1.2	0.33
6	prism	sisal	3.75	1.2	0.66
7	prism	sisal	4.25	1.2	0.66
8	prism	sisal	4.57	1.2	0.66
9	prism	sisal	9.83	1.2	0.66
10	prism	sisal	6.39	2.4	0.66
11	prism	sisal	6.51	2.4	0.66
12	prism	Palm	7.27	1.2	0.33
13	prism	Palm	7.27	1.2	0.33
14	prism	Sisal	6.07	2.4	0.66
15	prism	Sisal	6.07	2.4	0.66

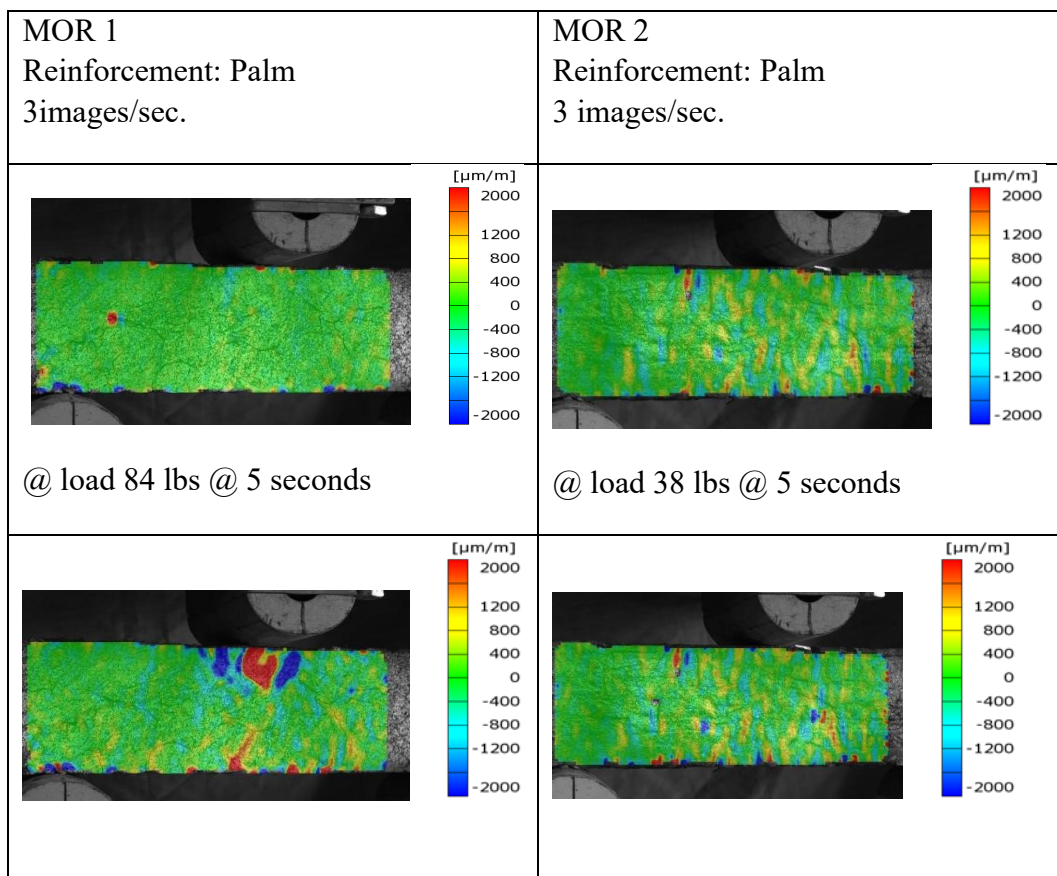
---

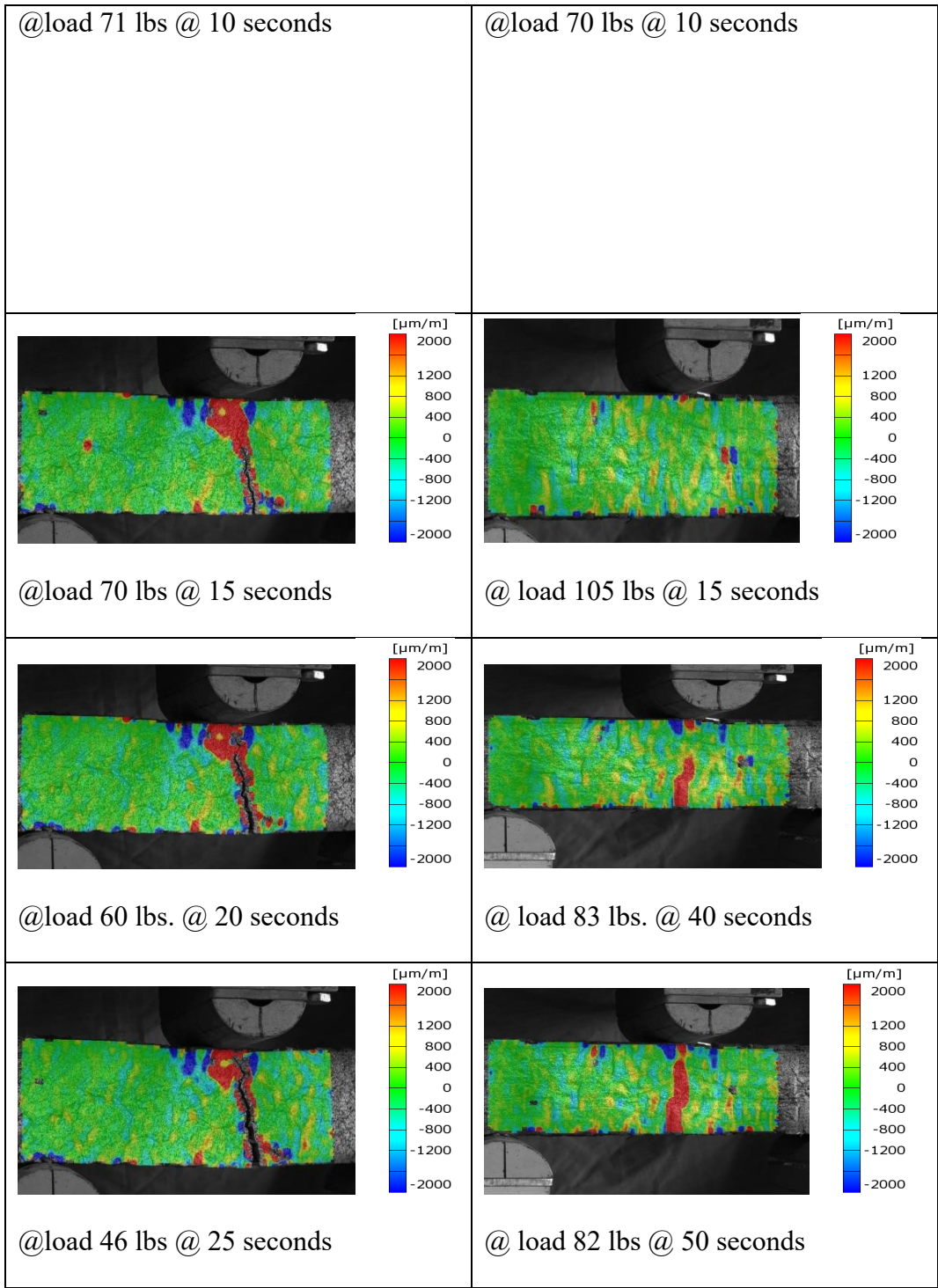
## Chapter Five

### Modulus of Rupture Test

#### 5.1 2017 Testing Procedure

Testing of MOR specimens 1, 2, 3, 4, 5, 5B, 6, and 7 were tested under 3-point loading. The loading was applied at a rate of 2.54 mm/min (0.1 inch/minute). One camera system was used to monitor the surface strains and deformations on the front longitudinal faces of the beams. Images of the surface strains along the longitudinal axis of the beam (x-direction) are shown in Figures 5.1 – 5.4, ARAMIS software was used for the analysis of crack development in the beam sample.





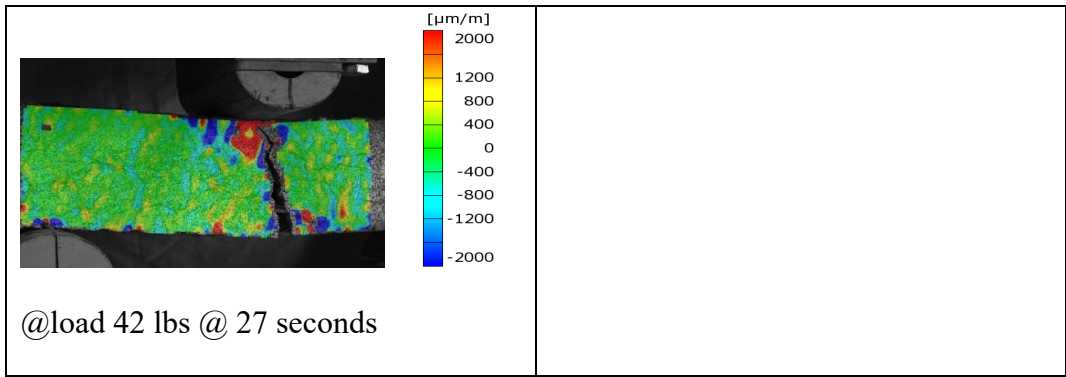


*Figure 5.1. Longitudinal strains for specimen 1 and 2 at different loads.*

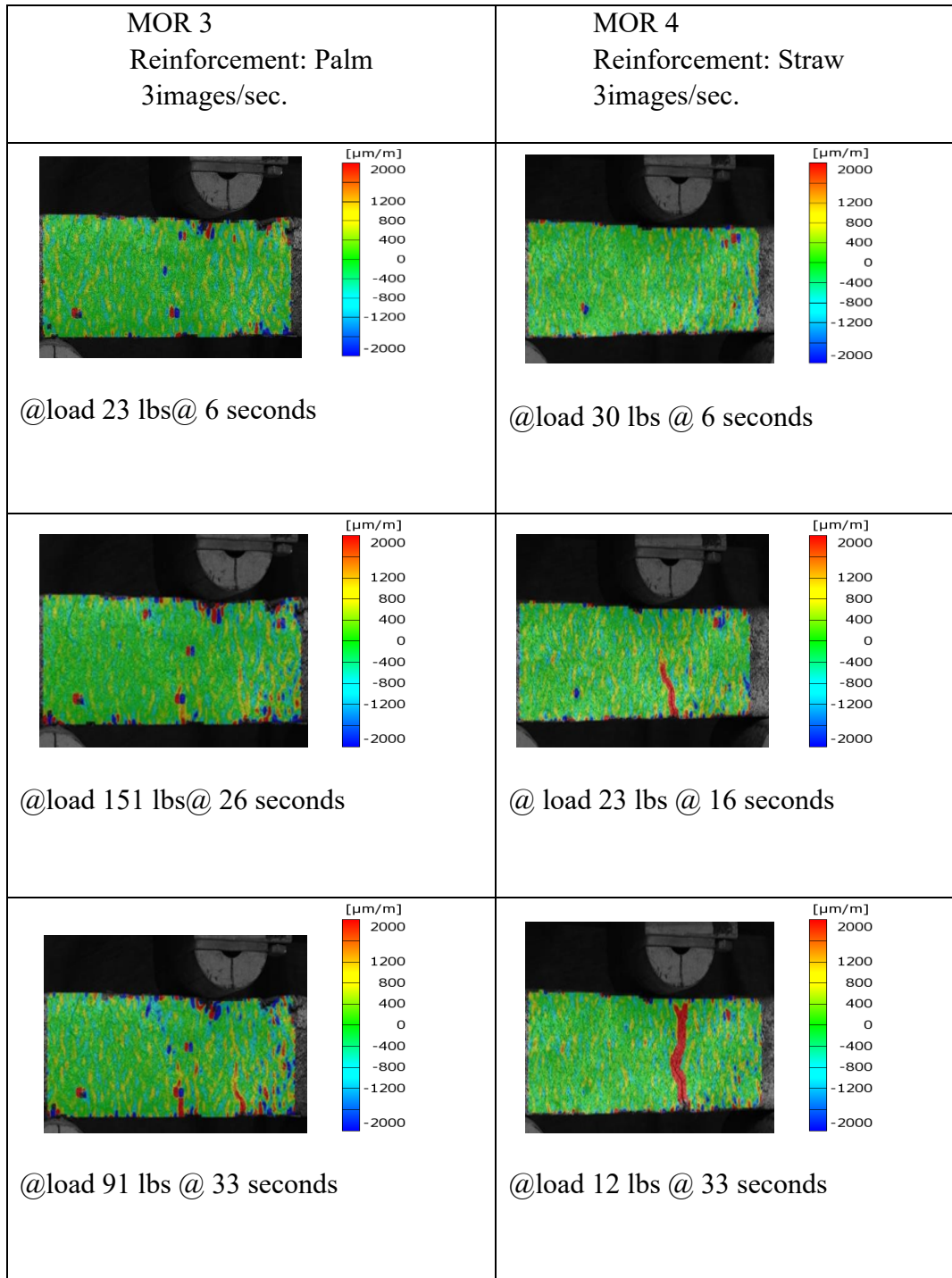


Figure 5.2. Longitudinal surface strains for MOR specimens 3 and 4



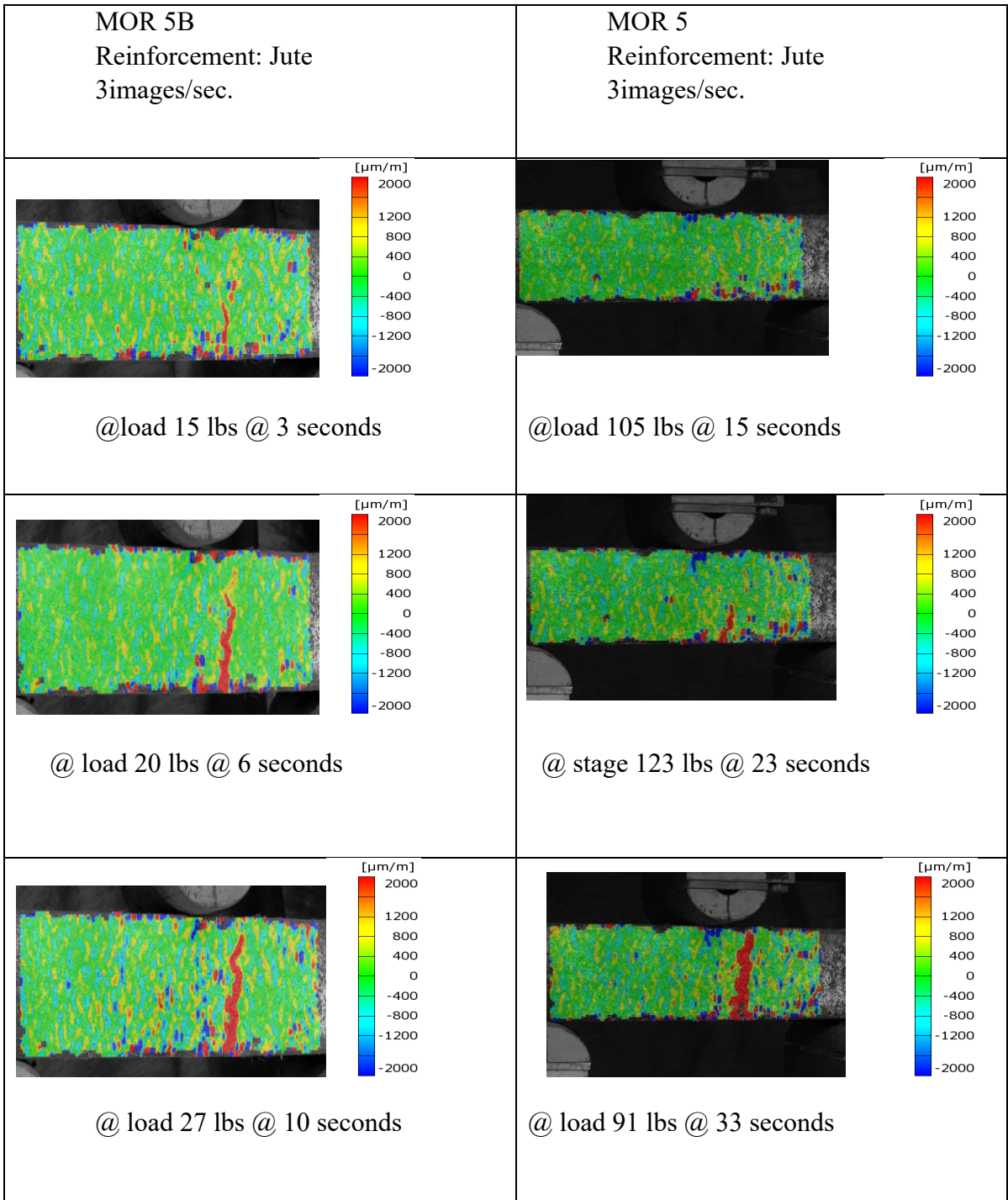


Figure 5.3. Longitudinal surface strains for MOR specimens 5B and 5

MOR 6	MOR 7
-------	-------

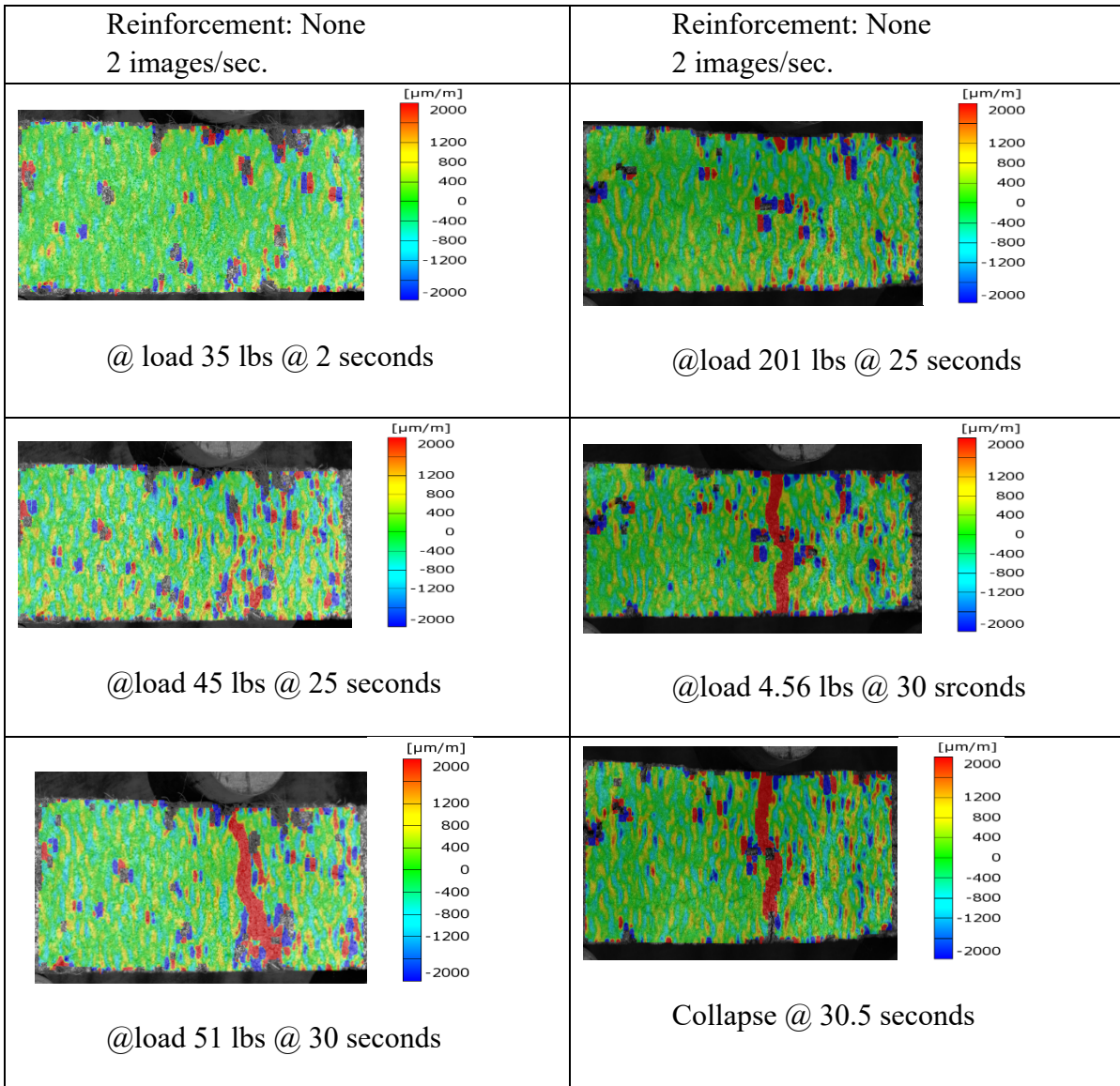


Figure 5.4. Longitudinal surface strains for MOR specimens 6 and 7.

### **5.1.1 Results**

Specimen 1 appears to crack very early in the loading process, failing around load 78 lbs. For specimen 2 the major flexural crack starts at load 130 lbs. Specimens 3 appears to be able to withstand the greatest load prior to any major flexural cracking with no significant cracking even after load of 151 lbs. Specimens 5B has a large flexural crack early in the loading process where 6 and 7 are much later.

Reinforcement plays an important role in the strength of the adobe. The adobe beam with reinforcement could resist higher load than the adobe without reinforcement. At the same time, the quality of the bricks also plays an important role in determining strength of the brick. There were a couple of cases where this was not true and was likely due to the quality of the brick that was manufactured.

### **5.2 2018 Testing**

Multiple adobe beams were developed and tested with varying levels of reinforcement in January 2018. The testing followed the same protocols as the July 2017 testing. The applied load along with corresponding load for different specimens with and without reinforcement is shown in Figure below.

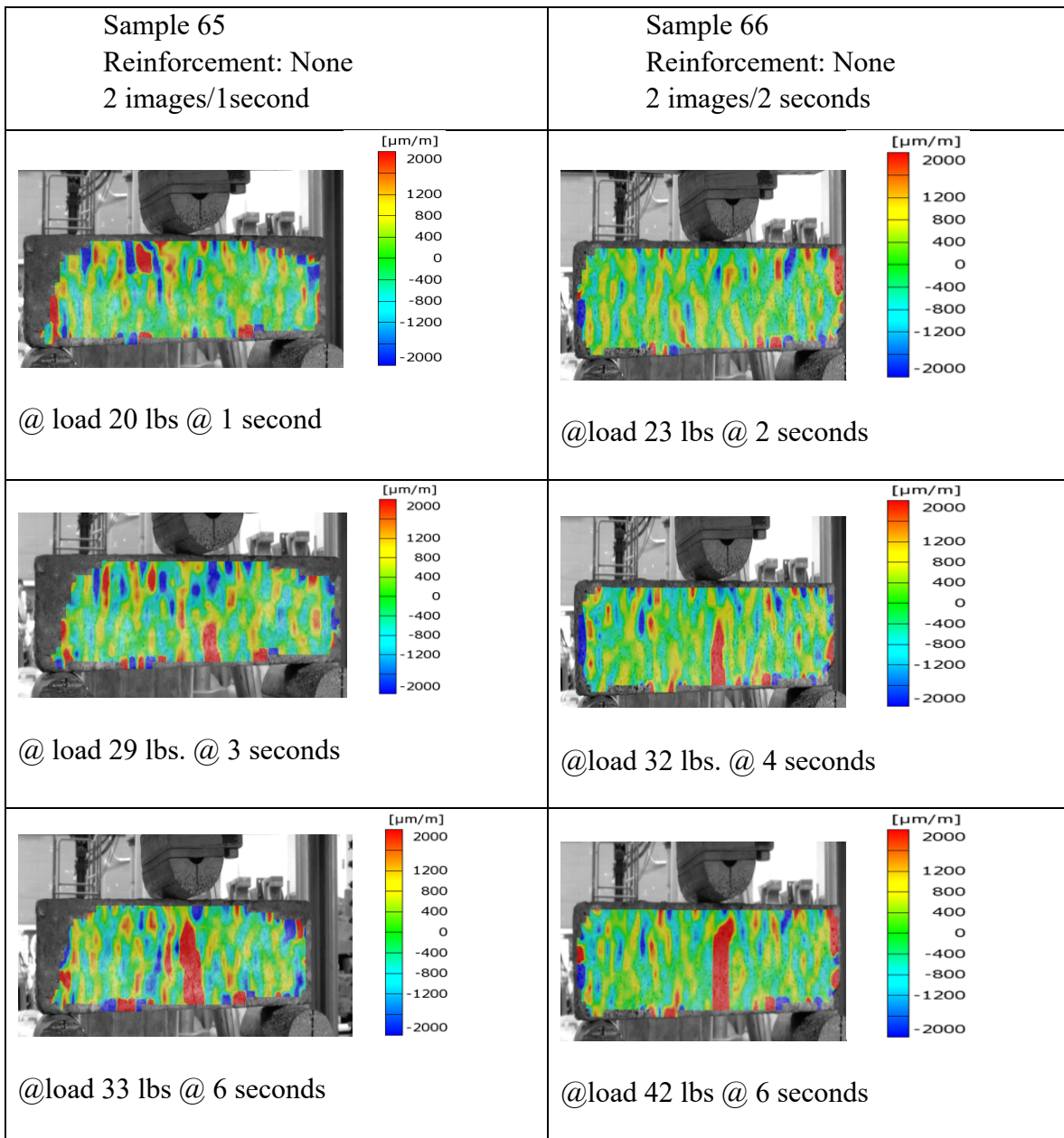


Figure 5.5. Longitudinal strain for specimen 65 and 66

<p>Sample 67 Reinforcement: Straw 2mages/1second</p>	<p>Sample 68 Reinforcement: Straw 2mages/1second</p>
--	--

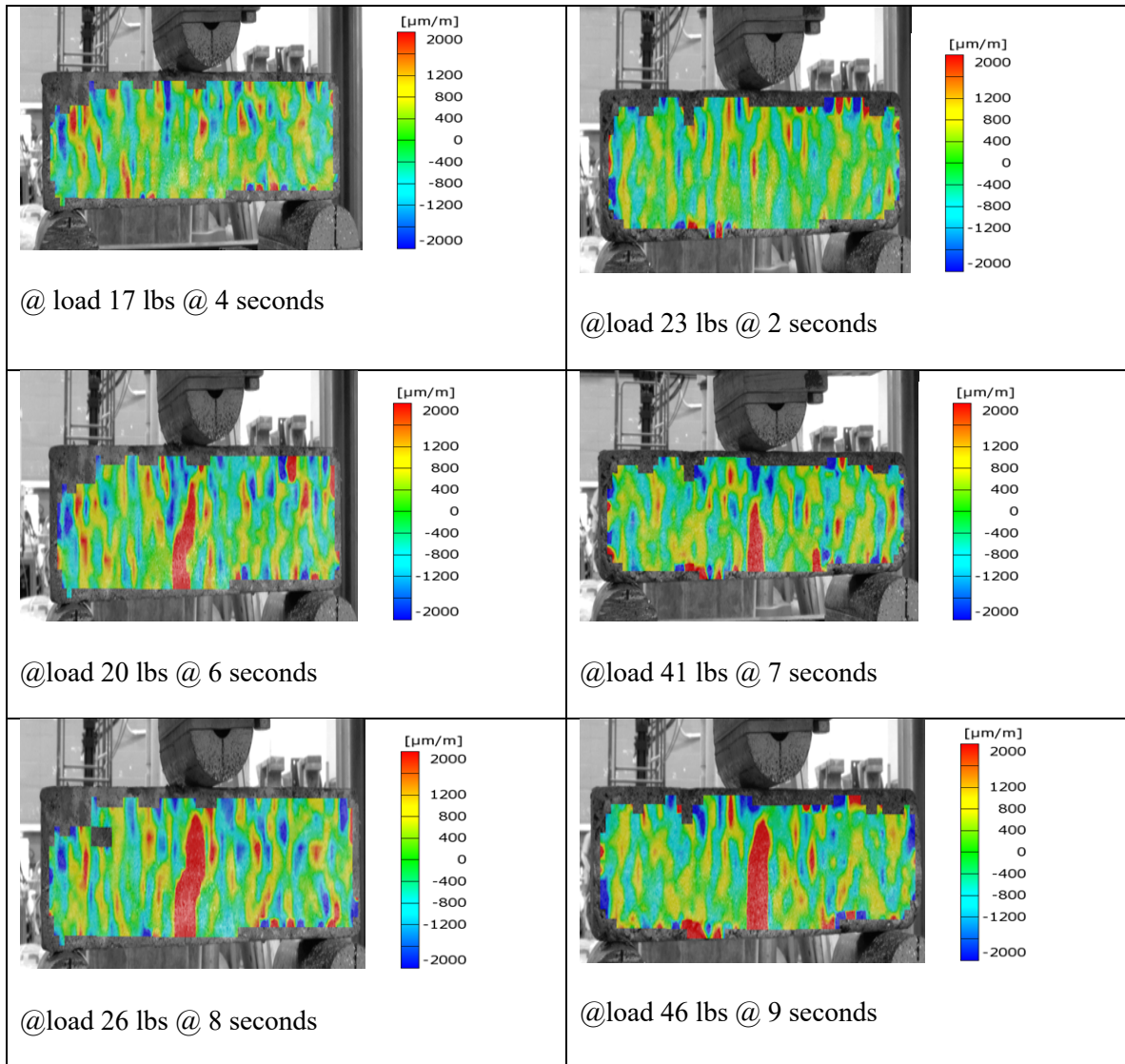


Figure 5.6. Longitudinal strain for MOR specimen 67 and 68.



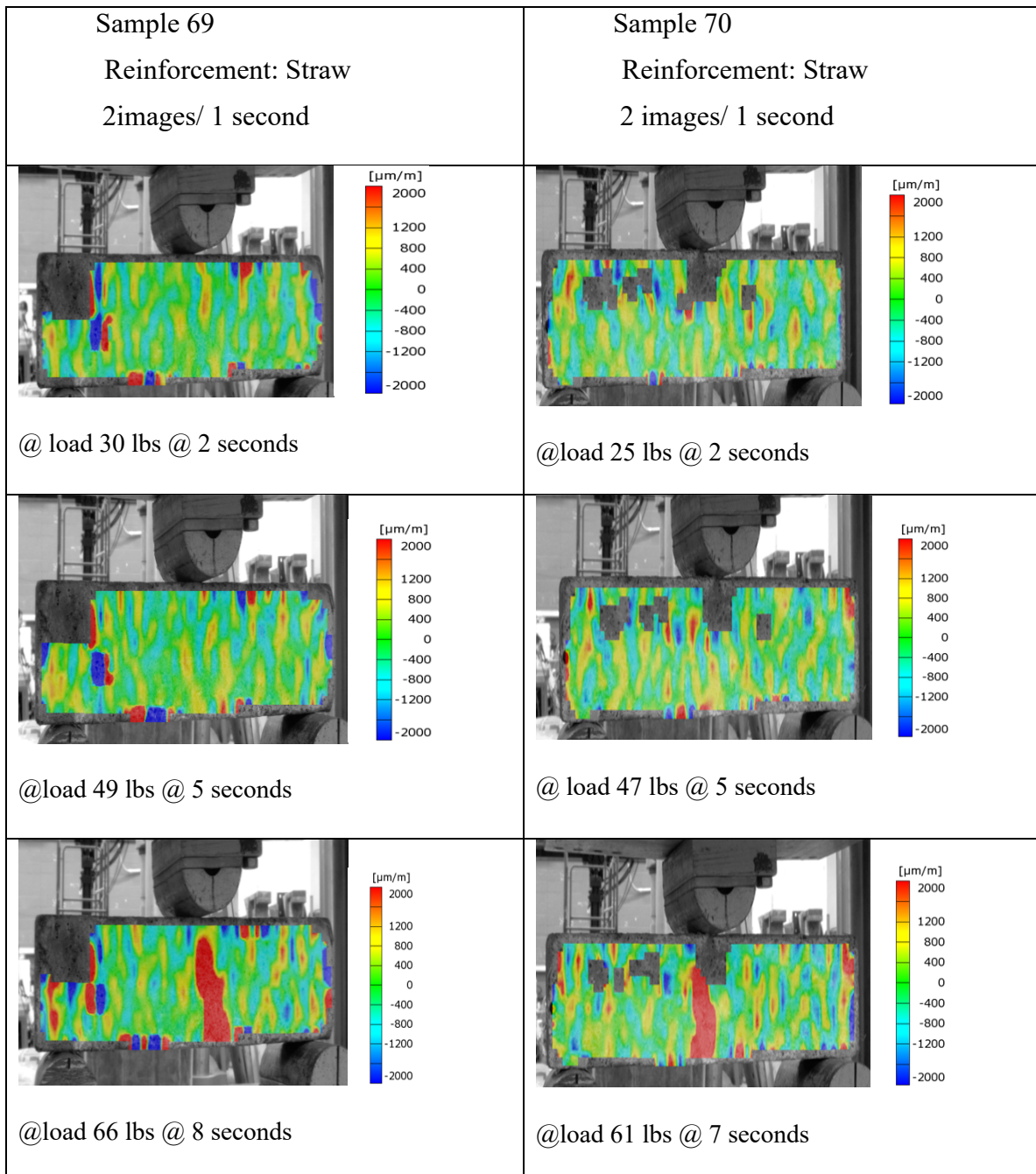


Figure 5.7. Longitudinal strains for specimen 69 and 70

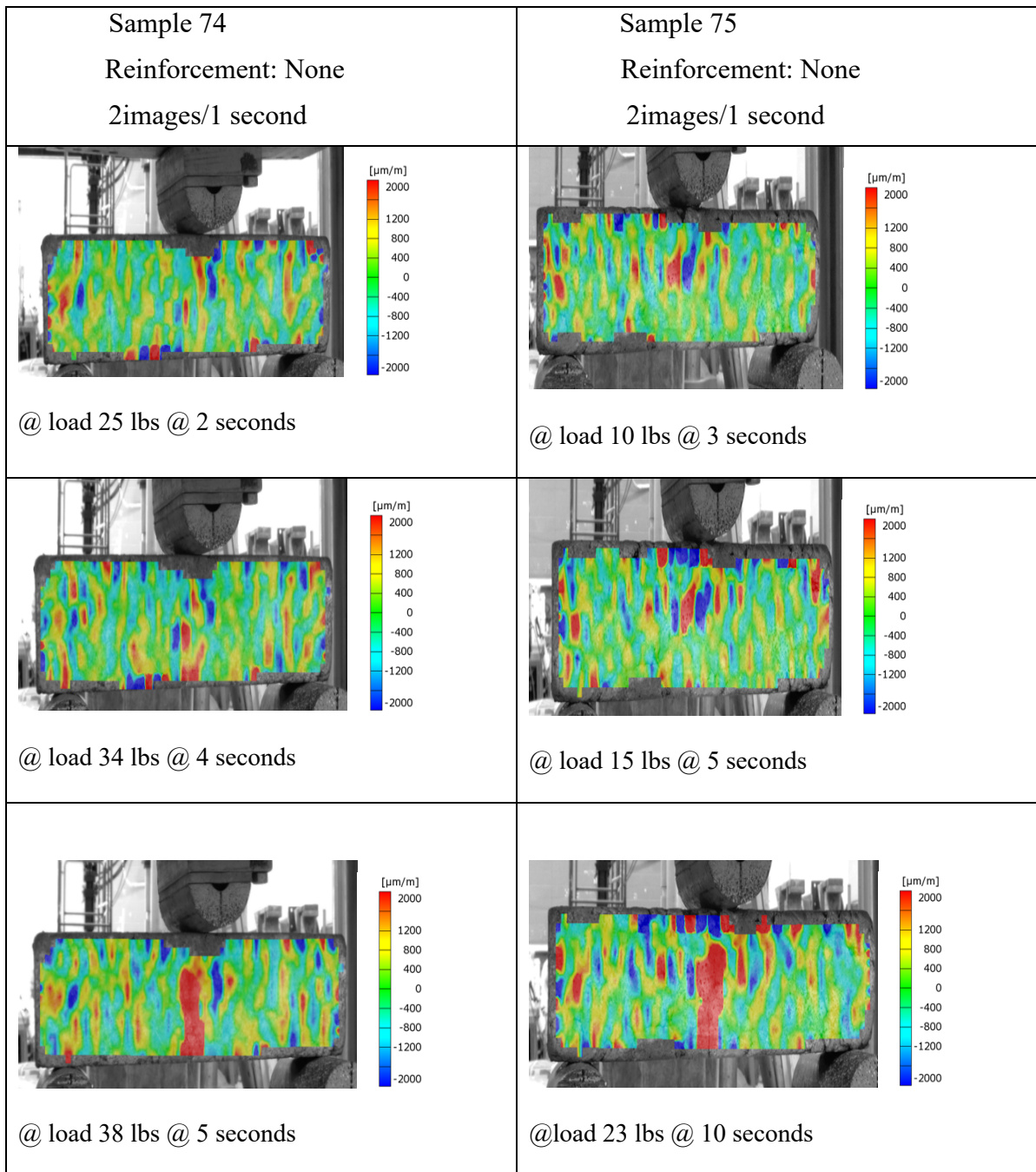


Figure 5.8. Longitudinal strains for specimen 74 and 75

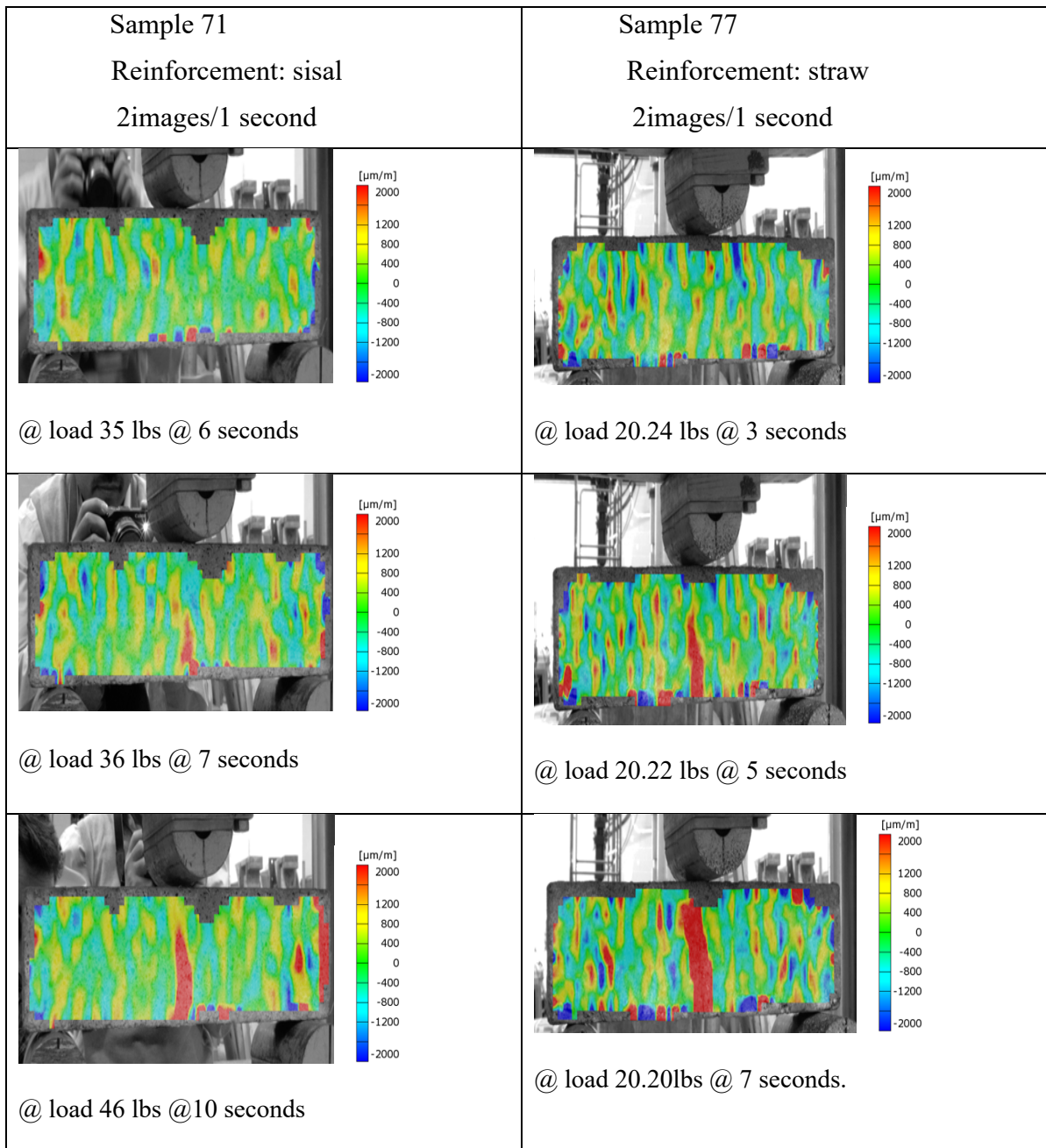


Figure 5.9. longitudinal strain for specimen 71 and 77



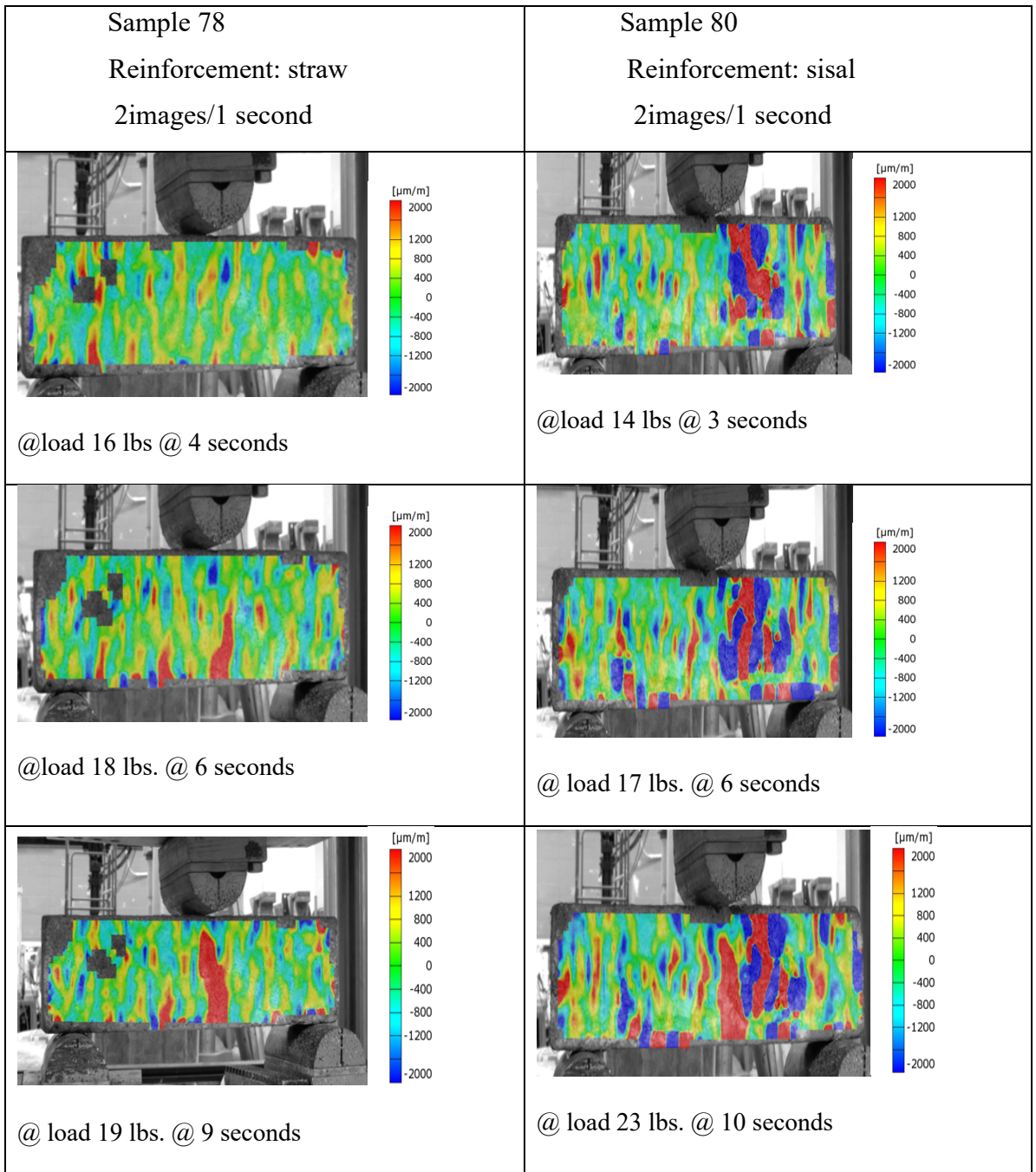


Figure 5.10. Longitudinal strain for specimen 78 and 80

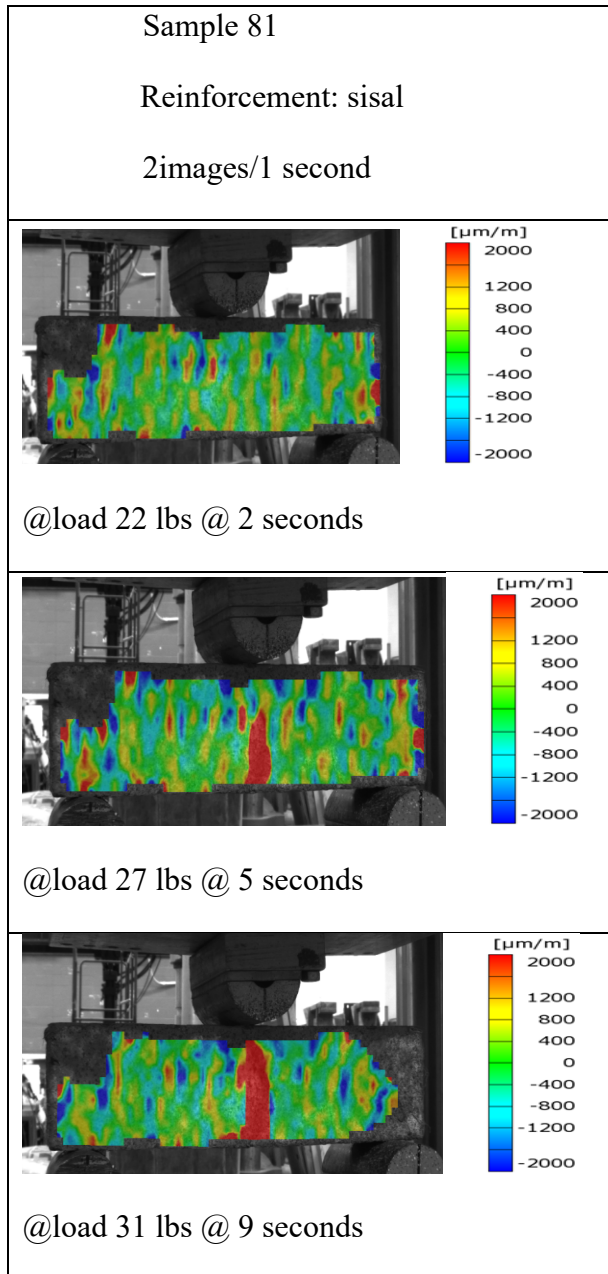


Figure 5.11. Longitudinal strains for sample 81.

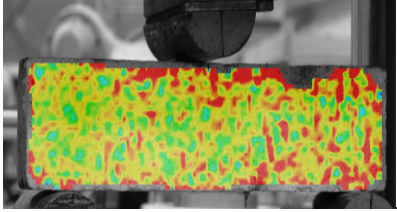
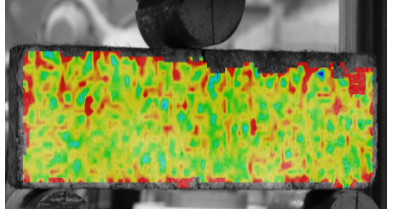
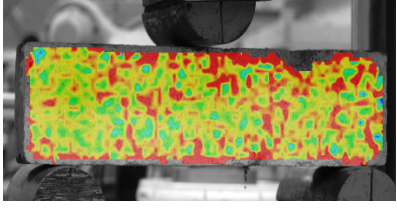
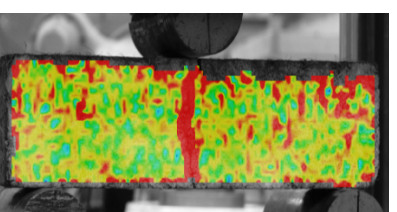
### 5.2.1 Results

Cracks start to appear early during the loading process in specimen 65 and 66 with no fibers. Specimen 67 and 68 with straw fibers had approximately the same loading capacity. Interestingly, specimen 69 and specimen 70 with straw fibers were able to

withstand the highest load of 76 lbs. and 75 lbs. respectively. Significant cracking starts to appear in specimen 71 with sisal fibers at a load 66 lbs. whereas full cracking is observed in specimen 77 with straw fibers at load 33 lbs. Large cracking is seen in specimen 81 with sisal fibers at an early stage.

### 5.3 2019 Testing

Additional specimens were tested following the same protocol as in 2017 and 2018.

MOR 202 Reinforcement: None 4 images/second	MOR 203 Reinforcement: Sisal 1 image/second
 <p data-bbox="256 1186 609 1228">@ load 14 lbs. @ 1 second</p>	 <p data-bbox="922 1186 1274 1228">@ load 23 lbs. @ 1 second</p>
 <p data-bbox="256 1533 397 1575">@ 129 lbs.</p>	 <p data-bbox="922 1543 1274 1585">@load 76 lbs. @ 2 seconds</p>

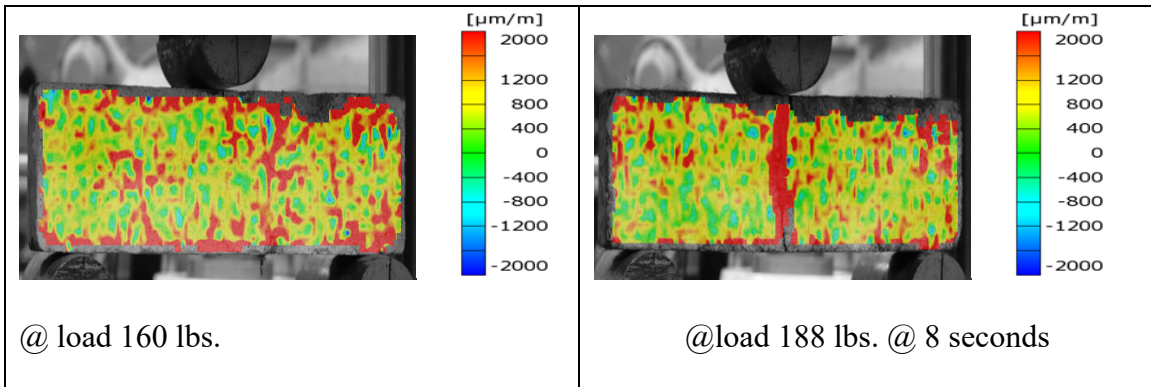
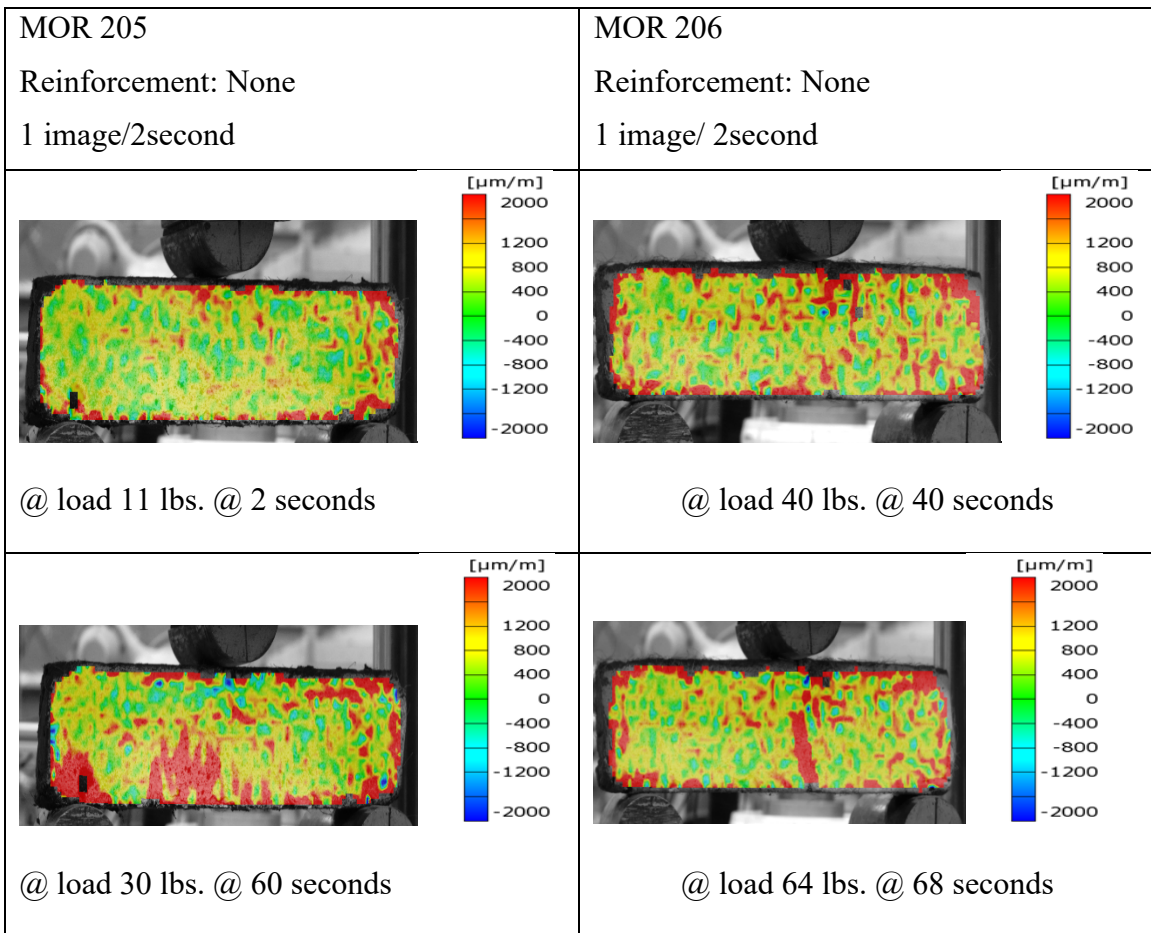


Figure 5.12. Major strain for specimen 202 and 203





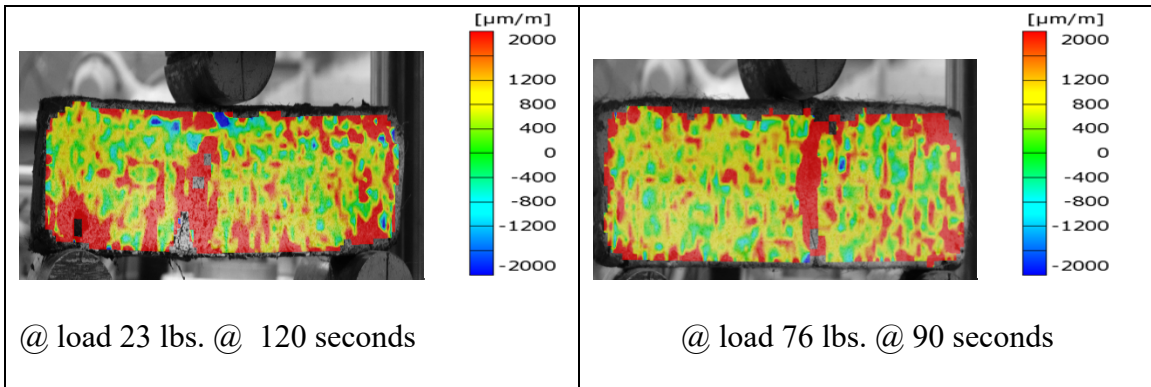
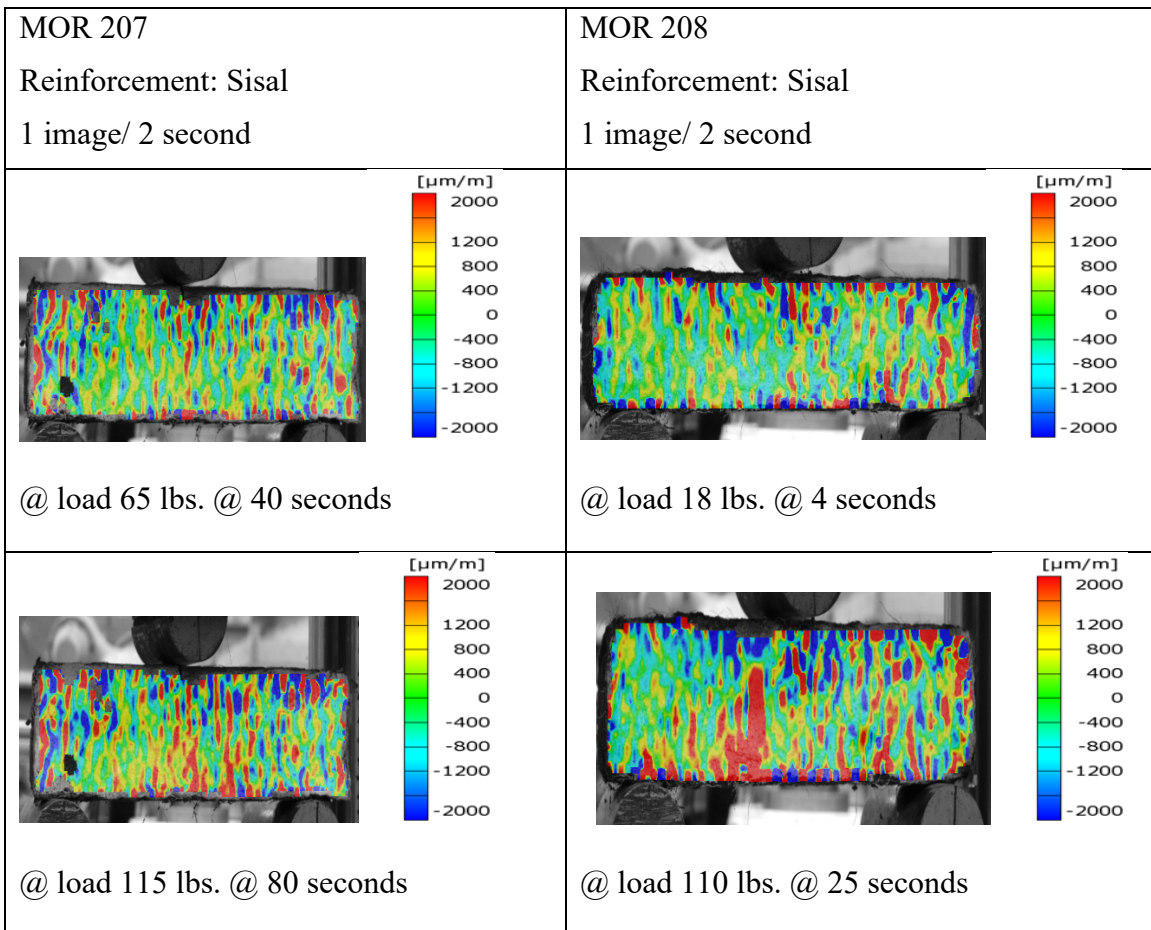


Figure 5.13. Major strain for specimen 205 and 206,



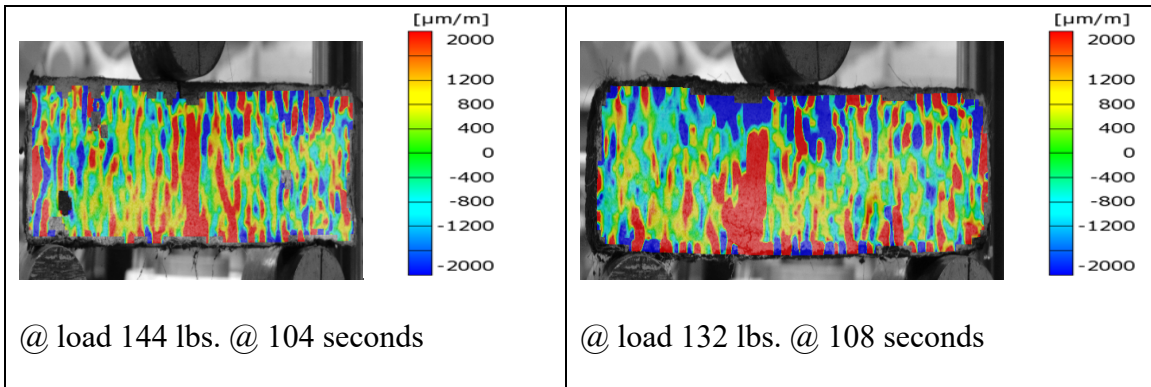
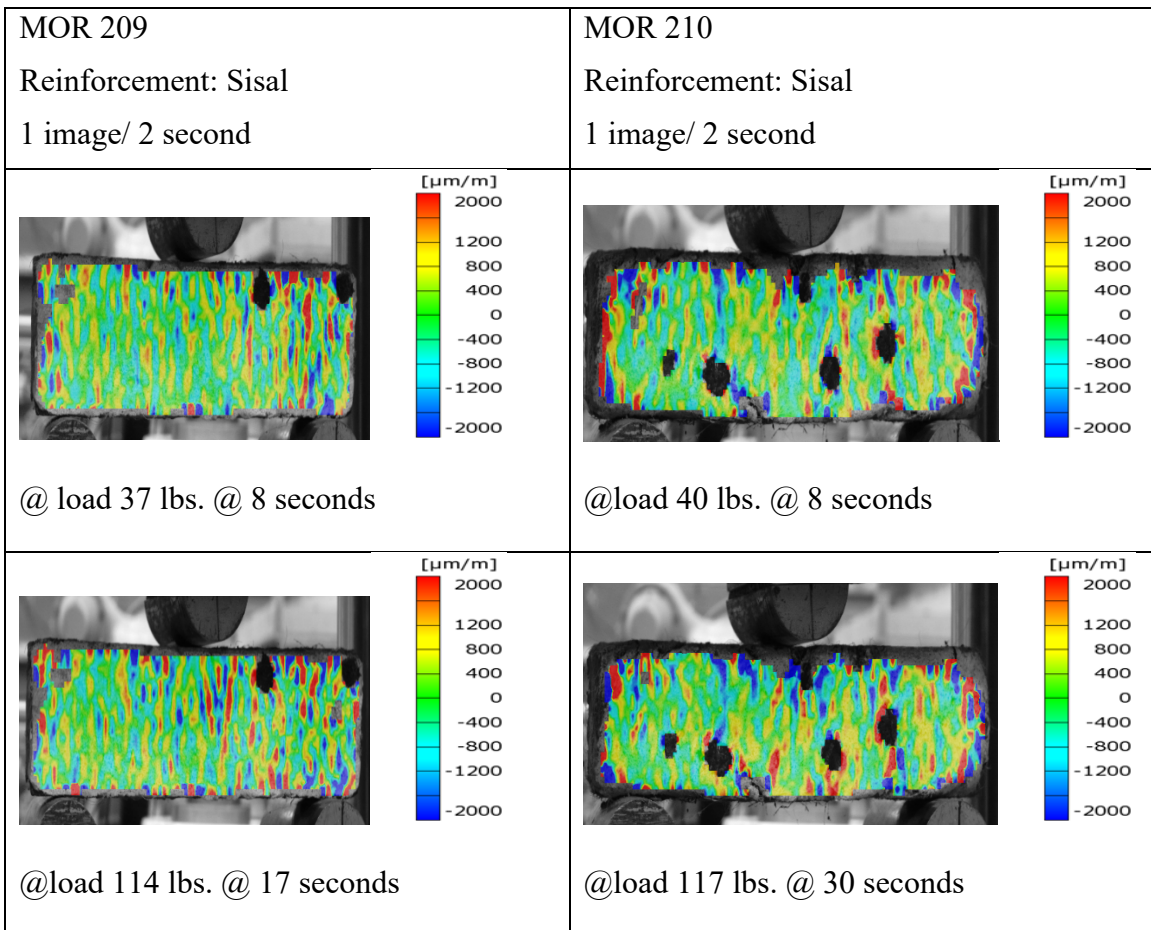
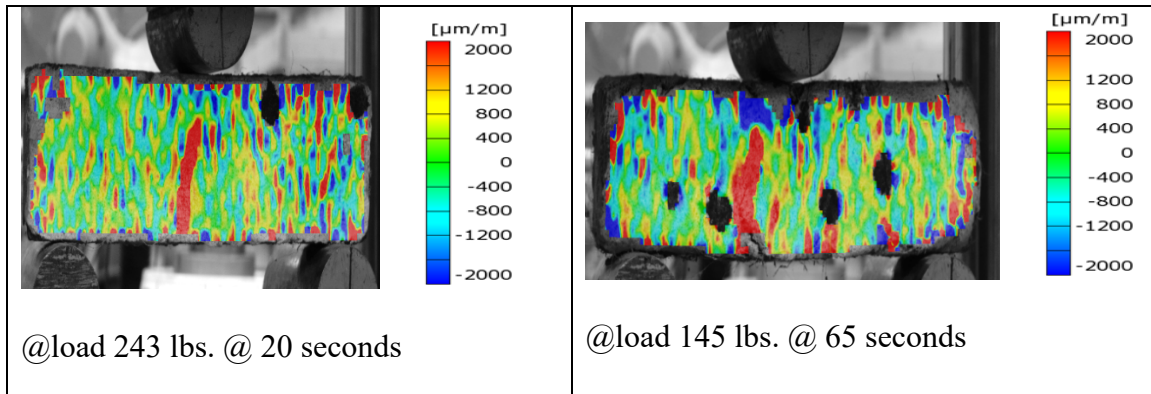


Figure 5.14. Longitudinal strain for specimen 207 and 208.





*Figure 5.15. Longitudinal strain for specimen 209 and 210.*

### 5.3.2 Results

In spite of having no reinforcement, failure in specimen 202 occurs quite late. Cracks start to appear in specimen 203 at a load of 76 lbs. Sudden failure of the beam does not occur even when cracks start to appear in specimen 203. Cracking starts to appear earlier in specimen 205 than specimen 206. Larger cracks appear in specimen 208 at loads of 110 lbs. whereas in specimen 207 small cracks start to develop around load 115 lbs. Significant cracking is seen at a load of 145 lbs. for specimen 210 whereas significant cracking is seen in specimen 243 at 243 lbs.

### 5.3 Conclusions

From the results of 2017, 2018, 2019 tests, it can be seen that the reinforced specimens were able to resist higher loads than the non-reinforced specimen. Cracks start to develop at very early stage for non-reinforced specimen, failing earlier at smaller loads. In the cases of the reinforced specimens, even after development of significant cracking, the structure did not collapse suddenly. The specimen slowly loses its strength as the fibers bridge the developing cracks preventing sudden failure of structure.

## Chapter Six

### Experimental Testing of Adobe Walls

Multiple wall specimens were tested during two different times. The walls were constructed using adobe bricks. This chapter will discuss the testing results from both tests, July 2017 and January 2018.

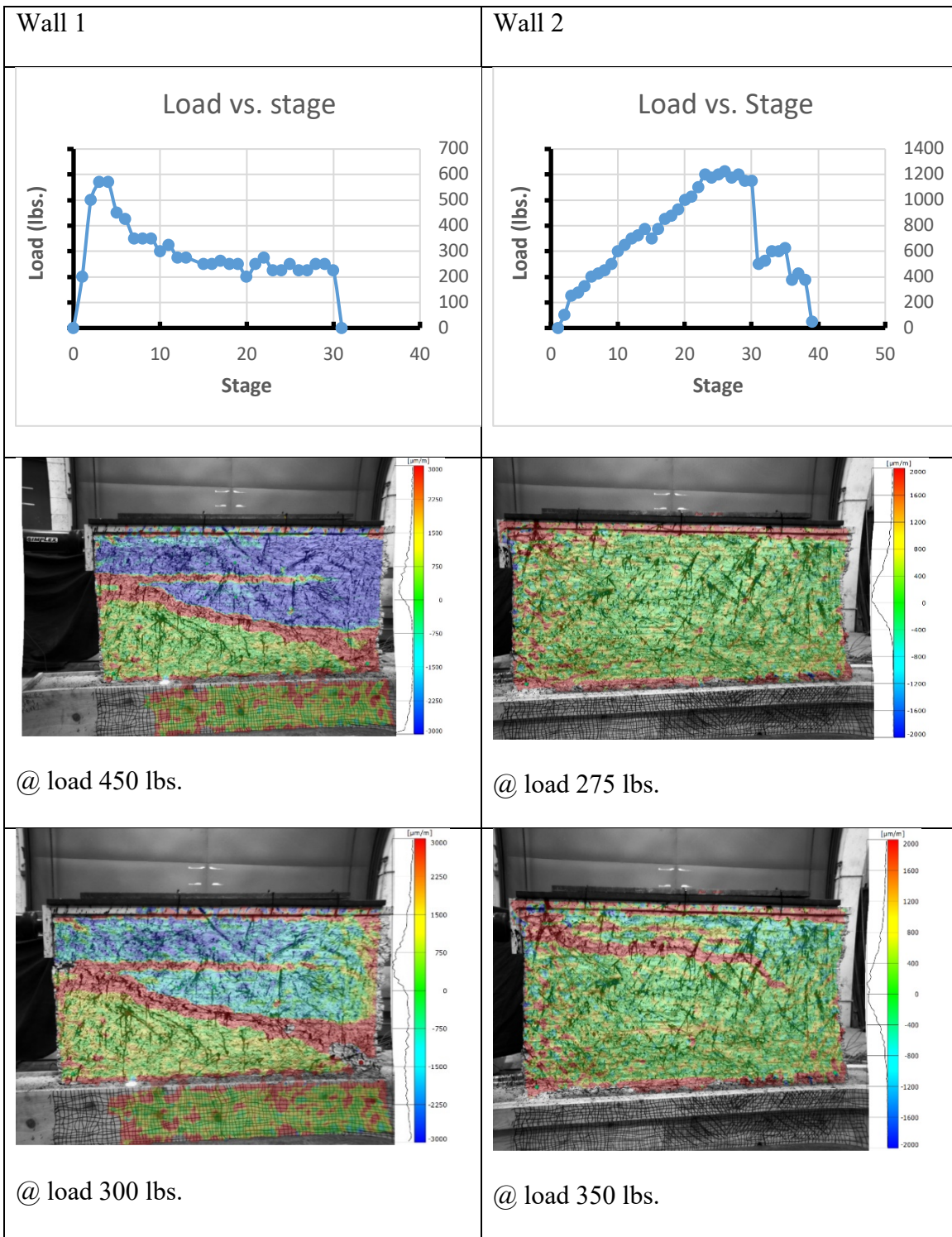
#### 6.1 July 2017 Testing

During July 2017, five walls were tested under lateral loading. The specimens follow the matrix outlined in Table 6.1. The load vs. stage curves for each wall are shown in Figure 6.1 , 6.2 and 6.3 along with images of the major strains on the face of the wall for different stages of the testing.

*Table 6.1. Matrix of Wall Test Specimens*

<i>Wall</i>	<i>NMSU (Davila 2019)</i>	<i>Date tested</i>	<i>Moisture</i>	<i>Reinforcement</i>
1	5	2017	3.03%	Reinf pattern1
2	7	2017	2.80 %	Reinf Pattern2
3	1	2017	3.86%	Reinf Pattern2
4	2	2017	4.26%	None
6	8	2017	4.48%	Reinf Pattern2
7	4	2018	1.77%	None
8	9	2018	8.55%	Reinf pattern2





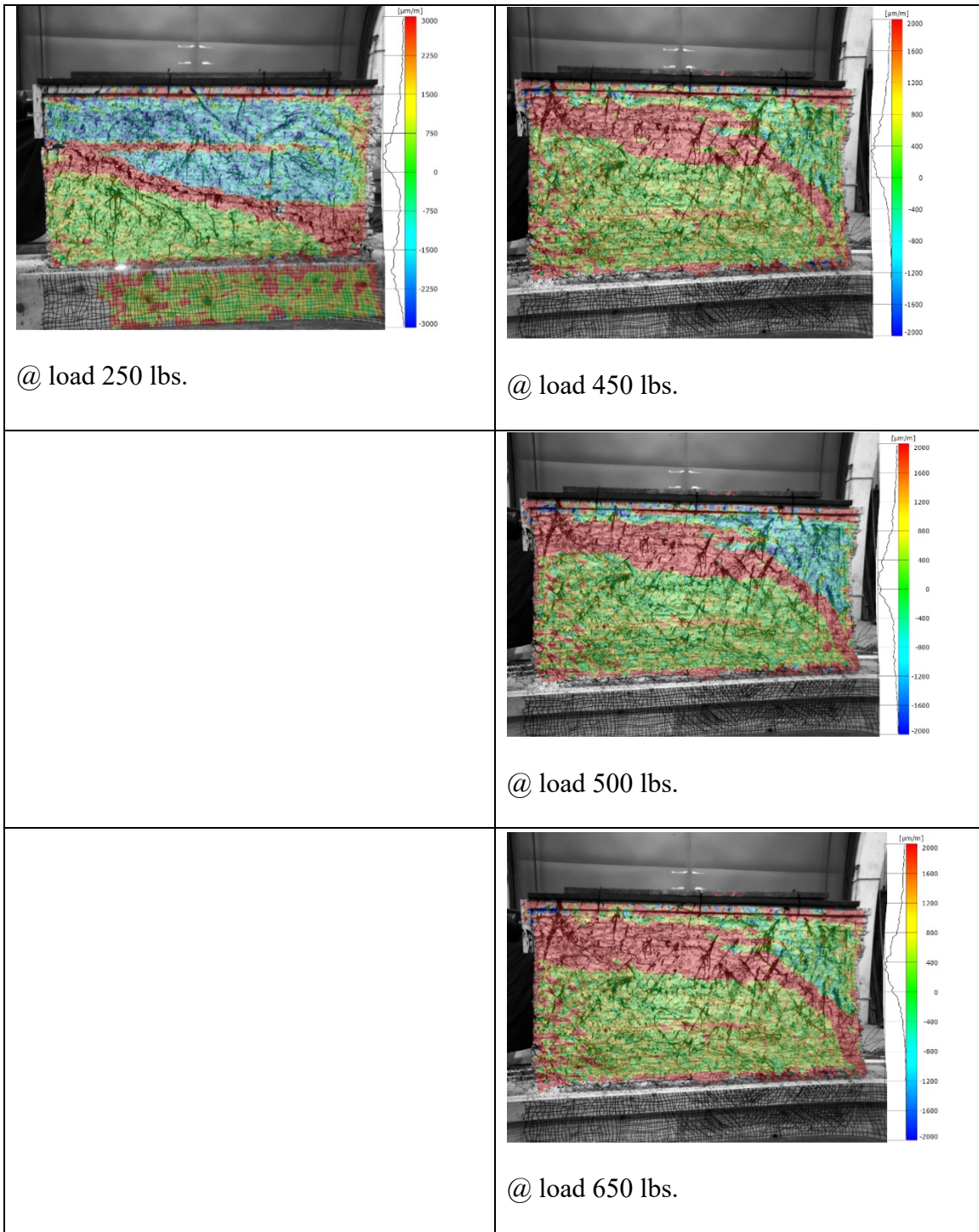
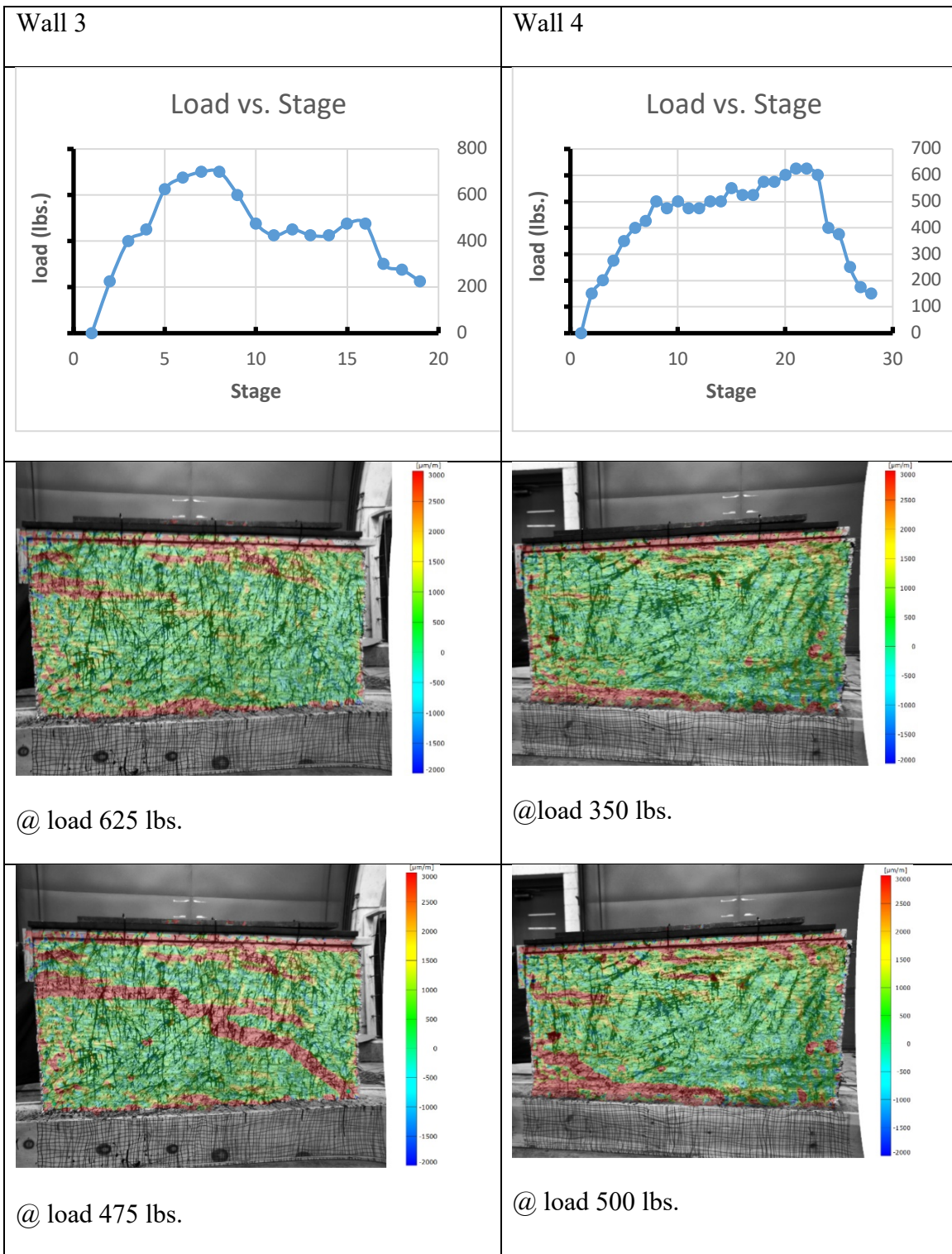
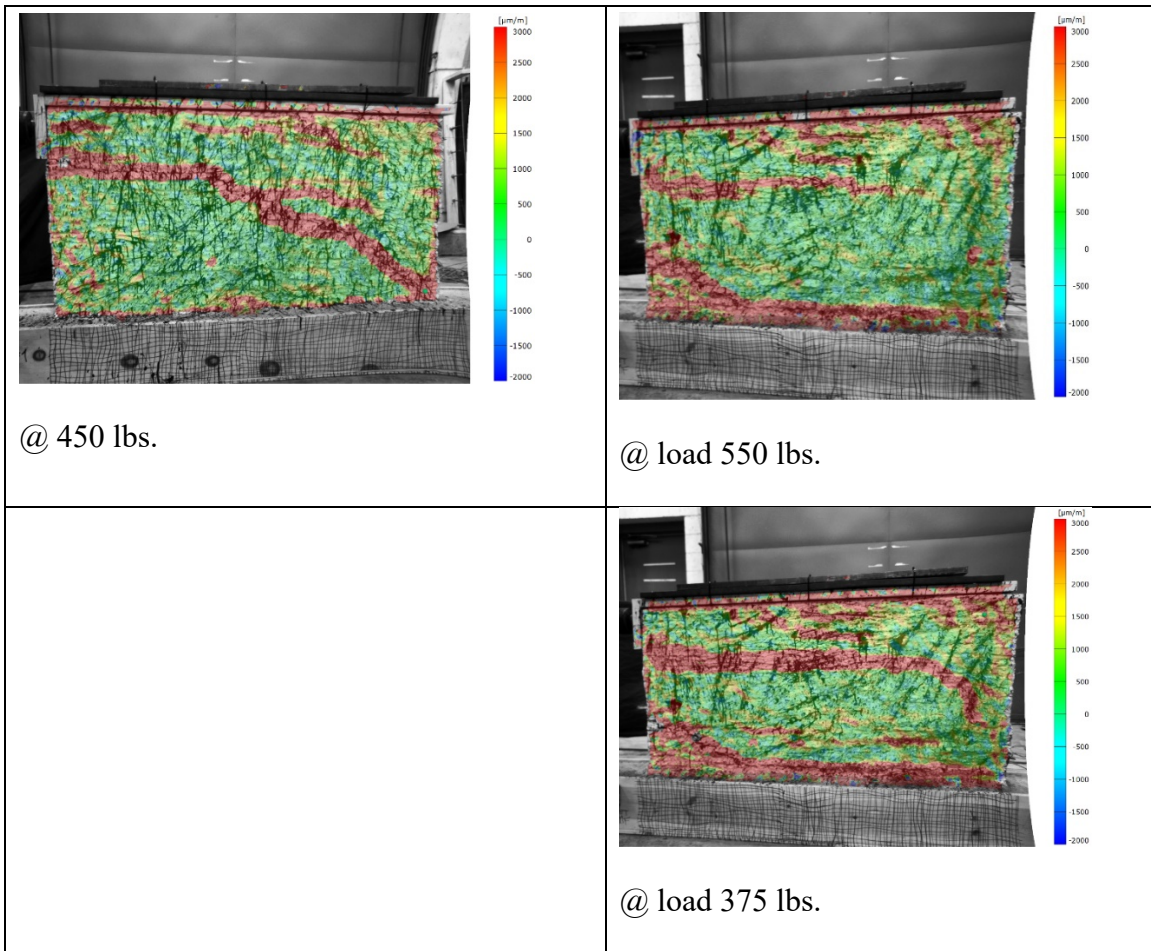


Figure 6.1. Major strain for Wall 1 and 2



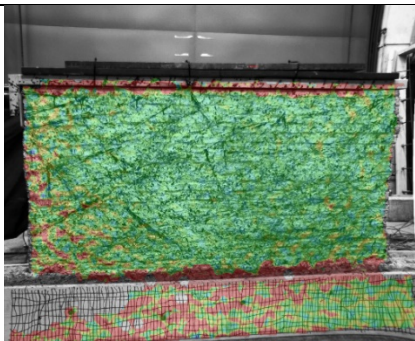
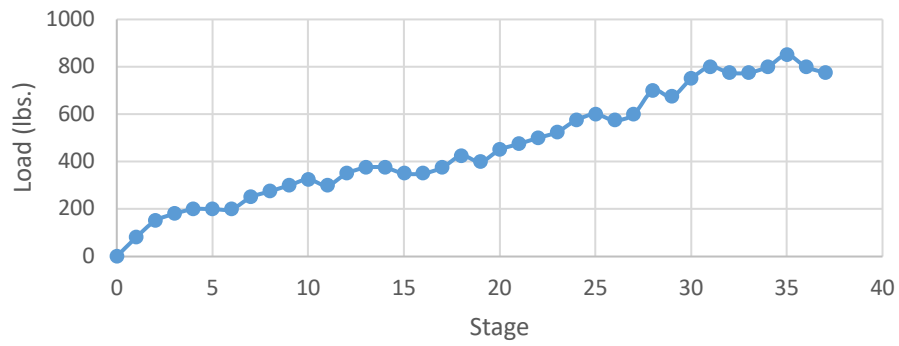




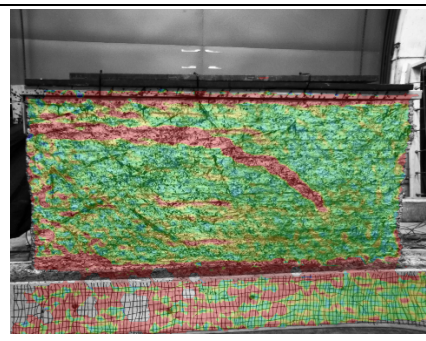
*Figure 6.2. Major strain for Wall 3 and 4*

# Wall 6

## Load vs. stage



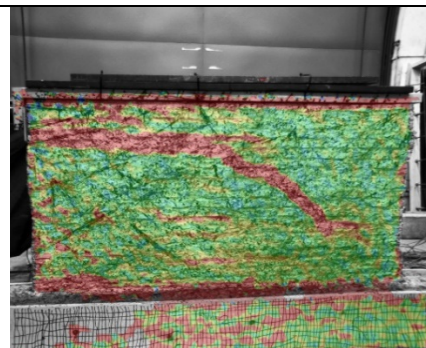
@ load 200 lbs.



@ load 750 lbs.



@load 325 lbs.



@ load 850 lbs.



Figure 6.3. Major strain for Wall 6

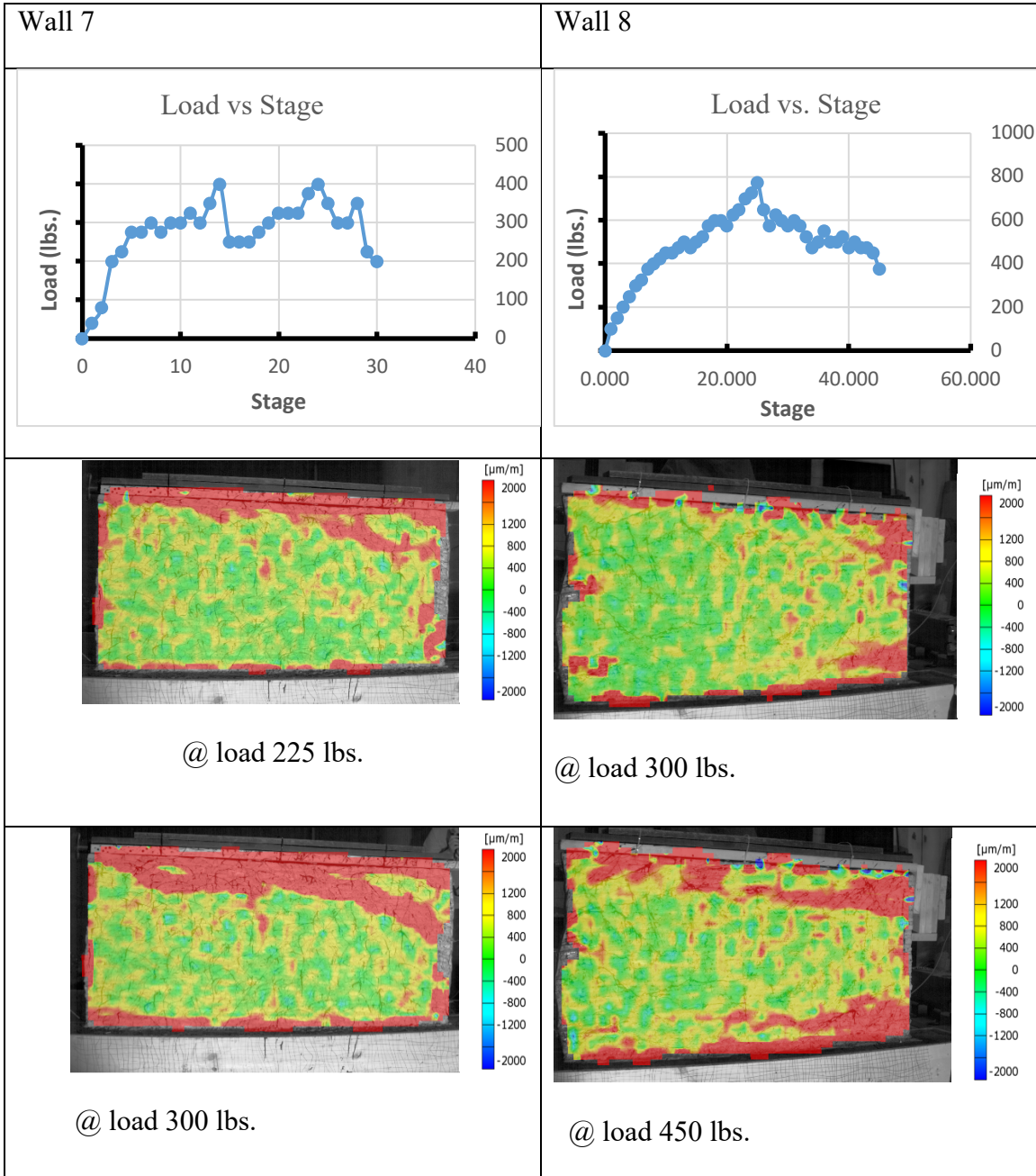
### **6.1.2 Discussion**

The data shows that reinforcement pattern 1 for the dry wall does not provide any additional strength beyond the non-reinforced dry wall. The maximum load is slightly less for the wall with reinforcement pattern 1 (650 lbs.) versus the non-reinforced wall (600 lbs.). Reinforcement pattern 2 increased the lateral strength of the wall significantly to 1220 lbs. Walls 4 and 5 both were considered wet and had no reinforcement and reinforcement pattern 2. The data shows that the wet wall with no reinforcement is weaker than the wet wall with reinforcement pattern 2.

### **6.2 January 2018 Testing**

Two additional walls were tested in January 2018 which correspond to walls 7 and wall 8 in Table 6.1. Lateral load was applied at the top left corner of the first wall whereas on the second wall, load was applied on the top right corner. The plots of load versus stage for both walls are shown in Figure 6.3. The in-plane horizontal displacements (y-direction and x-direction) are shown in figure 6.7 and 6.8 for both walls 6 and 7 for points A, B, C and D outlined in Figure 6.8.







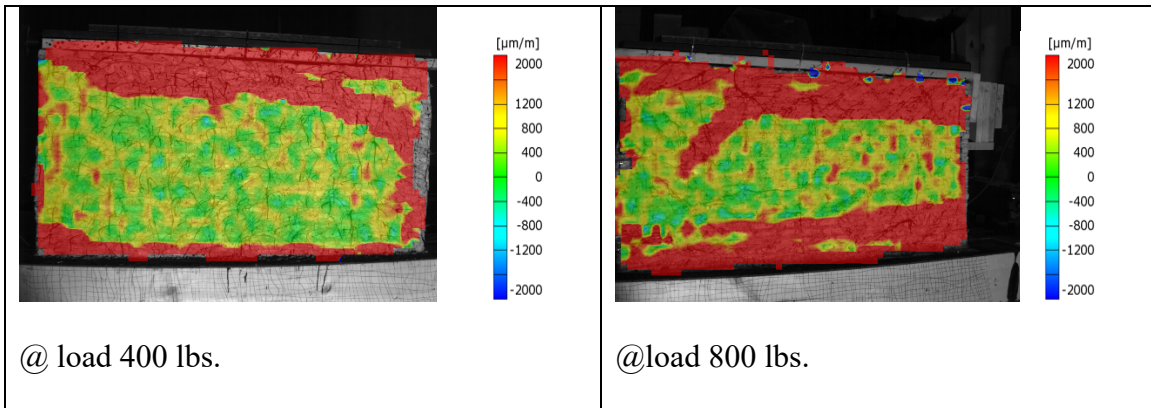


Figure 6.3. Major strains for Wall 7 and 8

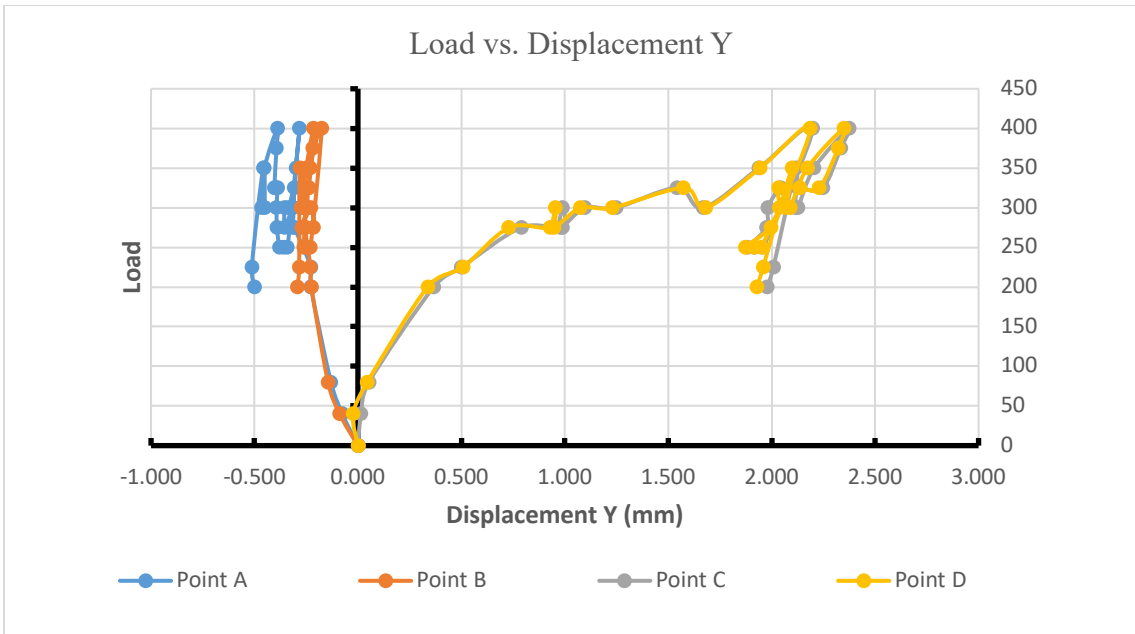


Figure 6.4. Load vs Vertical displacement for four points shown in Figure for Wall

7.

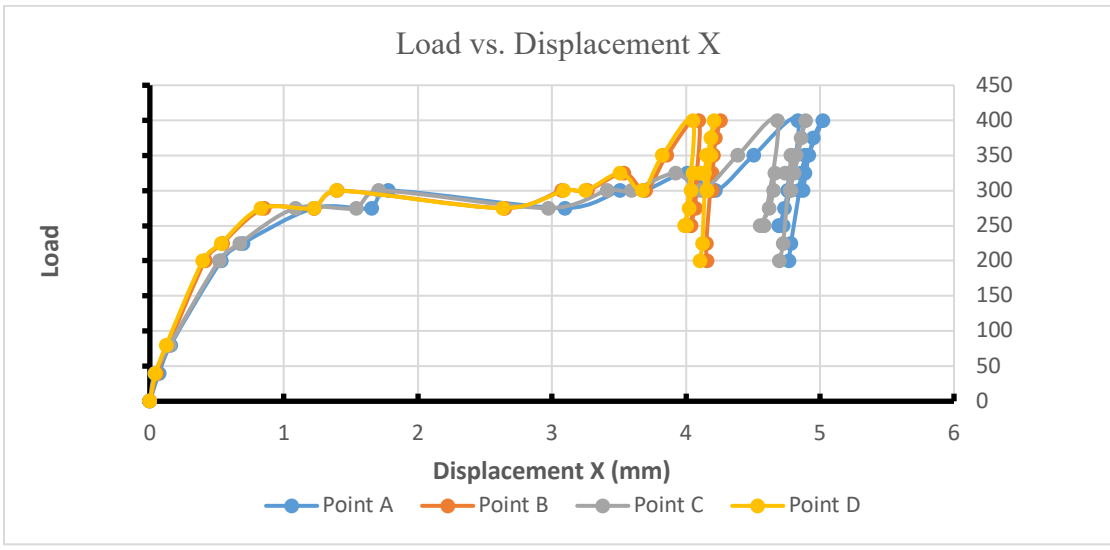


Figure 6.5. Load vs. Horizontal displacement for four points shown in Figure for Wall 7.

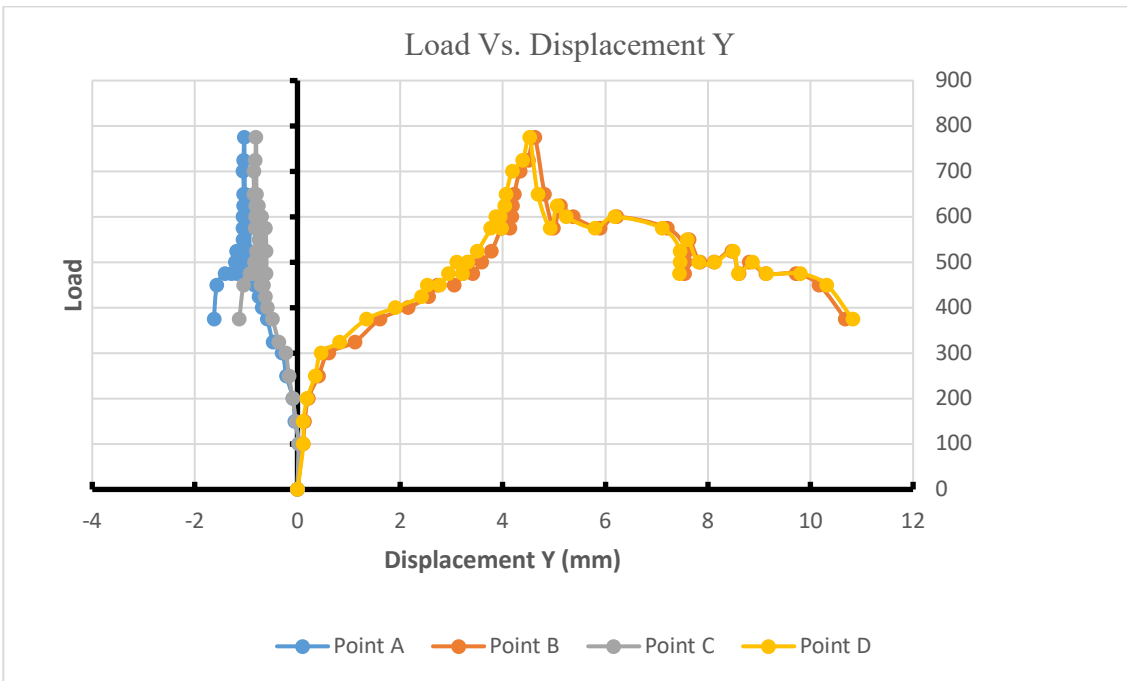


Figure 6.6. Load vs. vertical displacement for four points shown in figure for Wall 8.

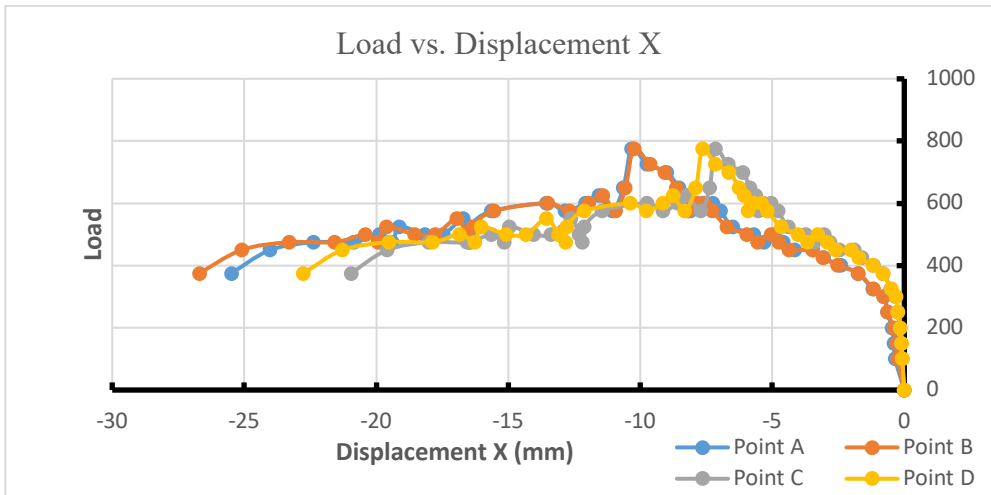


Figure 6.7 Load vs. horizontal displacement for four points shown in figure for Wall 8.

From the in-plane displacements the shear strain across the surface of the wall was determined for an applied load. The shear strain ( $\gamma$ ) was calculated using equation (1). Figure 20 illustrates the physical dimension used for the shear strain calculation.  $\delta_1$  and  $\delta_2$  are the extension or contraction of dimensions D1 and D2 respectively and can be positive (extension) or negative (contraction).

$$\gamma = \frac{\delta_1 D_1 - \delta_2 D_2}{2 h * L} \quad (I)$$

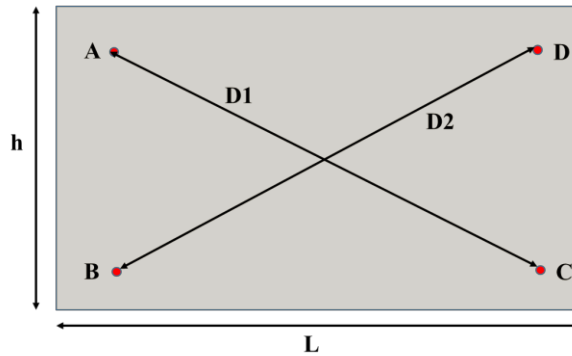


Figure 6.8. Illustration of dimensions used in equation (1)

### 7.2.2 Discussion

The peak load for Wall 7 with no fibers was roughly 400 lbs. and 800 lbs. for the Wall 8 with reinforcement pattern 2. From the displacement results, points A and D at the top corners of the wall have the highest amount of horizontal displacement and points B and C at the base of the wall have the smallest. Both A and D have a maximum horizontal displacement of roughly 5 mm (0.19 in.) for Wall 7 and a maximum horizontal displacement of approximately 25 mm (0.98 in.) for Wall 8. B and C move the least as they are closest to the continuously supported base of the wall. Figure 10 shows the vertical displacement (y-direction) for all 4 corners. In the case of Wall 7, the loading was applied in the upper left corner near point A. As the load was applied there was uplift to that side of the wall which created an upward movement in A and B and compressed C and D, the right side of the wall. For wall 8, the loading was applied at the top right corner of the wall which caused an upward movement in C and D and a downward (compression) movement of A and B. Upward displacements for both the walls from January 2017 were higher in

magnitude than the downward displacements likely due to the adobe brick being stronger and stiffer in compression than tension.

### 7.3 Summary and Conclusions

Load vs shear strain curves are plotted for all the wall tested in 2017 and 2018.

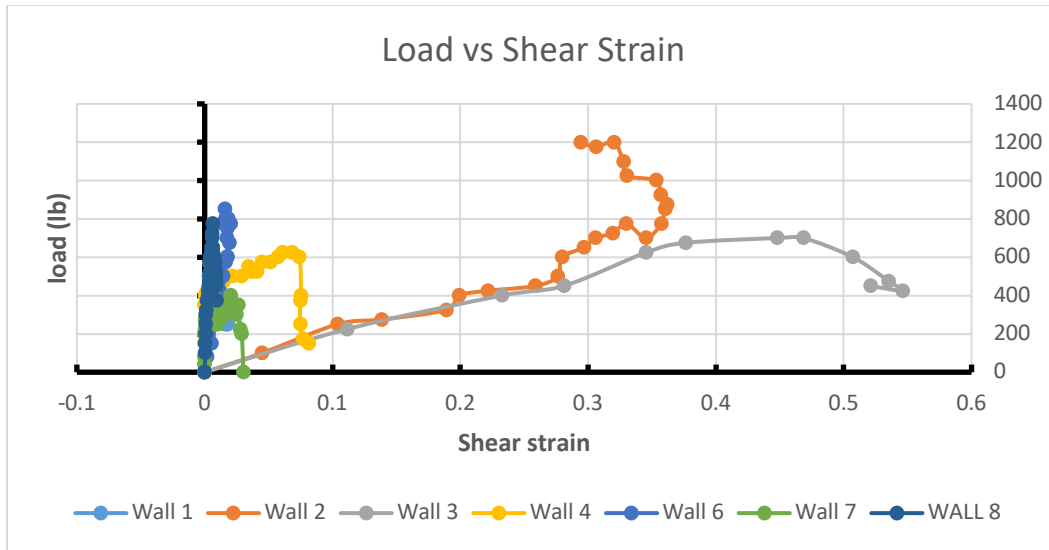


Figure 6.9 Load vs shear strain for all walls

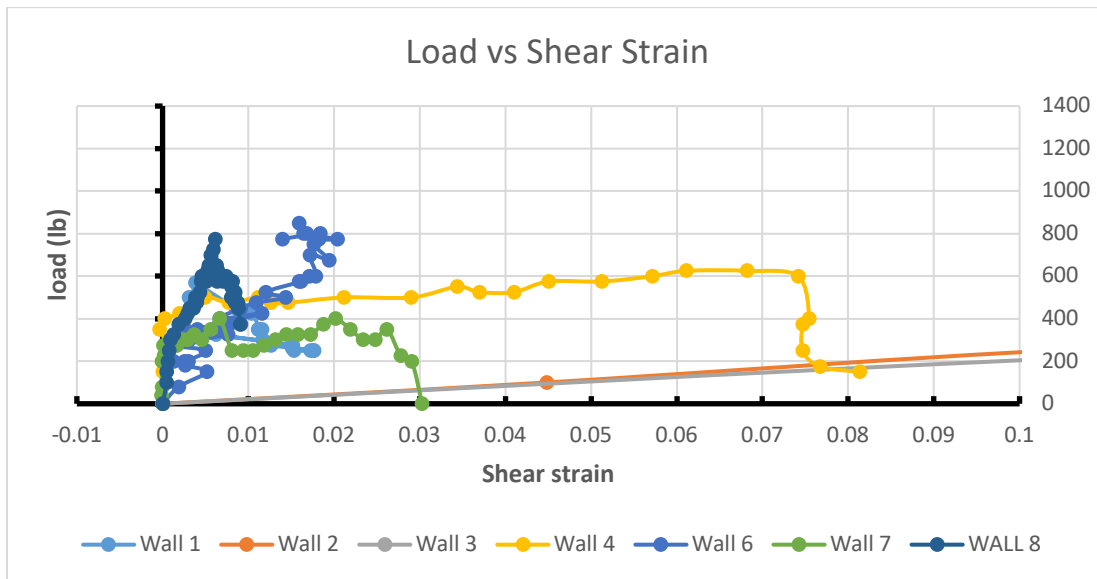


Figure 6.10. Load Vs Shear Strain

*Table 6.2. Summary of Wall tests with maximum load and shear strain at maximum load*

<i>Wall</i>	<i>Maximum load (lb)</i>	<i>Shear strain at maximum load</i>
1	600	0.004
2	1200	0.38
3	700	0.2
4	650	0.23
6	900	0.29
7	400	0.0006
8	800	0.03

The load vs. strain graph shows that for Wall 7, the magnitude of the shear strain was lower at for larger loading levels. The opposite is seen for Wall 8 with an increase in load producing larger shear strains. The wall with reinforcement pattern 2 seems to have maximum shear strain at load 1200 lbs.

The results from July 2017 and January 2018 testing shows that walls with reinforcement pattern 1 performed better than the walls which were not reinforced. Further, the walls that were dry had slightly higher lateral load capacity than the walls with moisture. Maximum shear cracking also occurred at lower loading levels for walls that were not reinforced.

## Chapter Seven

### Compression Testing for Modulus of Elasticity

This chapter discusses the compression testing of adobe prisms (cubes) for determining the Modulus of Elasticity at differing reinforcement and moisture levels. The testing was completed in January 2017 and March 2019.

#### 7.1 2017 testing

Five adobe cubes were constructed in New Mexico State university with varying moisture content and reinforcement. The specimens follow the matrix outlined in Table 4.1. IL5 and 2M camera system were used to monitor the surface strains and deformations on the front and back faces of the prisms respectively. ARAMIS software was used for the analysis of displacement.

Ten points were created in the mid of the specimen as shown in the figure 7.1 such that vertical displacement of each of the points were noted. Horizontal and vertical distance between the points is 25 mm.

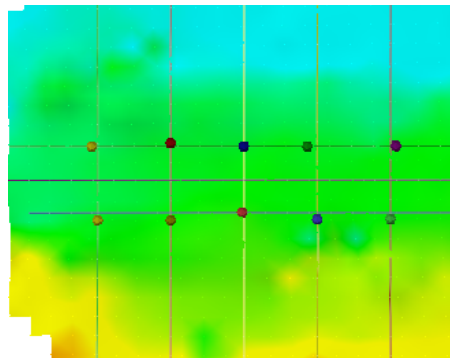


*Figure 7.1. Cube specimens showing top and bottom five points*

Stress data was obtained from the Tinius Olsen machine. Strain was calculated using equation II.

$$\text{Strain} = \frac{\Delta T - \Delta B}{L} \quad \text{_____ (II)}$$

$\Delta$  T = Average of top five points

$\Delta$  B = average of five bottom points

L = Length between top and bottom row of points.

Stress vs. strain graphs as shown from Figure 7.2 to Figure 7.6 were plotted. For the determination of the modulus of elasticity, average of strain from both the faces of the specimen was calculated and plotted against the respective stress.

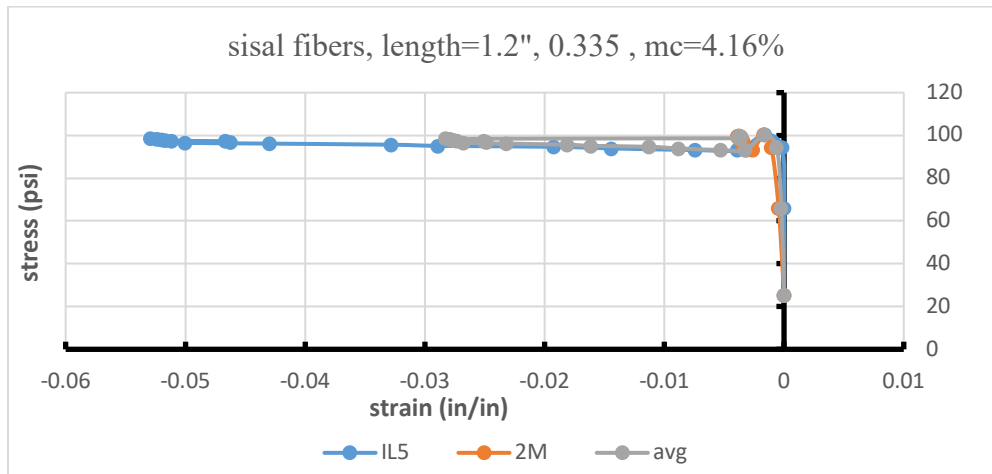


Figure 7.2. Stress vs. stress plots for specimen 1



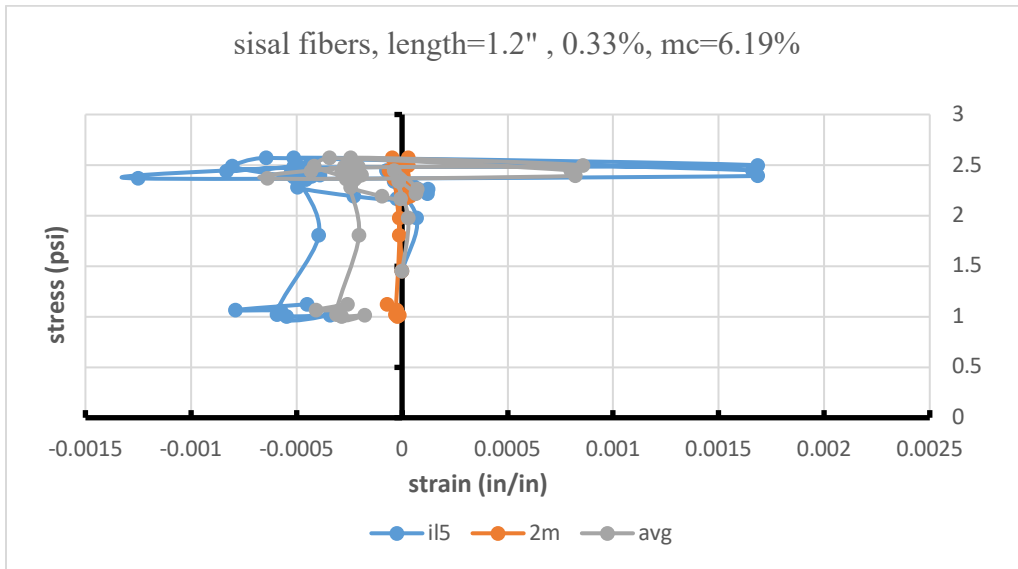


Figure 7.3. Stress vs. stress plots for specimen 2

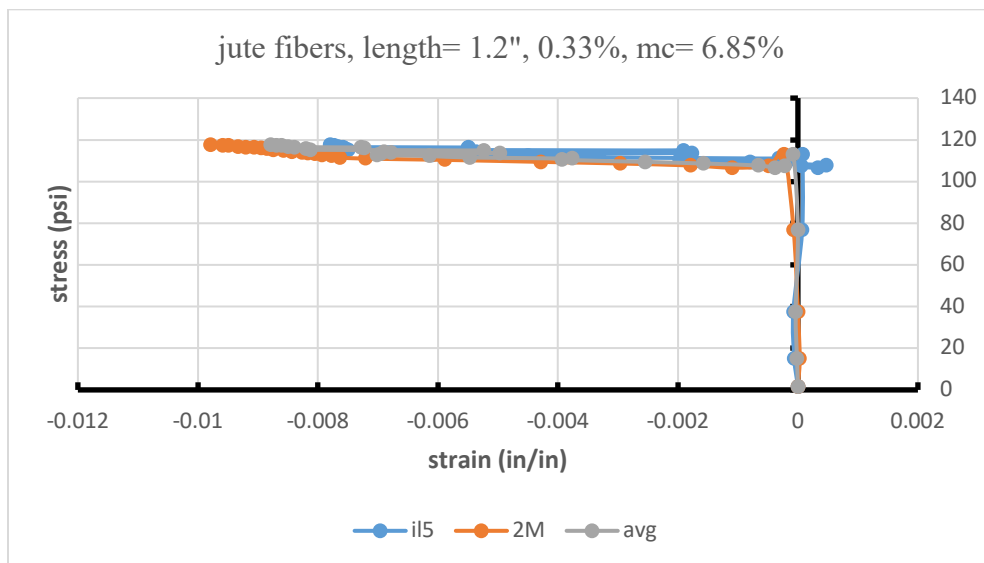


Figure 7.4. Stress vs. stress plots for specimen 3

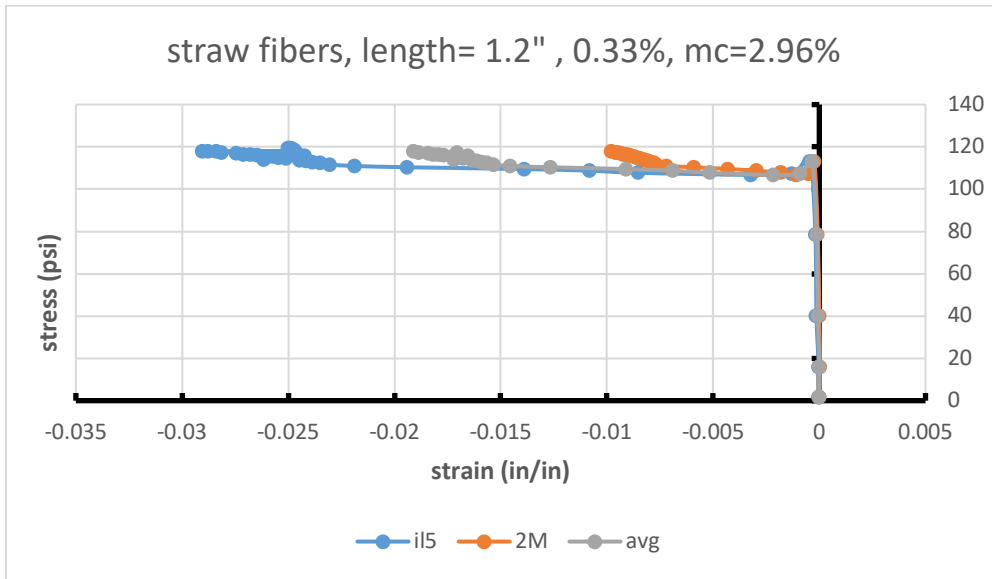


Figure 7.5. Stress vs. stress plots for specimen 4

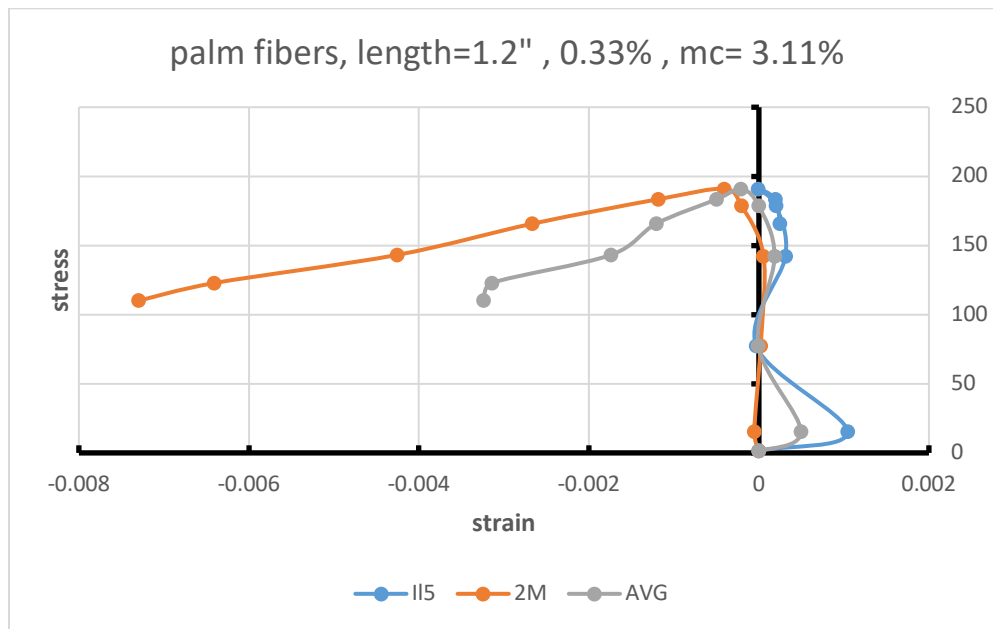
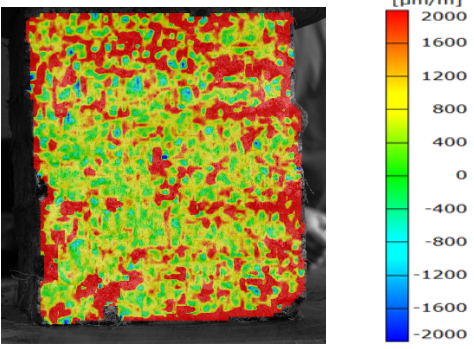
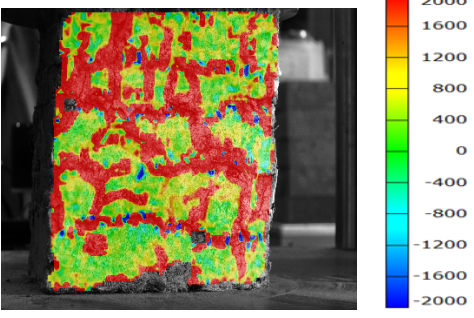
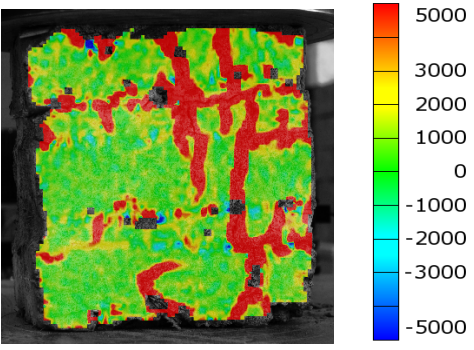


Figure 7.6. Stress vs. stress plots for specimen 5

Sample No.	Cracks at corresponding load.
2	 <p data-bbox="820 577 941 630">@ 84 lbs.</p>
3	 <p data-bbox="820 1018 941 1071">@ 3949 lbs.</p>
4	 <p data-bbox="820 1491 941 1543">@3862 lbs.</p>

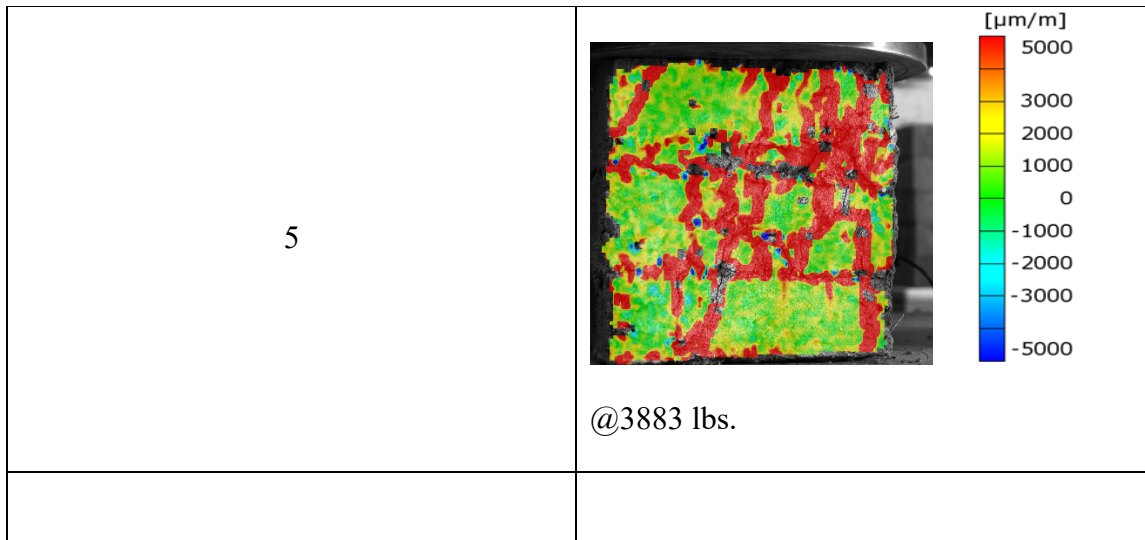


Figure 7.7. Major strains for specimen at particular loads.

### 7.1.1 Results

Following table presents the summary of the result from test 2017.

Table 7.1. Summary Results of compression test 2017

Sample No.	Fibers	Moisture content (%)	Maximum stress(psi)	Strain at maximum load (in/in)
1	sisal	4.16	100	-0.003
2	Sisal*	6.19		
3	jute	6.85	118	-0.0087
4	straw	2.96	119	-0.02
5	palm	3.11	110	-0.0032

The specimen with sisal fibers and moisture content 4.16% has lowest stress as compared with jute, straw and palm. Palm fibers shows to have a higher stress of 190 psi at small moisture content of 3.11 %. As seen, jute and straw

shows almost similar behavior. Tests for sample No. 2 took too long and proper results could not be obtained from that test.

### 7.2 2019 testing

An additional ten more compression tests were completed in March 2019. The Hispec and 2M camera system were used. The analysis was performed in similar manner as was performed for 2017 samples. Figure 7.8 to Figure 7.18 shows stress-strain curves for respective samples.

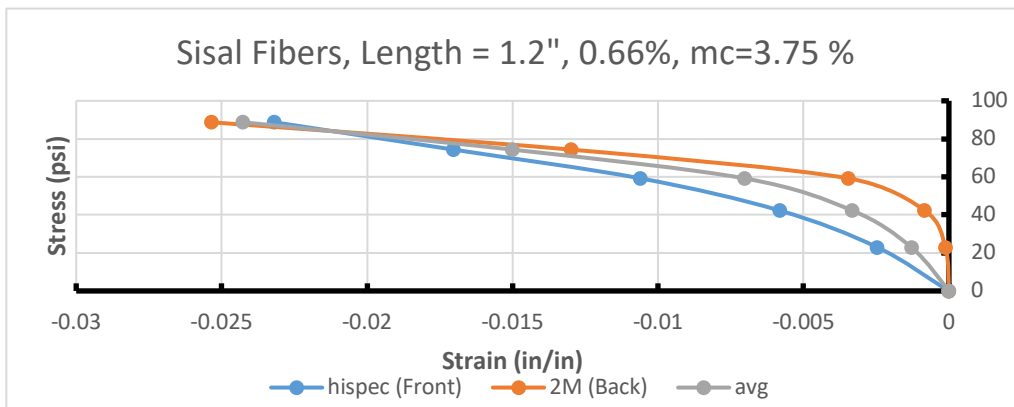


Figure 7.8. Stress vs. stress plots for specimen 6

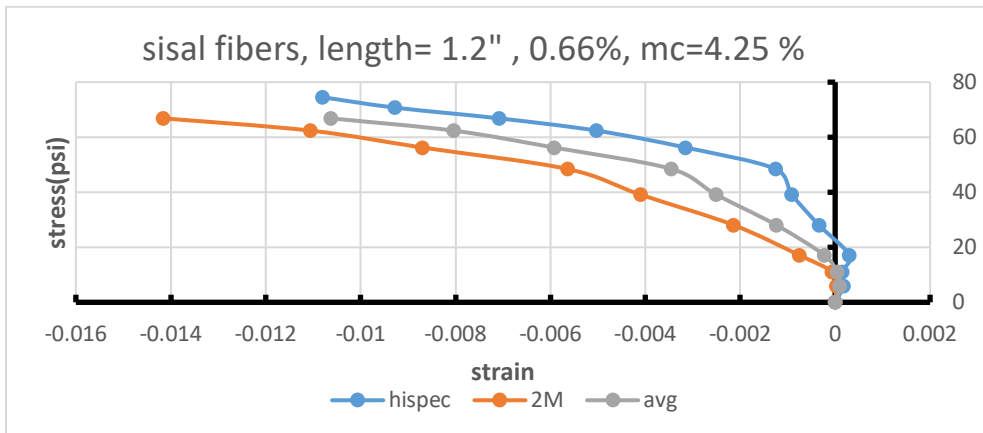


Figure 7.9. Stress vs. stress plots for specimen 7

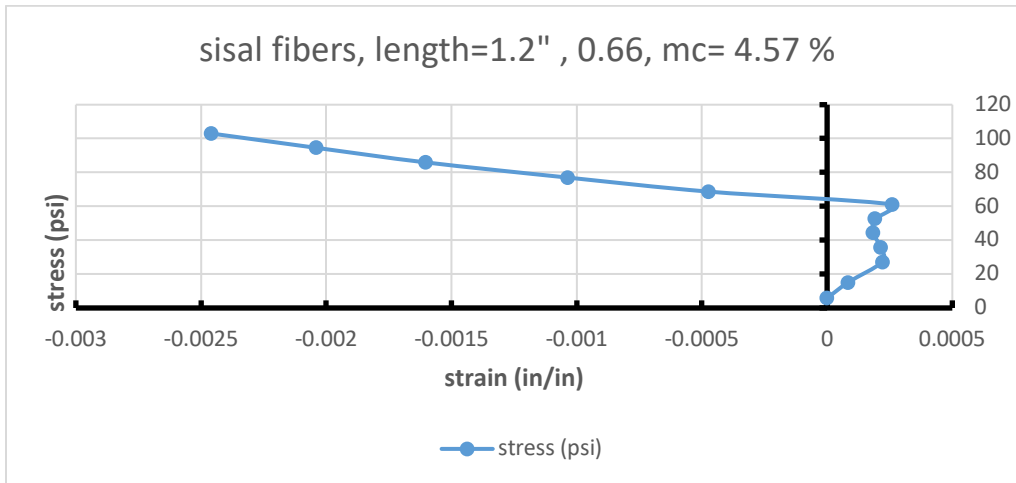


Figure 7.10. Stress vs. stress plots for specimen 8

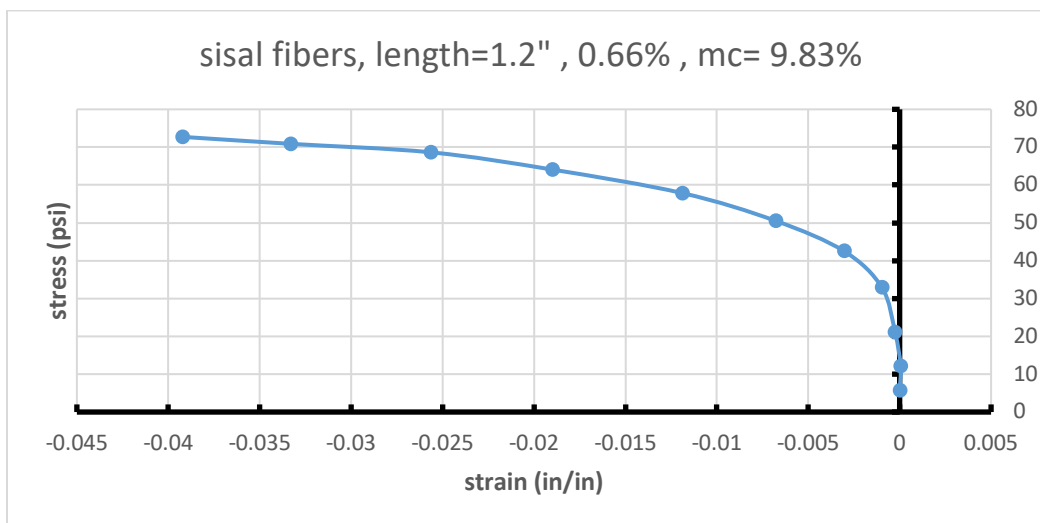


Figure 7.11.: Stress vs. stress plots for specimen 9

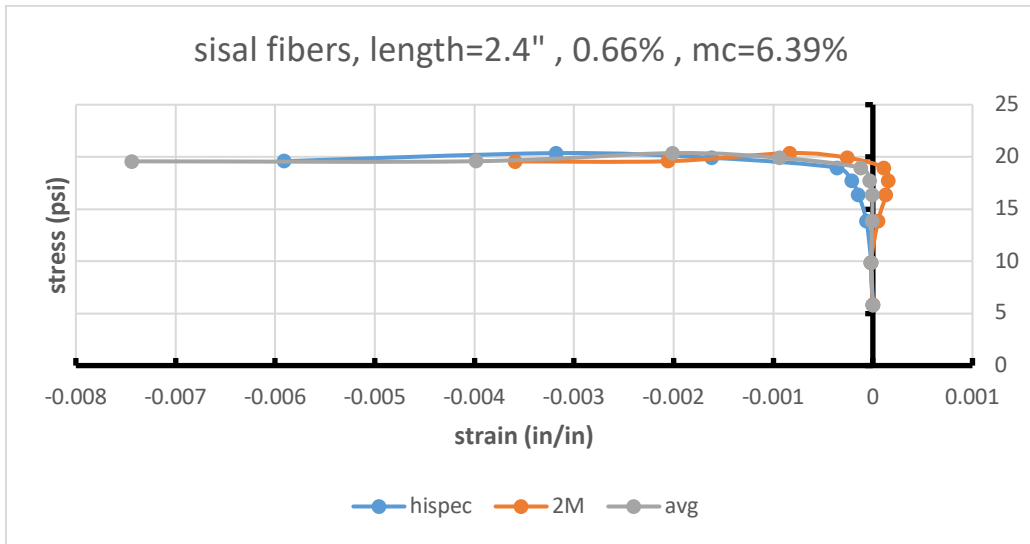


Figure 7.12. Stress vs. stress plots for specimen 10

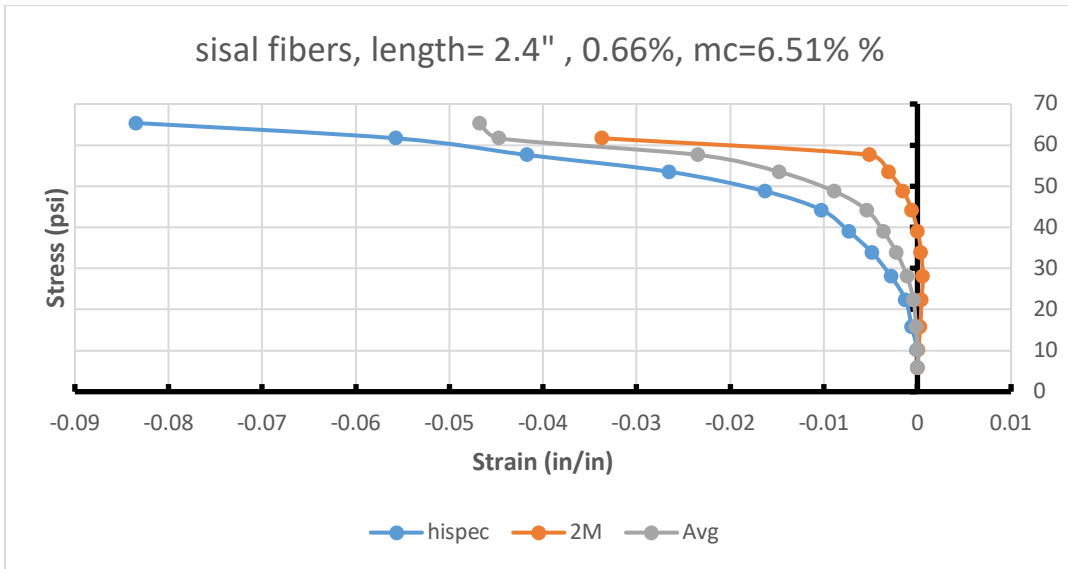


Figure 7.13. Stress vs. stress plots for specimen 11

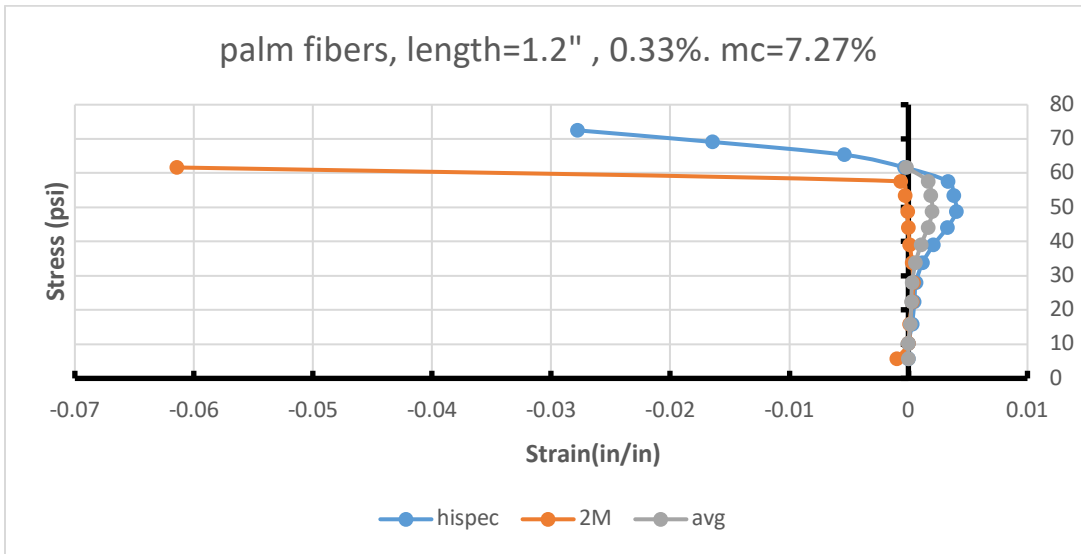


Figure 7.14. Stress vs. stress plots for specimen 12

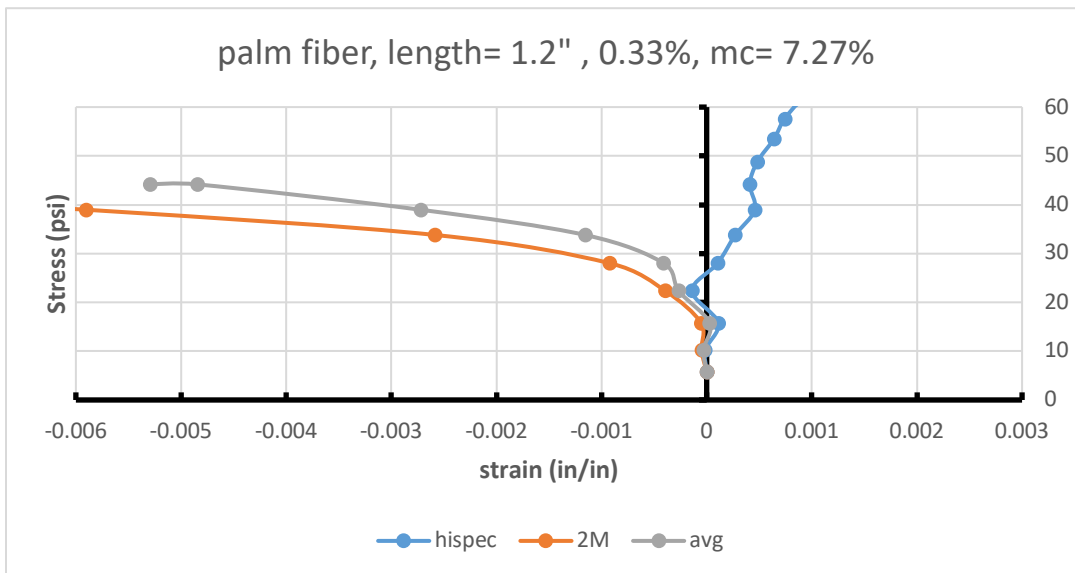


Figure 7.15. Stress vs. stress plots for specimen 13



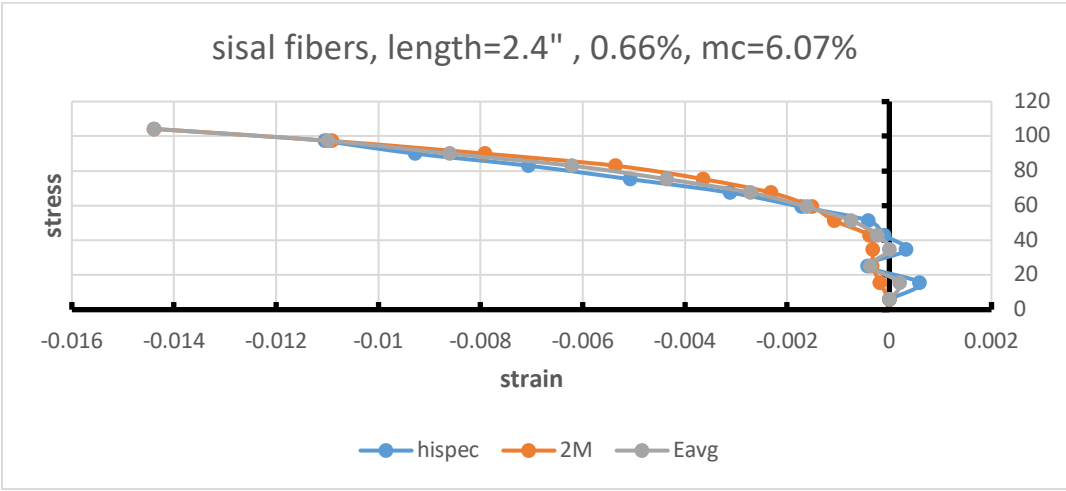


Figure 7.16. Stress vs. stress plots for specimen 14

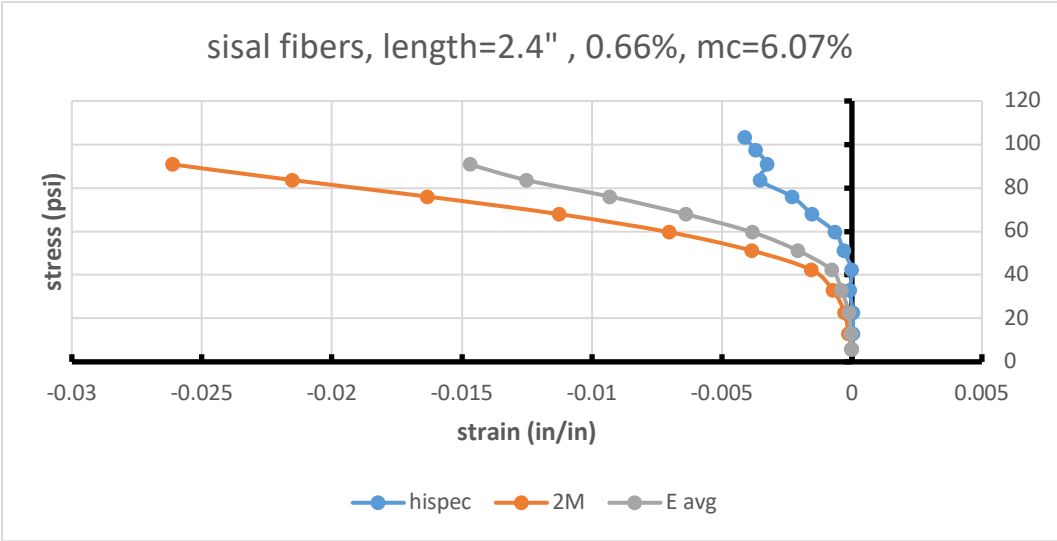
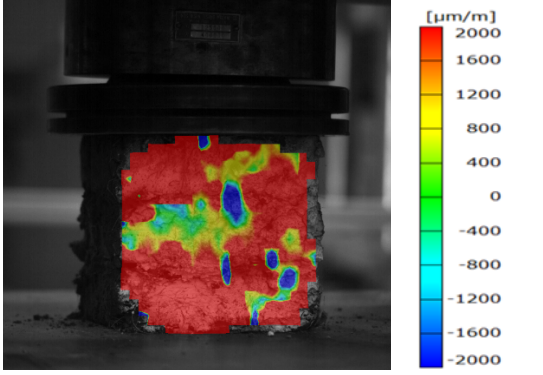
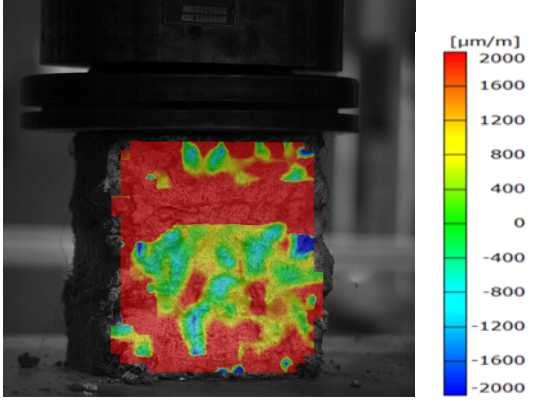
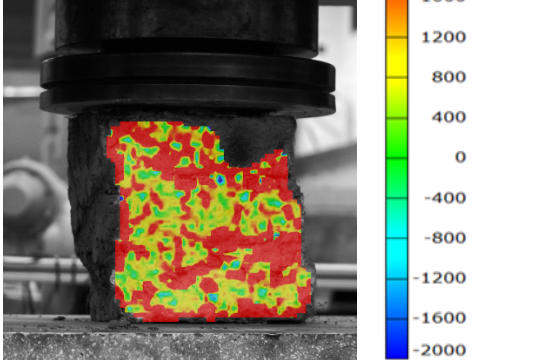
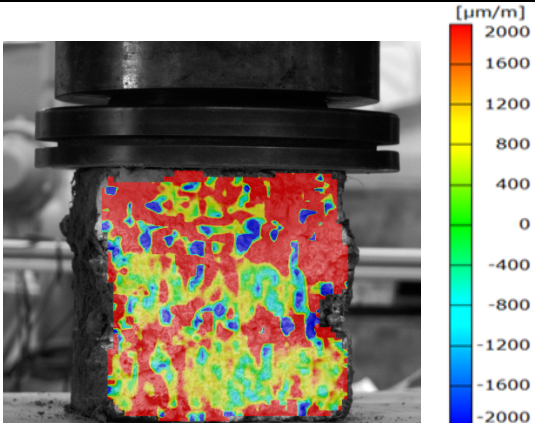
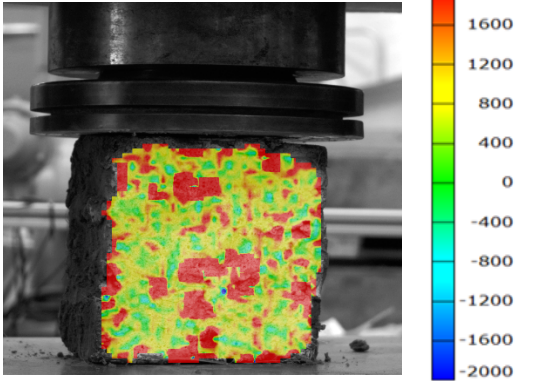
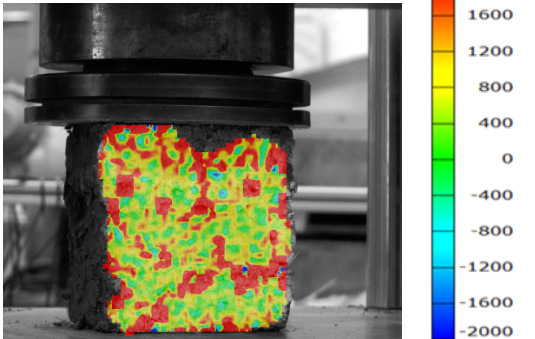


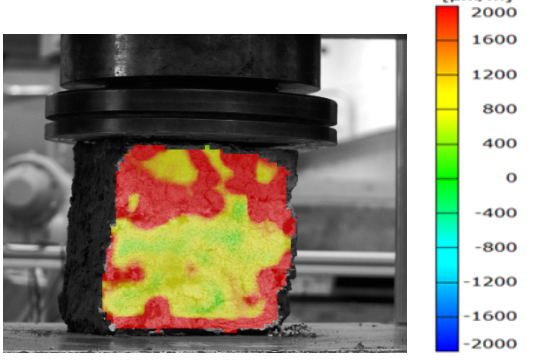
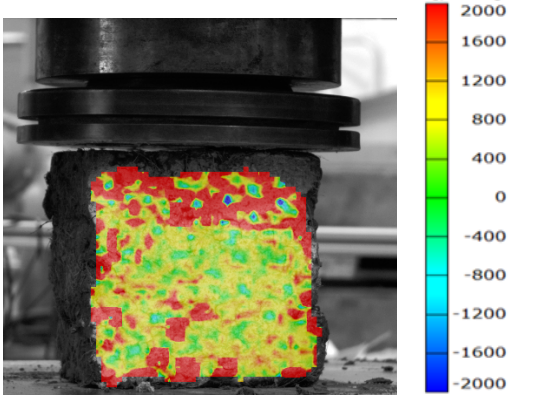
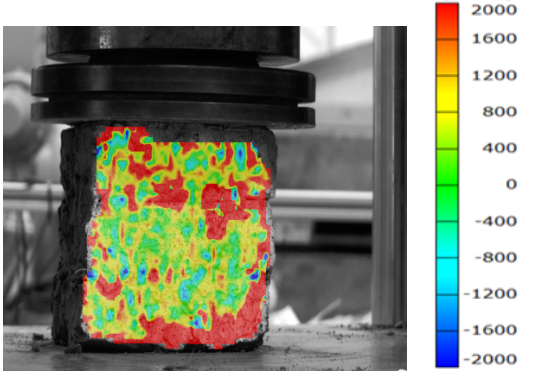
Figure 7.17: Stress vs. stress plots for specimen 15

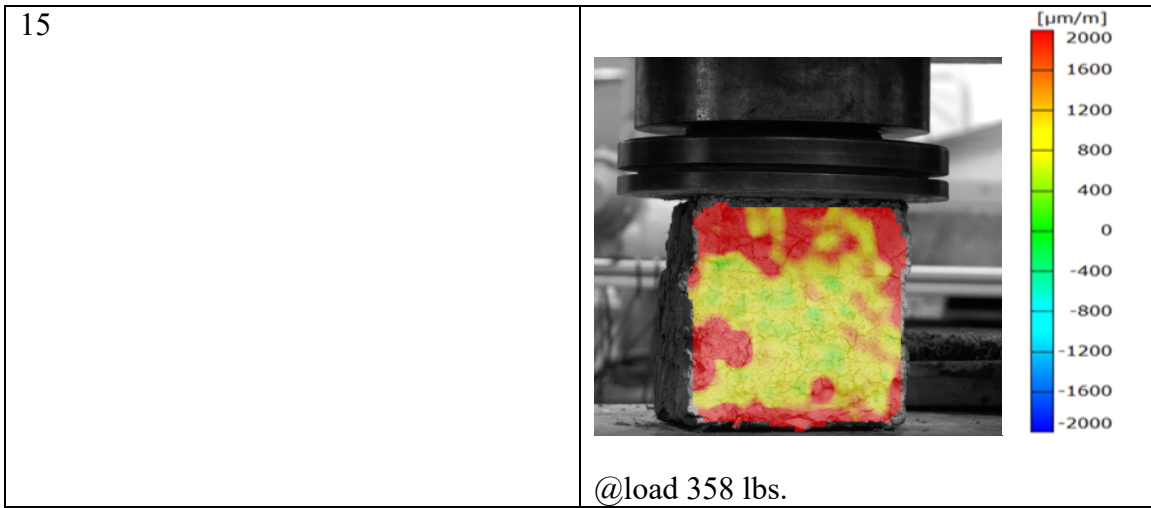
7.2.1 Result

Patterns showing cracks in each specimen is presented below

Specimen	
6	 <p data-bbox="824 819 1039 850">@ load 2072 lbs.</p>
7	 <p data-bbox="824 1323 1023 1354">@ load 984 lbs.</p>
8	 <p data-bbox="824 1858 1023 1890">@ load 951 lbs.</p>

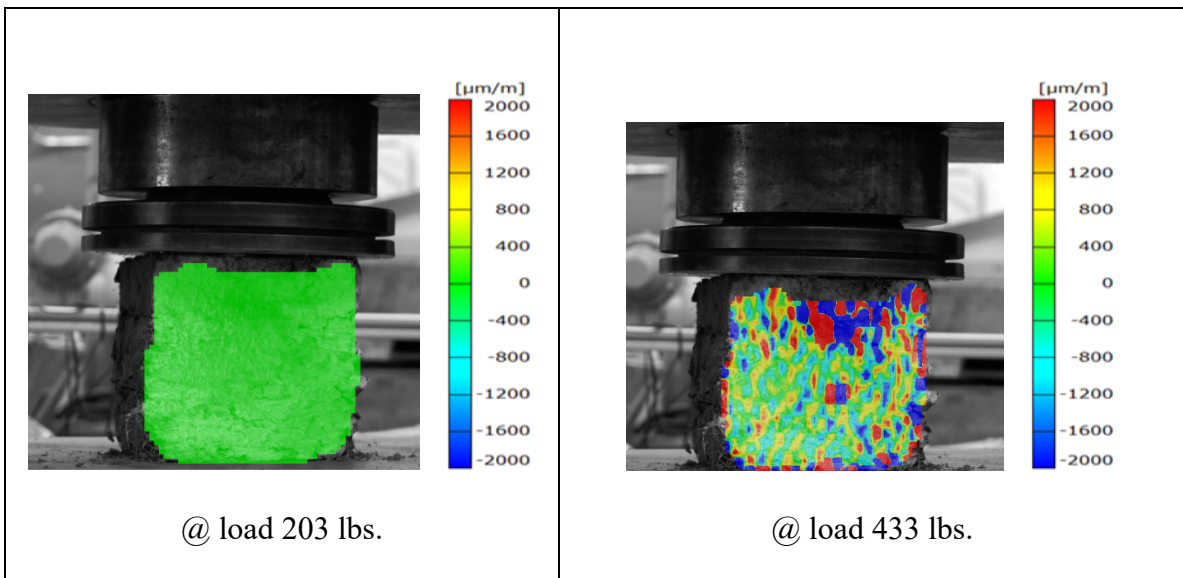
<p>9</p>	 <p>@ load 1768 lbs.</p>
<p>10</p>	 <p>@ load 540 lbs.</p>
<p>11</p>	 <p>@ load 453 lbs.</p>

12	 <p>@ load 485 lbs.</p>
13	 <p>@ load 553 lbs.</p>
14	 <p>@ load 1183 lbs.</p>



*Figure 7.18. Major strains for specimen at particular given loading condition.*

Figure 7.17 shows an example of how crack development in specimen can be tracked using ARAMIS.



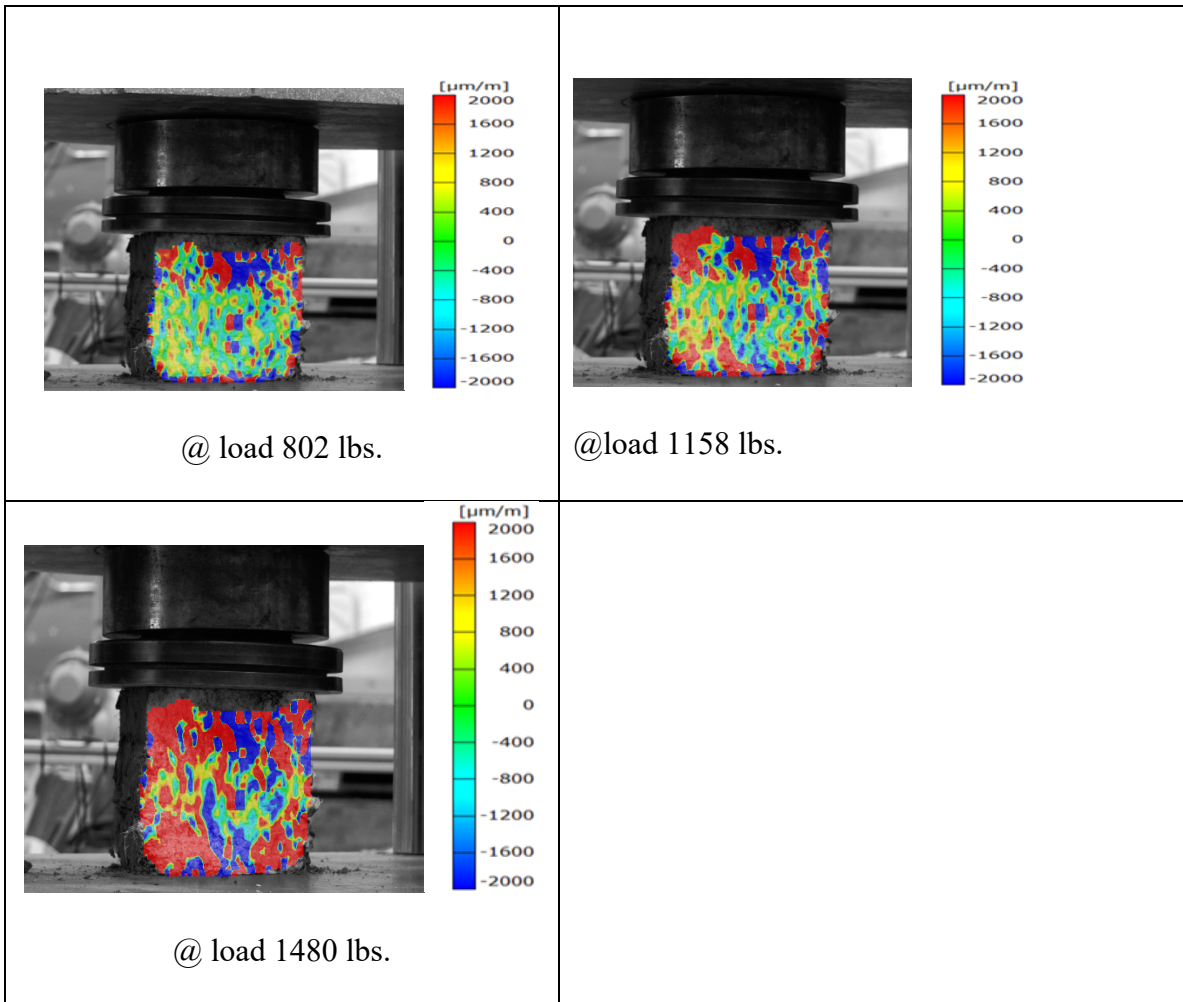


*Figure 7.19. Major strains for different loads for specimen 6.*

Table 7.2. Summary of Results of compression test 2019

Sample No	fibers	Fiber length	Stress (psi)	Strain at maximum load (in/in)
6	sisal	1.2	88	-0.024
7	sisal	1.2	70	-0.010
8	sisal	1.2	103	-0.002
9	sisal	1.2	72	-0.04
10	sisal	2.4	19	-0.007
11	sisal	2.4	65	-0.046
12	palm	1.2	65	-0.002
13	palm	1.2	48	-0.002
14	sisal	2.4	104	-0.014
15	sisal	2.4	103	-0.004

### 8.3 Analysis and Discussion

Each sample was analyzed separately and then summarized for the determination of modulus of elasticity. At first, strain values from front and back surface of the specimen were averaged. Modulus of elasticity was calculated using equation III.

$$E = \frac{\sigma}{\epsilon} \quad \text{(III)}$$

Where, E = Modulus of elasticity

$\sigma$  = Difference between the stress of corresponding stage with the initial one

$\gamma$  = Difference between the strain (average strain from the front and back face) of the corresponding stage with initial one.

Some of the readings included relative movements between the prisms and the machine head. So, the first reading is not considered. The next four readings are considered for determination of Modulus of elasticity which is represented by  $E_2$ ,  $E_3$ ,  $E_4$  and  $E_5$  as shown in Figure 30. The strain values from both the faces are averaged for all the samples except for sample No.8 and sample No. 9 as images of only the front face for these specimens were available.

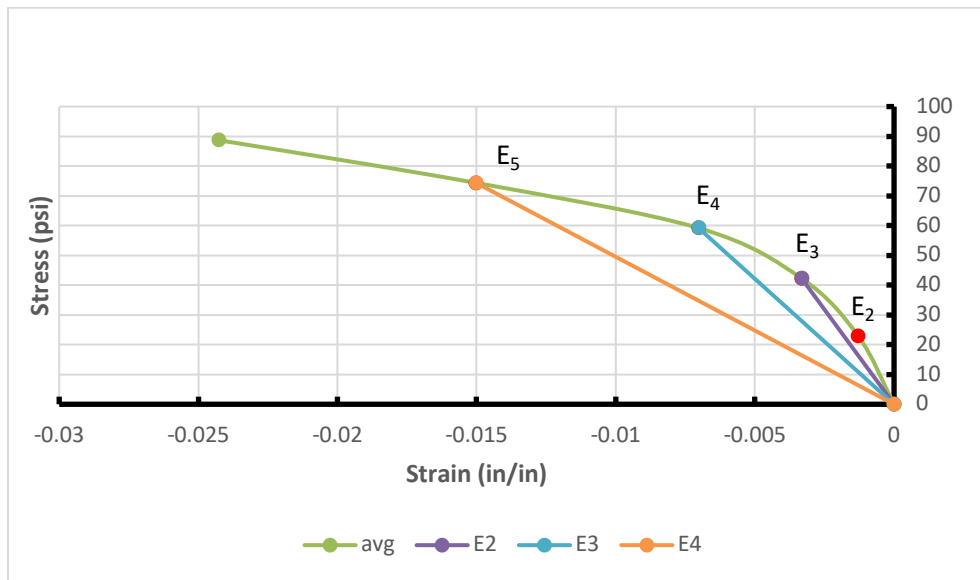


Figure 7.20. Graph showing  $E_2$ ,  $E_3$ ,  $E_4$ ,  $E_5$

This approach yields those four values for the modulus of elasticity. The following table (Table 7.3) shows the summary of calculations. Values highlighted in red in the table were eliminated from the overall averages at the bottom because they were positive. Values in pink in the table were eliminated because they were too large (negatively) and do not come close to values available in the literature.



Table 7.3. Calculation of Modulus of Elasticity

Fiber	Index	Length	%	Mc	E2 (psi)	E3 (psi)	E4 (psi)	E5 (psi)
sisal	6	1.2	0.66	3.75	-12,729	-8,426	-4,952	-3,656
sisal	7	1.2	0.66	9.76	287,535	-74,167	-22,566	-15,598
sisal	8	1.2	0.66	4.57	97,050	140,721	210,376	245,152
sisal	9	1.2	0.66	9.83	-61,255	-27,909	-12,097	-6,597
sisal	10	2.4	0.66	14.63	-1,258,150	-2,048,578	-425,137	-108,331
sisal	11	2.4	0.66	17.39	-39,258.	-15,608	-8,706	-5,168
sisal	14	2.4	0.66	9.14	65,698	66,404	70,809	46,825
sisal	15	2.4	0.66	8.14	593,651	-83,038	-68,579	-28,684
palm	12	1.2	0.33	14.29	-51,389	2805,316	-154,840	-61,362
palm	13	1.2	0.33	8.13	-140,167	-67,419	-46,538	-21,747
sisal	1	1.2	0.33	4.16	-115,214	-45,939	-21,173	-12,909
sisal	2	1.2	0.33	6.19	-26,887	11,005	11,444	-54,144
jute	3	1.2	0.33	6.85	-959,477	428,478,261	-1,413,999	-484,262
straw	4	1.2	0.33	2.96	649,096	-631,535	-335,890	-118,894
palm	5	1.2	0.33	3.11	-13,781,068	765,143	-118,876,792	-908,320
Average=					-51,122	-46,072	-42,431	-39,735

% = Percentage of fiber content.

Mc= Percentage of moisture content.

E= Modulus of elasticity at corresponding stage.

Table 7.4. Comparison of Modulus of Elasticity values with Literature Values

Reference	Year	E <sub>Average</sub>	E range (psi)	Notes
-----------	------	----------------------	---------------	-------

Blondet and Vargas	1978	30,458	29,000 - 32,000	Calculated from full scale specimens
Silviera et al.	2012	29,660	7,400 - 65,000	Bricks recovered from houses, strain from movement of platens of compression machine
Silviera et al.	2012	24,275	13,600 - 49,300	Bricks recovered from land dividing walls, strain from movement of platens of compression machine
Aguilar et al.	2017	116,175	*67,900 - 165,000	~1500 year old brick E measured with platens from 0 - 33% of $f_c$
Aguilar et al.	2017	21,320	*15,500 - 27,100	~1500 year old brick E measured with DIC from 30 - 60% of $f_c$
From Literature			7,400 - 165,000	
* +/- One Standard deviation				
UT Tyler / NMSU	All	73,700	12,800 - 140,000	E2
UT Tyler / NMSU	All	39,800	3,650 - 118,000	E5

Values for modulus of elasticity obtained from different experiments is presented in Table 7.4. From the comparison, the obtained values in this research is within the range obtained by other authors.

Hence.

- The calculated value of modulus of elasticity for the adobe in the current project is between 39,000 and 51,000 psi, depending on the method used (how far out on the stress strain curve the value is taken)
- No comments on the Fiber length, percentage of fiber or moisture content can be made, because not enough specimens of each type were tested.

## Chapter Nine

### Summary and Conclusions

#### 9.1 Summary from Wall Tests

A total of seven wall tests were monitored with DIC under lateral loading from a single point load at the top of the wall. The wall specimens were designed and constructed in the Structural Engineering and Materials Laboratory at New Mexico State University (NMSU).

From the July 2017 testing, following points could be summarized,

- The peak load for the wall with reinforcement pattern 1 is 650 lbs. which slightly more than the wall with no reinforcement i.e., 600 lbs.
- The lateral strength of the wall with reinforcement pattern 2 increased to 1200 lbs.
- Wet wall with no reinforcement seems to be weaker than wall with reinforcement pattern 2.

From January 2018 testing, following points could be summarized,

- The peak load for the dry wall without reinforcement was 400 lbs. whereas for the wet wall with reinforcement was 800 lbs.
- For both the walls, upward displacement was higher than the downward displacement.

Overall, for the wall tests:

- DIC was useful in determining the failure mode and initiation points.

- The DIC results show that the walls failed primarily by large diagonal shear cracking. The load versus shear deformation behavior was able to be captured using DIC.

## 9.2 Summary from Modulus of Rupture Tests

3-Point Bend test on adobe was performed to determine the Modulus of Rupture (MOR) of the material. The beams were constructed then tested in the Structural Engineering and Materials Laboratory at NMSU using a Tinius Olson axial loading machine. The beams constructed contained no reinforcement, straw fibers and sisal fibers as reinforcement. Each of the individual beam samples were tested under loading condition while being monitored by the DIC system.

The results from July 2017 and 2018 can be summarized as follows:

*Table 9.1. Summary of MOR test*

Sample No	Reinforcement	Maximum Load (lbs.)
65	None	35
66	None	58
74	None	45
75	None	28
67	Straw	60
68	Straw	50
69	Straw	79
77	Straw	28
78	Straw	30
71	Sisal	70

80	Sisal	35
81	Sisal	35

### 9.3 Summary from Prism Tests

- The calculated value of modulus of elasticity for the adobe in the current project is between 39,000 and 51,000 psi, depending on the method used (how far out on the stress strain curve the value is taken).
- No comments on the Fiber length, percentage of fiber or moisture content can be made, because not enough specimens of each type were tested.

### 9.4 Overall Conclusions

The walls which were dry performed better than the walls which were wet. Similarly, Reinforced adobe structure were able to resist higher load and cracking developed at higher loading cycle. However, proper care should be taken during the specimen preparation as quality of the bricks might also play an important role in improving the strength of adobe structure.

Therefore,

- DIC can be used to measure strains in adobe.
- Crack development can be tracked using DIC.
- Composition of materials in adobe plays significant role in determining Modulus of Elasticity.
- DIC measured the value of E to be in between 3,650 psi to 140,000 psi.

- Reinforcement prevents sudden failure of structure and can resist higher loads.
- Fibers bridge cracks and allow large deformations before failure.
- The calculated value of modulus of elasticity for the adobe in the current project is between 39,000 and 51,000 psi, depending on the method used (how far out on the stress strain curve the value is taken).
- No comments on the Fiber length, percentage of fiber or moisture content can be made, because not enough specimens of each type were tested.

## Future Work

More tests need to be performed to understand the effect of moisture content and fibers in adobe structure.

In Prism test, a critical component is missing. Specimen with no reinforcement need to be examined first in order to study whether the added fibers helps in increasing strength or not.



## References

- Aguilar, M. . (2017). Mechanical characterization of the structural components of Pre-Columbian earthen monuments: Analysis of bricks and mortar from Huaca de la Luna in Peru. *Case Studies in Construction Materials*, 16-28.
- Aydilek, O. E. (2002). Digital Image Analysis to Determine Pore Opening Size Distribution of Nonwoven Geotextiles. *Journal Of Computing In Civil engineering*. doi:16. 10.1061/(ASCE)0887-3801(2002)16:4(280)
- Bergliv, E. (2016). Laboratory study on two-dimensional image analysis as a tool to evaluate degradation of granular fill materials. *Nordic Geotechnical Meeting*, (pp. 461-470).
- Blondet, V. (1978). Seismic strength of adobe masonry. *Material and Structures*, 253-258. doi:10.1007/BF02472107
- C. Galan-Marin, C. R.-G. (2010). Clay-based composite stabilized with natural polymer and fibre. *Construction and Building Materials*, 1462-1468.
- Caporale, P. A. (2015). Comparative micromechanical assessment of adobe and clay brick masonry assemblages based on experiment data sets. *Composite Structures*, 120, 208-220.
- D.M. Herbert, D. G. (2011). The development of a new method for testing the lateral load capacity of small-scale masonry walls using a centrifuge and digital image correlation. *Construction and Building Material*, 4465-4476.
- Davila, E. (2019). *Laboratory Study on the Behavior of Laterally Loaded Adobe Walls*. Las Cruces, NM: New Mexico State University Master's Thesis.

- F. Tootoonchy, B. A. (2015). Experimental in-plane behavior and retrofitting method of mud-brick walls. *International Journal of Civil Engineering*, 191-201.  
doi:10.22068/IJCE.13.2.191
- Fayyad, L. (2014). Application of Digital Image Correlation to Reinforced Concrete Fracture. *Procedia Material Science*, 1585-1590.
- Fulvio Parisi, D. A. (2015). Experimental characterization of Italian composite adobe bricks reinforced with straw fibres. *Composite Structures*, 122.  
doi:10.1016/j.compstruct.2014.11.060
- Illampas, C. I. (2014). Laboratory testing and finite element simulation of the structural response of an adobe masonry building under horizontal loading. *Engineering structures*, 362-376.
- Illampas, L. C. (2017). Validation of the repair effectiveness of clay-based grout injections by lateral load testing of an adobe model building. *Construction and Building Materials*, 174-184. doi:10.1016/j.conbuildmat.2017.07.054
- K.M.A. Hossain, M. L. (2007). Stabilized soils for construction applications incorporating natural resources of Papua New Guinea. *Resources Conservation & Recycling*.
- Kabir, F. F. (2018). Experimental study on shear responses of clay adobe beams reinforced randomly distributed short fibres. *Materials Science and Engineering*, 433, p. 012016. doi:10.1088/1757-899X/433/1/012016
- Lees, J. &. (2017). Experimental investigation of crack propagation and crack branching in lightly reinforced concrete beams using Digital Image Correlation. *Engineering Fracture Mechanics*. doi:10.17863/CAM.9155

- Lutfullah turanli, A. S. (2010). Strengthening the structural behavior of adobe walls through the use of plaster reinforcement mesh. *Construction and Building Materials*, 1747-1752.
- M. J. McGinnis, S. B. (n.d.). Application Of Multiple Digital Image Correlation Sensors In Earthquake Engineering. *National Conference in Earthquake Engineering*.
- Manning, M. P. (2016). Behavior Comparison of Prestressed Channel Girders from High Performance Concrete and Locally Developed Ultra-High Performance Concrete. *Proceedings of the Transportation Research Board 95th Annual Meeting*. Washington, DC.
- McGinnis, M. J. (2005). Application of 3D Digital Image Correlation to the Core-Drilling Method. *Experimental Mechanics*, 45(4), 359-367.
- McGinnis, M. J. (2009). Structural Aspects of Residential Housing that Compromise Fire Fighter Safety. *ASCE Structures Congress*, (p. Poster). Austin, TX.
- McGinnis, M. J. (2012). 3-D Digital Image Correlation – An Underused Asset for Structural Testing. *ASCE Structures Congress*. Chicago, IL.
- McGinnis, M. J. (2013). Experimental Evaluation of a Multi-Story Post-Tensioned Coupled Shear Wall Structure. *ASCE Structures Congress*. Pittsburgh, PA.
- McGinnis, M. J. (2015). Digital Image Correlation For Bridge Inspection: Impact of Using Commercial Grade Cameras. *16th European Bridge Conference*. Edinburgh, Scotland.
- McGinnis, M. J. (2015). In situ stresses in Bridge Beams. Part I: Concrete Stresses. *Magazine of Concrete Research*, 67(9), 459-466.

- McGinnis, M. N. (2009). Structural Aspects of Residential Housing that Compromise Fire Fighter Safety. *ASCE Structures Congress*, (p. Poster). Austin, Texas.
- Michelle Holloman, M. M. (2013). Testing and Analysis of a Post-Tensioned Coupled Wall System Monitored With Multiple Digital Image Correlation Systems.
- Monika H, S. U. (2017). Characterisation of Jute Fibre reinforced Adobe Brick and Brick masonry. *International Journal of International Research Trends in Engineering and Technology*.
- Pablo de Heras Ciechowski, m. C. (2012). Development and Implementation of a Web-Enabled 3D Consultation Tool for Breast Augmentation Surgery Based on 3D-Image Reconstruction of 2D Pictures. *Journal of Medical Internet Research*. doi:<https://dx.doi.org/10.2196%2Fjmir.1903>
- Qualiarini, I. (2010). the influence of natural stabilizers and natural fibres on the mechanical properties of ancient Roman adobe bricks. *journal of Cultural Heritage*, 309-314. doi:<https://doi.org/10.1016/j.culher.2009.11.012>
- Quintilio Piattoni, E. Q. (2011). Experimental analysis and modelling of the mechanical behaviour of earthen bricks. *Construction and Building Materials*, 2067-2075.
- Rodriguez, J. E. (2012). Particle shape determination by two-dimensional image analysis in geotechnical engineering. *Nordic Geotechnical Meeting*.
- Schmidt, T. G. (2003). Pull-field dynamic displacement and strain measurement using advanced 3D image correlation photogrammetry: Part 1. *Experimental Techniques*, pp. 47-50.

Silveira, V. ., (2012). Mechanical properties of adobe bricks in ancient constructions.

*Construction and Building Materials*, 36-44.

doi:<https://doi.org/10.1016/j.conbuildmat.2011.08.046>

Smith. (1982). *Adobe bricks in New Mexico*. New mexico: Authority of State of New mexico.

Tyson, J. (2010). optical 3D Deformation and Strain Measurement., (pp. 147-164).

Vargas, B. B. (1986). Seismic strength of adobe masonry. *Materials and Structures*, 253-258.